A STUDY OF RATING CURVE & FLOOD ROUTING USING NUMERICAL METHODS

Prateek Kumar Singh

Department of Civil Engineering

National Institute of Technology, Rourkela

A STUDY OF RATING CURVE AND FLOOD ROUTING USING NUMERICAL METHOD

A dissertation submitted to the

National Institute of Technology, Rourkela
in partial fulfilment of the requirements
of the degree of
Master in Technology

in

Civil Engineering

By

Prateek Kumar Singh

(Roll Number: 215CE4286)

Under the supervision of

Prof. K. K. Khatua

June, 2017

Department of Civil Engineering

National Institute of Technology, Rourkela

Department of Civil Engineering

National Institute of Technology, Rourkela

June 02, 2017

Certificate of Examination

Roll Number: 215CE4286

Name: Prateek Kumar Singh

Title of Dissertation: <u>A STUDY OF RATING CURVE AND FLOOD ROUTING USING NUMERICAL METHOD</u>

The undersigned, after examining the thesis mentioned above and the official record book (s) of the student, hereby state my approval of the dissertation submitted in partial fulfillment of the requirement of the degree of Masters in Technology in Civil Engineering at National Institute of Technology, Rourkela. We are satisfied with the volume, quality, correctness, and originality of the work.

(External Examiner)

Date:

Department of Civil Engineering

National Institute of Technology, Rourkela

K. K. Khatua

Professor   June 02, 2017

Supervisor's Certificate

This is to certify that the work presented in this dissertation entitled *"A Study of Rating curve and Flood Routing Using Numerical method"* by *"Prateek Kumar Singh"*, Roll Number: 215CE4286 is a record of original research carried out by him under my supervision and guidance in partial fulfillment of the requirements of the degree of *Master in Technology* in *Civil Engineering*. Neither this dissertation nor any part of it has been submitted for any degree or diploma to any institute or university in India or abroad.

- - - - - - - - - - - - - - - - -
K. K. Khatua

Principal Supervisor

DEDICATED TO

MY Nation

Declaration of Originality

I am Prateek Kumar Singh bears a Roll Number: 215CE4286 want to affirm that this dissertation entitled *"A Study of Rating curve and Flood Routing Using Numerical method"* is an original work carried out for the partial fulfillment of Masters' degree in NIT Rourkela. It does not comprise any material previously published or written by another person, nor any material presented for the award of any degree or diploma of NIT Rourkela or any other institution. Any contribution made to this research by others, with whom I have worked at NIT Rourkela or elsewhere, is explicitly acknowledged in the dissertation. Also, the works of other authors cited in this dissertation have been duly acknowledged under the section "Bibliography".

I am fully aware that in case of my non-compliance detected in the future, the Senate of NIT Rourkela may withdraw the degree awarded to me based on the present dissertation.

June 02, 2017

Prateek Kumar Singh

NIT Rourkela

Acknowledgment

Abstract

The stage discharge curve, depth-averaged velocity and boundary shear stress distributions are essentially determined for the flood extenuation scheme. The difficulties aroused in prediction of these parameters are usually due to the 3D nature of the fluid flow in open channel. The current study represents different analytical model for velocity distribution, boundary shear stress and stage-discharge curves and their application to the trapezoidal compound channel. The analytical solution to the depth-integrated Navier-Stokes equation is used for the same and their results are validated using experimental data. These parameters are not easy to predict because of the three-dimensional characteristics of the flow field. The model proposed by Shiono and Knight (1988, 1991) is compared with those by Ervine et al. (2000), Kordi et al. (2015) and K-ε model (ANSYS) through numerical modelling. This test shows that secondary flow parameter plays a vital role and its significance proliferates near side slope where momentum transfer from the main channel to flood plain is observed. The contrast in the results are shown with the help of lateral variation in percentage error.

The flood routing is an important technique to determine the flood peak attenuation and the duration of the high water levels through channel routing. Beside stage-discharge curve, hydrographs also plays a vital role in flood prediction and forecasting. The present study shows the application of hydrological methods for channel routing, the constant coefficient Muskingum-Cunge (MC) methods on the River Brosna, Co. Offaly in Ireland. The results obtained are validated by two software packages MIKE 11 and HEC-RAS beside that the method ensuring the mass balance of the model is tested in terms of water storage. The results of all the tests are plotted and verified with respect to the mass conservation criteria. Data sets of the River Brosna, Co. Offaly in Ireland is taken from the Elbashir (2011) for the November 1994 flood event.

Keywords: Shiono Knight Method, Extended SKM, Secondary parameters, compound channel, Open channel, Muskingum-Cunge, Mass conservation

Contents

List of Figures

List of Tables

Nomenclature

$\bar{\mathrm{v}}$	Time-averaged spanwise velocity
$\bar{\mathrm{w}}$	Time-averaged vertical velocity
$\bar{u}$	Time-averaged streamwise velocity
Δt	Computational interval
Δx	Spatial Weightage factor
A	Area of the compound section
b	Bottom width of main channel
B	Over all width of compound channel
C	Volume fraction
C	Courant number
C_d	Dynamic celerity
C_o, C_1, C_2	Routing Coefficients
D	Cell Reynold's number
D_m	Hydraulic depth
f	Darcy-Weisbach Friction factor
F_r	Froude's number of the flow
g	Acceleration due to gravity
g	Gravitational acceleration
h	Height of main channel up to floodplain bed
H	Total depth of flow in compound channel
H	Water depth
h_v	Velocity head
i	Stands for local values in the ith cell or node
I	turbulence intensity
k	Turbulence kinetic energy
K	Ervine's coefficient for K-method
L	Non prismatic length of converging compound channel
L	Reach length
n	Manning's roughness factor
P	Wetted perimeter of the compound channel section

Q	Discharge
q	The unit flow rate
Q_{actual}	Actual discharge
Q_o	References discharge
R	Hydraulic mean radius of the channel cross section (A/P)
R_e	Reynolds number of the flow
S	Valley slope
S	Storage
S_f	Friction slope
S_o	Bed slope
t	Time
T	Top width
U	Instantaneous streamwise velocity
U_*	Shear velocity
u'	Streamwise fluctuation velocity
U_d	Depth-averaged streamwise velocity
V	Instantaneous spanwise velocity
v'	Spanwise fluctuation velocity
W	Instantaneous vertical velocity
w'	Vertical fluctuation velocity
x	Cartesian coordinate in the streamwise direction
y	Cartesian coordinate in the spanwise direction
z	Cartesian coordinate in the vertical direction
β	Ratio of kinematic celerity to the average longitudinal velocity
Γ	Secondary flow term
ϵ	Rate of dissipation of turbulent kinetic energy k
ϵ_{yx}	Kinematic eddy viscosity
λ	The dimensionless eddy viscosity
λ	Eddy viscosity coefficient
μ	Dynamic viscosity of water
v	Kinematic viscosity of water
ρ	Density of flowing liquid
σ_k	Turbulent Schmidt number
τ	Point boundary shear stress

τ_d Bed shear stress lateral distribution

$\tau_{xx}, \tau_{xy}, \tau_{yx}$, and τ_{yy} The depth integrated Reynolds stresses in appropriate directions

$\Gamma 1$ Helical secondary current

$\Gamma 2$ Transverse convection term

ϵ The eddy viscosity

Note: - The symbols and abbreviations other than above have been explained in the text.

Chapter 1

INTRODUCTION

1.1   General

Estimation of the flow discharge with respect to the stage and the time is one of the main parameters in the flood management projects. The insurance companies have also acknowledged the importance of the prediction of the flow discharge. Estimation of flow discharge leads to evaluate the flow depth in streams is necessary to estimate the risk of insurance of projects located on the floodplains. The stage-discharge curve is very crucial for the prediction, computation and the forecast of flood in a natural river system. When a flood occurs, the flow depth increases arbitrarily which in turn causes overbank flow. The overbank flow is usually very different from that of the inbank or single channel flow. The characteristic of the floodplain in the overbank flow plays a vital role, whereas the difference in the flow of water in the floodplain and the main channel generates strong lateral shear layer and large-scale turbulence (Sellin 1964; Perkins 1970; Wormleaton and Merrett 1990; Ackers 1992; Tominaga and Nezu 1991; Bousmar and Zech 1999). The occurrence of large eddies due to the vertical vortices and helical secondary flows is most substantial feature in the longitudinal direction (Rodi 1980). Ignorance of such coherent structure may always lead to the error, in prediction of the velocity and the boundary shear stress distribution.

Velocity distribution and boundary shear stress distribution is the key feature for the prediction of the water surface profile, compound open channel design, and sediment and pollutant transport in the overbank flow. Many modelling techniques are presented in the past literature for the prediction of the velocity distribution, such as single channel method, divided channel method (Lotter 1933; Te Chow 1959), coherence method (Ackers 1992, 1993; Lambert and Sellin 1996), weighted divided channel method (Lambert and Myers 1998), exchange discharge model (Bousmar and Zech 1999), lateral discharge method using Reynolds averaged Navier-Stokes equation (RANSE) (Shion and Knight 1988,1991; Ervine et al. 2000) and so on. The prediction of the boundary shear stress distribution in a gravity flow channel is very significant because this is that parameter which influence flow

structures in the channel, the conveyance capacity and the transportation of the sediments in the channel (Knight 1981; Graf 1991; Knight and Sterling 2000; Sterling et al. 2008).

On the other hand, climate change is another factor affecting the hydrological processes, which has profoundly changed the approach of the engineers in the past few decades. Further, engineers and hydrologist face problems related to the hydrology of the ungauged basin because of the unavailability of the morphological, hydrological and hydrometric data for the basins, especially in the developing and under-developed countries (Perumal and Price 2013). These problems of hydrological non-stationarity and ungauged basins necessitates decision making based on the hydrological models that are numerically governed solution for the basic equation of flow which are integral to these hydrological component processes.

Flood routing is another approach for the flood planning and management. Study of flood wave movement in the channel and Natural River is one of the most important hydrological investigation using the basic governing equation of flow. Many studies have been performed which showed the consistency of such hydrological routing methods. Ponce (1981) and Merkel (2002) showed the consistency of the MC method (constant parameter) and developed the outflow hydrograph using different step and time size interval. Reid (2009) suggested more research on the short reaches and small drainage area, which are the conventional cases experienced while the application of the hydrological channel routing method.

The difficulties in dealing with a small channel are the milder slope, which lack good quality flow data, which are most significant for modelling and comparison purpose. These aspects influence the precision of the two approaches and introduce sources of error in the assessment process.

1.2   Velocity distribution

In a circular duct, the profile is considered parabolic for laminar flow conditions. However, the velocity profile in open channel flow is usually turbulent and fluctuates because of friction generated at the bottom and sidewalls. The velocity increases as we move away from the boundaries in either lateral or longitudinal direction, or it would indicate that the maximum velocity would occur at the midway from both side boundaries and over the free surface away from the bottom wall. Other factors like secondary flow current usually does

not make the ideal condition possible for the location of maximum velocity and hence the velocity dip near surface comes into the picture. In case of rectangular channel, the point of maximum velocity on a vertical line would occur close to the water surface if the vertical line is taken at the centre. As we move closer to the banks, the point of maximum velocity will tend to move downward. In contrast to narrow rectangular channel if wide rectangle channels are considered the maximum velocity will occur closer to the water surface in wide channels.

Some of the important observations regarding the velocity distribution in open channel flow are as follows:

1. The velocity at the depth of 0.6 times the total flow depth from the water surface level is considered as the depth average velocity in general. This has important application since discharge is sometimes calculated from the contour diagram through area-velocity method. Rather calculating velocity at every point and then averaging it to obtain the average velocity, it would be more convenient to measure the average velocity at a particular point which is 0.6y below the water surface, and where y is the flow depth at that vertical line.

2. An even more accurate method to estimate the average velocity is to measure the point velocity at two different location i.e. 0.2y and 0.8y from the water surface. Note that these locations are nearly identical with the location of Gauss points, which are numerically integrate an arbitrary function with best possible accuracy using two points the values of Gauss points are $0.5[1 \pm (1/\sqrt{3}\,)]$, i.e. 0.79 and 0.21 of the flow depth.

3. The magnitude of the surface velocity is almost 5-25% more than that of the average velocity. The channel dimension and flow characteristics play significant role in determining the exact ratio of the surface velocity and average velocity. This ratio remains more or less constant for a given channel under comparable flow conditions.

1.3 Boundary shear stress

The average boundary shear stress on the channel has been shown (through a balance of driving and resisting forces under uniform flow conditions) to be equal to ρgRS where R is the hydraulic radius, S is the bed slope in uniform flow condition and ρ and g are density of fluid and acceleration due to gravity respectively.
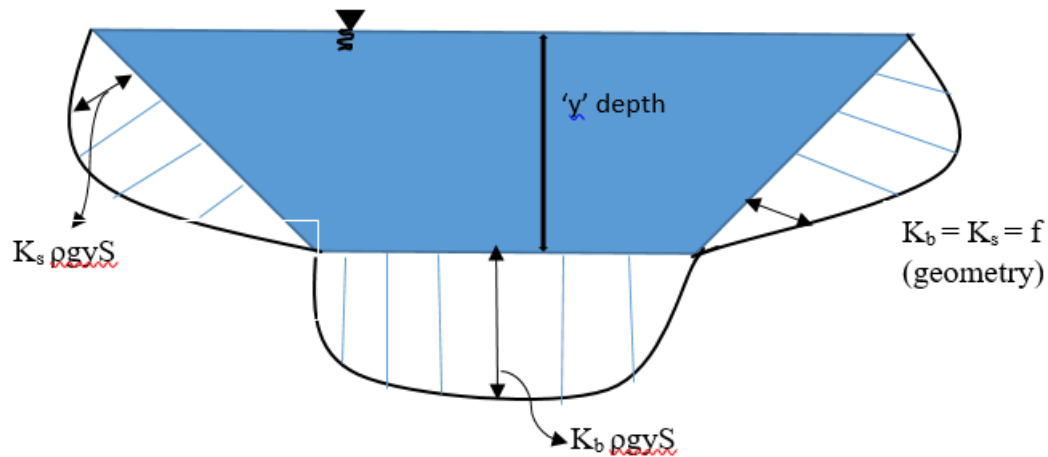
Figure 1 Shear stress distribution on the boundary of a trapezoidal channel

However, the variation of shear stress near wall and bottom is very different and thus may not be considered constant or equal to theoretical value. For example trapezoidal channel has shear stress distribution as shown in Fig. 1. The variation in the shear stress may vary with the bed width, side slope and even to the depth ratio. Similarly, the shear stress variation in the rectangular channel depends on the aspect ratio. Guo and Julien (2005) gave a graphical relation relating the average shear to ρgyS. Instead of using hydraulic radius flow depth is used since for wide channels, these would be almost identical.

Since we are generally concerned with the maximum shear stress at any point on bed or sides (e.g. to analyse the stability of a sediment particle), it is desirable to look at the maximum shear stress on the bed as well as sides (since the stability analyses for particles on sides and those on the channel are different). It is found that the maximum shear for the trapezoidal channel with side 2H:1V is around 75% of ρgyS on the sloping sides while it is almost ρgyS for the bed.

1.4 Stage discharge

The relationship within the water-surface stage (i.e. the water depth) and the coincident flow discharge in an open channel is known as stage-discharge relation or rating curve or just rating. This relationship is either empirical or theoretical which are can be used interchangeably since they are practically the same. The dependability on a rating curve as a tool is very high in surface hydrology since discharge data can be extrapolated from stage-discharge relationship at gauging station. However, the accuracy of this relationship is another concern. The formulation of rating curve is mostly dependent on the empiricism,

which necessitates an extensive theoretical background to establish a significantly accurate tool to compute discharge from measured flow depth. The wide applicability of the rating curve as a tool to estimate discharge in natural and/or artificial open channel and its extensive use in the field of hydrology makes it more demanding. Its application to the field of hydrology first came to knowledge in early XIX century where it was practiced to measure the discharge of a stream at suitable time using a current meter or other methods (Rantz 1982; ISO 1100-2, 1998). The corresponding stage is measured by regression or fitting the data set with power or exponential curve (see Fig. 2), a curve of the stage against discharge can then be useful to obtain the empirical equation depending upon the availability of data. One of the oldest methods of collecting current discharge data is to measure water level with gauges and then using the stage-discharge equation to estimate the flow discharge. The difficulty aroused during flood time is unrealistic for direct measurement of discharge in open channel in terms of risk of life, cost and time.

1.4.1 Hydraulics governing stage-discharge relationships

The stage-discharge relation in the open channel flow is dependent on the downstream condition from the gauge station. The channel conditions and characteristics understanding are very essential for the stage-discharge relationship and thus it is a very crucial component in developing rating curves. Three types of control are identified based on the channel and flow characteristics.

– A section control affects the low flow depths;

– A channel control affects the high flow depths;

 – Both types of flow controls affect the intermediate flow depths.

The sequence of section and channel control can occur at some stages. A section control is defined as the explicit cross-section of a channel, which is downstream from the gauge station having water level gauge regulating the relation between gauge height and discharge at the gauge. A section control such as rock ledge, a sand bar, a severe constriction in the channel, or an accumulation of debris can be identified as a natural feature section control. Similarly, a fabricated section control such as a small dam, a weir, a flume, or an overflow spillway is identified as the artificial section control. A pronounced drop of the water surface can be easily found in the field over section control, which signifies the meaning of control section itself, Fig. 3.
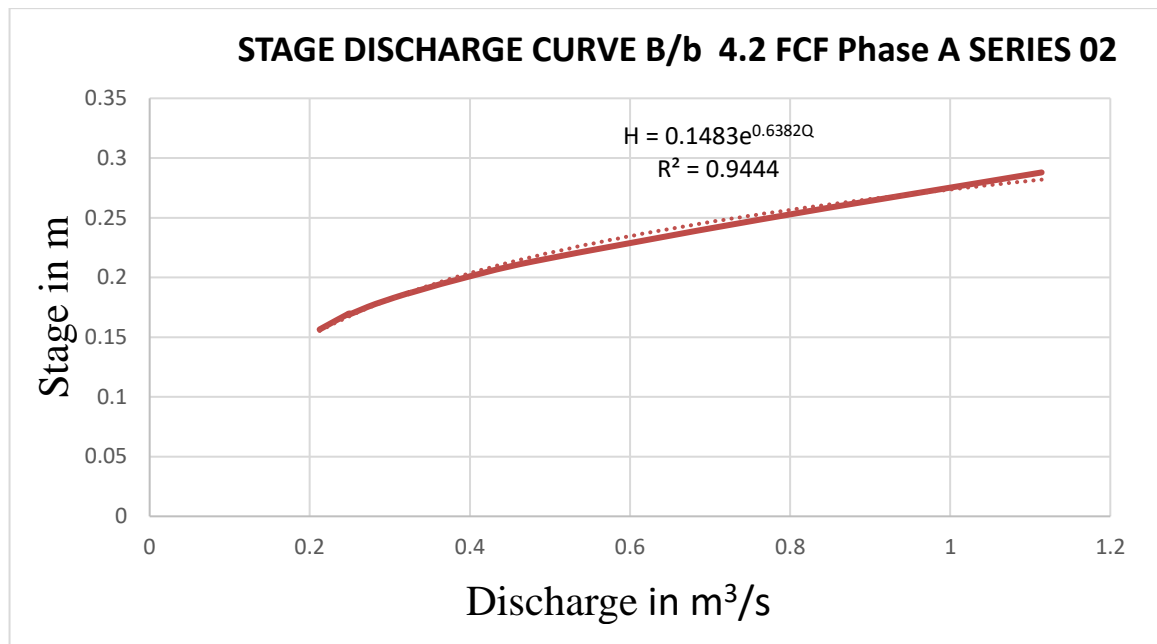
Figure 2 Stage Discharge Curve for B/b 4.2 Flood channel facility phase A series 02

Sometimes when the flow depth increase limitlessly these section controls get flooded and inundated in such a way that it no longer regulates the discharge in relation to the flow depth. At this particular instant, the drop is no longer visible, and flow either is controlled over another section control downstream or through the channel characteristics such as hydraulic geometry and the roughness of the channel downstream (i.e. channel control). A sequence of features throughout a reach downstream from a gauge is required in channel control. These features include channel size, shape, curvature, slope, and roughness. Dependency of the stage-discharge relation to the channel reach length can be extremely variable. A much longer reach is able to control the relation of the stage-discharge over the channel length of the flat or very milder channel, whereas very short channel reach may control the stage-discharge relation for the steeper channels. In addition, the magnitude of flow is also another parameter, which affects the length of channel control. The difficulty to define the length of a channel control reach is such a problem, which can be solved through numerical methods. As discussed above, the combination of the section and channel control are found in some of the specific stages, such as short range in stage between section-controlled and channel-controlled segments of the rating (Fig. 3). The development of stage-discharge curves where one control feature changes to another or combination of controls are possible or where number of measurement are handful, usually needs a wide understanding of the flow characteristics, in order to make a possible interpolation between measurements and extrapolation beyond respectively the lowest or highest measurements. This becomes

extremely reasonable where fluctuation of the controls is very high and have altered frequency time after time, resulting in a variation of the positioning of segments of the stage-discharge relation. The term transition zone is used where part of the resulting rating curve is regulated through both section and channel control. Both the controls acting simultaneously is usually a rare condition, though a combination control may be possible where each has a partial controlling effect. Plotting procedures are always used to identify the control and their behavior according to the stage-discharge relation. The characteristic of the transition zones, in particular, is distinguished through a change in slope or shape on the stage-discharge relation. The stage-discharge relationship for stable controls, such as fabricated structures are usually easy and have very less problem in terms of maintenance and calibration. For unstable controls problem arises in multiple when backwater occurs. In addition, segment of stage-discharge relation changes abruptly in unstable controls when severe flood or any other rare event occurs.
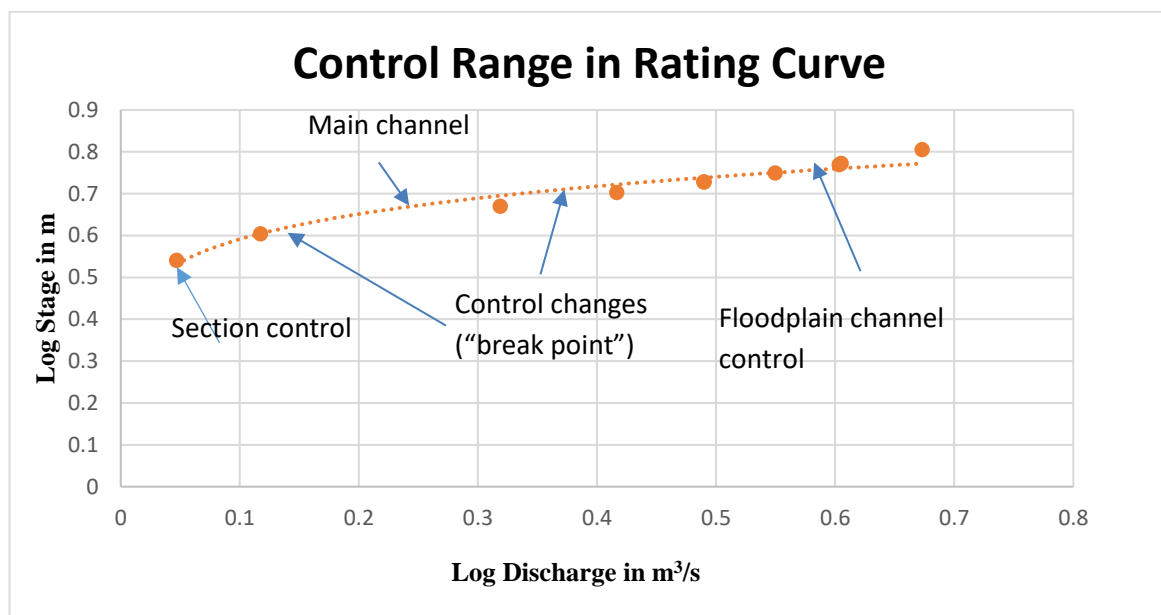
Figure 3 Schematic representation of controls range in rating curve

1.5 Flood hydrograph

The term hydrograph is a graphical representation of variation of discharge over a given period for a catchment area Fig. 4. It can also be stated as the response of a catchment area for a given input as rainfall intensity.

The total volume of water from a rainfall are not considered as a total input since the initial losses and the base flow (i.e. the flow through the ground water source) is excluded from

the volume and the remaining volume of water is denoted as the surface run-off or the quick response.
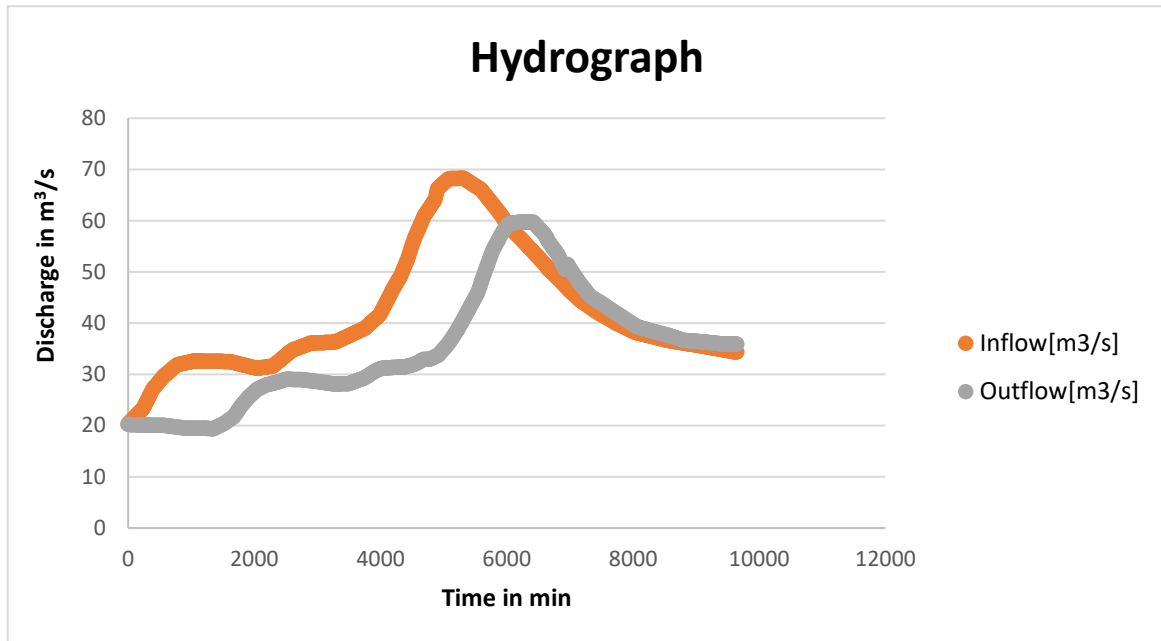
Figure 4 Hydrograph of inflow and outflow flood event 1994 River Brosna, Ireland

Iisrflow are also part of the quick response. As the name suggests the quick response are the volume of water that enters the stream immediately after the rainfall. As shown in the Fig. 5, a hydrograph has a rising limb, point of inflection, upper crest and then the recession limb. The characteristic of the curve shows the response of the catchment in a unique way where primarily during the rainfall the peak is built for over a period. The division of the
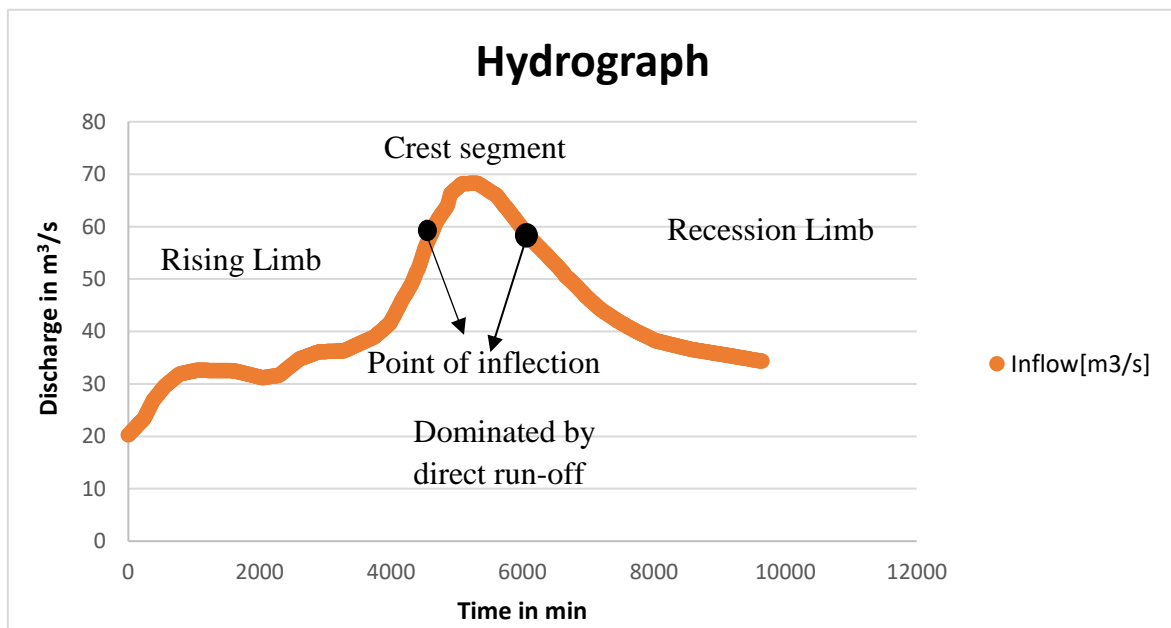
Figure 5 Hydrograph elements

base flow from the hydrograph is transitional and called as base flow separation, which have been proposed to distinguish surface run-off from the base flow.

1.5.1 Base flow separation

In many hydrographs analyses, a relationship between surface-flow hydrograph and the excess rainfall (i.e. rainfall minus losses) is sought to be established. The surface run-off hydrograph is obtained from the total run-off hydrograph through the technique called base flow separation. The graphical technique is established on locating the base flow recession points on the graph, which lies on the falling and the rising limb of the quick flow response. Another method called filtering techniques operate on the complete hydrograph data for obtaining the base flow hydrograph (Connected Water 2006).

1.5.2 Graphical separation method

Graphical techniques vary in complexity and they include:

- An empirical approach, which is based on the different parameters related to the characteristic of the catchment area Eq. 1.1. The basic idea behind this formulation is to find a point along the falling limb, which indicate the start of base flow recession on the curve.

  $D = 0.827 \ A^{0.2}$ (1.1)

  Where, D is the number of days between the storm crest and the end of the quick response flow and A is the catchment are in square Kilometres.

- The constant discharge method assumes that a constant discharge of base flow occurs throughout the storm hydrograph.

- The constant slope method is established on the link between the start of the rising limb and the point of inflection on the falling limb. This method assumes the instant base flow response to the rainfall event, hence it is more suitable for the topography where base flow dominant.

- The concave method considers the initial recession in the base flow during the rising limb by projecting the decrease in the hydrograph trend prior to rainfall event to directly to the line joining the centre of the crest line perpendicular to horizontal axis. This projection is then connected to the point of inflection on the falling limb of a storm hydrograph.

Han (2010) suggested the constant discharge method and the constant slope method because of their simplicity and wide applicability.

1.5.3 Filtering separation methods

Another method, which is also used, for the base flow separation is the data processing or filtering procedures. This method uses the automation index of the base flow response of the catchment area. The ratio of base flow to the total flow calculated from the storm hydrograph smoothing and separation procedure using daily discharge are called as a base flow index (BFI) or reliability index (Tallaksen and van Lanen 2004).

1.6 Flood routing

A mathematical method to calculate variations in the magnitude and celerity of a flood wave when it proliferates down the river or across the reservoir is called flood routing. As the flood wave moves downstream its peak and the whole shape of the flood wave transforms throughout the movement (Tewolde 2005).

Considering the storage effect of the reservoir, the peak of the outflow hydrograph always have less attenuation in comparison to the inflow hydrograph. This relative decrement in the peak of the two consecutive hydrograph is attenuation Fig. 6. In addition, there is a translation, which indicates the delay in time of the peak discharge Fig. 6 while delay in travel time of the water mass moving downstream is called as lag time (Heatherman 2008).
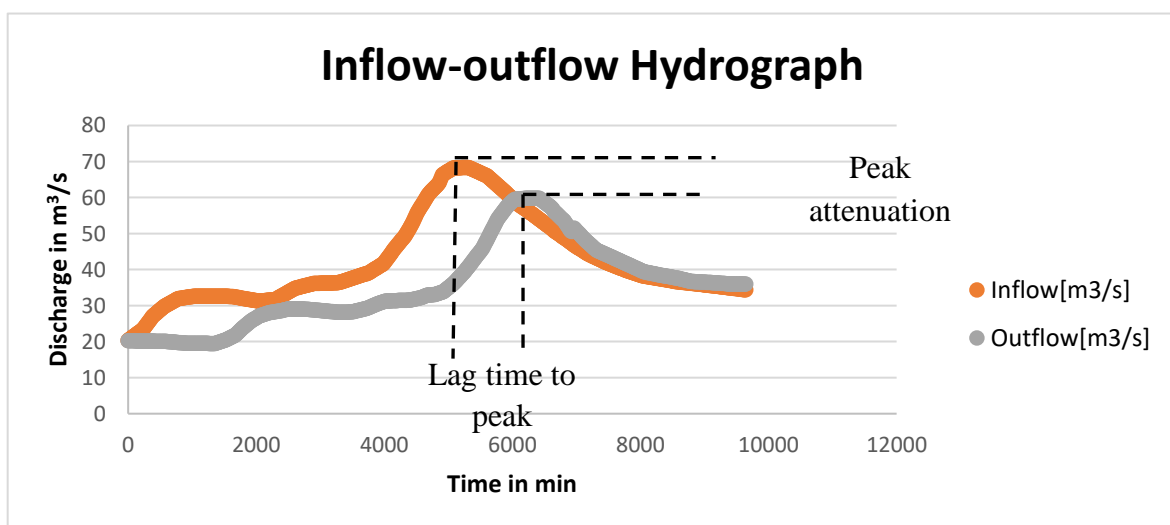
Figure 6 Flood routing hydrograph for natural river Brosna, Offaly, Ireland Elbashir (2011)

The inflow hydrograph is considered as the flow of water at the upstream while the outflow hydrograph is the consequence of the inflow hydrograph at the downstream section. Flood hydrograph can be broadly classified as the reservoir routing and the channel routing (Subramanya 2009). However, the main difference explicitly depends on the outflow hydrograph for both the type i.e. when determined over the spillway is called reservoir routing and when estimated over the river reach is called channel routing (Chadwick and Morfett 1993).

1.6.1 Kinematic, dynamic wave speed and Froude number

In numerous past studies, researchers suggested that the travelling of flood wave is explained by the wave 'celerity' (Heatherman 2008). In an open channel flow, the dynamic celerity 'c_d' is defined as the small disturbance or wave in the direction relative to the depth of the average velocity flow. To travel long enough wave must have low amplitude, long periods and negligible losses of energy.

$$c_d = \sqrt{gy} \quad \text{for wide rectangular channel} \tag{1.2}$$

$$c_d = \sqrt{gD_m} \quad \text{for channel in general} \tag{1.3}$$

Where, $D_m = A/T$ i.e. ratio of Area of the channel to the top width of the channel called hydraulic depth.

From the equation above, c_d is called as dynamic celerity and its unit is m/sec, g is the acceleration due to gravity m/sec^2, y is the depth of the flow in m, A is the area of the channel in m^2 and T is the top width of the channel in m.

The flow can be characterized by the dimensionless quantity called Froude number, which can be defined as the ratio of the average velocity 'V' of the flow to the dynamic celerity.

$$F_r = \frac{V}{\sqrt{gy}} \tag{1.4}$$

When the wave velocity surpasses the water velocity, the disturbance travel upstream and downstream, as well as the upstream depth of flow is affected by the downstream control. This case in particular is called as subcritical flow and the Froude number is less than one. In contrast to this when the flow velocity is more than the dynamic celerity than the supercritical flow is said to occur where Froude number is more than one and the disturbance now travel downstream only. The net possible case is when the velocity and dynamic

celerity is equal then the flow is called critical with Froude number equal to one (Chadwick and Morfett 1993).

Kinematic waves 'c$_k$' move with much lower velocities in contrast to the dynamic waves, which are characterized by quick attenuation, and higher velocities. Singh (1996) defined the Kinematic waves as the slope of the discharge-area rating curve. However, it can be estimated as the product of mean velocity and a factor called β. Table 1 shows the value for the factor β for various channel shapes.

Table 1 Factors for computing wave speed from average velocity (US Army Corps of Engineers, 2008

Channel shape	Factor $\beta = \frac{c_k}{V}$
Wide rectangular	1.67
Wide parabolic	1.44
Triangular	1.33
Natural channel	1.5

1.6.2 Distributed and lumped models

Commonly, the flood routing techniques are either lumped or distributed models. Lumped models consider complex parameters of flow behaviour between the upstream and downstream section of the channel. However, in the distributed models, more features of the flow behaviours are given at the points in between the reach located at the station from upstream to downstream section of the channel. Thus a model requiring lumped parameter are called hydrological routing, and flow routing through distributed parameter models is called hydraulic routing (Chin 2000).

1.6.2.1 Hydraulic method

When the flow computation is varied in both time and space (Mays and Tung 2002) then that type of flood routing technique is called hydraulic routing. Because of its computational ability over both space and time, this procedure is becoming popular for flood routing.

Hydraulic routing is exercised through the continuity equation as well as the momentum equation of motion of unsteady flow (Subramanya 2009) Eq. 1.5 and 1.6.

$$\frac{\partial A}{\partial t} + \frac{\partial Q}{\partial x} = 0 \tag{1.5}$$

$$S_f = S_o - \frac{\partial y}{\partial x} - \frac{v}{g}\frac{\partial v}{\partial x} - \frac{1}{g}\frac{\partial v}{\partial t} \tag{1.6}$$

Where t is time, x is the distance down the channel, y is depth of flow, v is the mean cross sectional velocity, A is the area, Q is discharge, g is the acceleration due to gravity, S_f is the frictional slope, S_o is the bed slope, $\frac{\partial y}{\partial x}$ is the longitudinal gradient of water profile, $\frac{v}{g}\frac{\partial v}{\partial x}$ is the convective acceleration slope and $\frac{1}{g}\frac{\partial v}{\partial t}$ is the local acceleration slope. The magnitude of other terms are usually very less as compared to the bed slope S_o.

This one dimensional continuity and momentum equation presented by the Barre de Saint-Venant (1871) are famously known as the St. Venant equations. Ignoring all other terms in the kinematic wave equation except pressure gradient term $\frac{\partial y}{\partial x}$, the diffusive wave equation becomes :

$$S_f = S_o - \frac{\partial y}{\partial x} \tag{1.7}$$

The pressure gradient term plays an important role in modelling the wave propagation and the storage effect within the channel for mild slope and steeply falling and rising hydrographs. Diffusive wave approximation equation simulates well, most of the flood wave travelling in the mild sloped river channels having some physical diffusion (Boroughs et al. 2002).

The full dynamic wave equation is those equations, which uses all the terms in the momentum equation. Its applicability is more often in the dam break analysis because it counters the backwater effects that other model neglect (Boroughs et al. 2002). The solution of such equations is more sophisticated, they use numerical modelling through high level computing techniques using implicit and explicit finite difference algorithm. Otherwise, it can be solved through the method of characteristics (Chin 2000). Other than this modelling techniques, one can also go for software packages which simulate momentum equation through different numerical schemes, commonly used are one dimensional HEC-RAS (Hydraulic Engineering Centre's- River Analysis System) or MIKE 11 (DHI) to perform steady and unsteady flow river hydraulics calculations.

The demerits related to such model is the complexity of the model solution, problem of convergence and it often leads to the numerical unstable solution. Such model also requires costly computational resources and computation time. Other simplified methods were improved to assist the computation, generally hydrological method that is easy, requires low computational resources and less time consuming (Johnson 1999).

1.6.2.2 Hydrological methods

The basis of continuity equation i.e. the mass balance of inflow, outflow and the volume of storage remain conserved is used in hydrological methods for channel routing. This method of channel routing requires storage-stage-discharge behaviour to establish the outflow for each time step (Guo 2006). Hydrological method considers mathematical practices that initiate translation or attenuation to an inflow hydrograph (Heatherman 2008).

The equation presented below is continuity equation Eq. 1.8:

$$\frac{dS}{dt} = I_{(t)} - O_{(t)} \tag{1.8}$$

where S is the storage between upstream and downstream in m^3, t is the time in s and $I_{(t)}$ and $O_{(t)}$ are the inflow at upstream and outflow at downstream respectively in m^3/s.

Over the finite interval of time between t and t+Δt Eq. (7) can be written in finite difference form as:

$$\frac{S_1 - S_2}{\Delta t} = \frac{I_1 + I_2}{2} - \frac{O_1 + O_2}{2} \tag{1.9}$$

where subscripts 1 and 2 refers to two consecutive times t and t+Δt respectively (Chin 2000).

A hydrological method, which initiates with continuity equation and comprises the dispersion form of the momentum equation, known as the MC (Johnson 1999) is used here for flood routing of Brosna River Offaly, Ireland (Elbashir 2011). The derivation and application of this method are discussed in further chapters.

1.6   Aim and Objectives

This research program has been pursued with the following principal aims:

- To study modelling techniques based on the Lateral discharge method using Reynolds Averaged Navier-Stokes Equation (RANSE) model for the computation of Stage discharge.
- To study the effects of secondary flow in compound channels through calibration coefficient Γ and k which was given by Shiono and Knight (1991) and Ervine et al. (2000).
- To analyse the lateral variation of depth averaged velocity and boundary shear stress at different relative depths for compound channels.
- To substantiate the analytical solution results produced by four different methods with/without secondary flow term by means of a numerical method called K-ϵ (standard eddy viscosity model using ANSYS-Fluent).
- To study the application of hydrological flood routing technique using the constant variable MC method for a river Brosna Offaly.
- To examine the steady state and mass conservation condition of the constant parameter MC method using mass balance equation and storage equation based on prism and wedge storage principle.

Apart from the principal aims, following sub objectives can be enumerated as below:

- To analyze the depth averaged velocity distribution and the boundary shear stress distribution curves for non prismatic compound channels with a B/b ratio of 2.2 for three different relative depths as 0.100, 0.245 and 0.500.
- To analyze the depth averaged velocity distribution and the boundary shear stress distribution curves for non prismatic compound channels with a B/b ratio of 4.2 for three different relative depths as 0.111, 0.242 and 0.479.
- To validate the results for analytical and numerical solution using percentage error analysis for each relative depth.
- To validate the stage discharge curve using the data presented in the FCF phase A series 02 and 03 (www.flowdata.bham.ac.uk).
- To analyze the stage hydrograph plot for 8 Km reach of river Brosna Offaly taken from Elbashir (2011).

- To validate the results obtained from the constant parameter MC method with the two software packages, namely HEC-RAS (US Army Corps) and MIKE 11 (DHI).

1.7 ORGANISATION OF THE THESIS

This thesis has been organized into six chapters, including Introduction. **Chapter 1** is the 'INTRODUCTION', which contributes a concise background of the rating curves, flood routing terminologies and aims & objectives of the present study undertaken.

Chapter 2 contains a brief appraisal of literature on compound river sections. All these subjects are considered in two different sections. The first section is about the different modelling techniques for depth-averaged velocity distribution, boundary shear stress distributions and stage discharge curve for compound channels. The second section is about different approaches of flood routing.

Chapter 3 describes the theoretical background of different modelling techniques and the important parameters related to them.

Chapter 4 deals with the results and discussions of the SKM with/without secondary flow term, K-method, extended SKM and K-ϵ model. It presents the results of depth averaged velocity distribution, boundary shear stress distribution and stage discharge curve for the two compound channel. In the next section, flood routing results are illustrated through the validation of the hydrologic routing technique (i.e. MC method) with the two software packages. Beside this water storage, analysis is done for the outflow hydrographs obtained.

Chapter 5 is error analysis, which compares the predicted depth averaged velocity with the measured depth-averaged velocity. Error analysis is also done to illustrate the contrast among all the contending models against extensive experimental datasets for ascertaining the efficiency of different models. The relative percentage error analysis is done in which the relative percentage error is plotted against the cross sectional lateral position. For outflow flood-hydrograph water conservation analysis is done and represented in the table.

In **Chapter 6** some conclusions and scope for future work are drawn from the results obtained for the compound channels. The chapter also illustrates the scope of this study for the field engineers and for the future studies.

Chapter 2

LITERATURE REVIEW

2.1 Stage Discharge, velocity distribution and boundary shear stress

In the past several years, many attempts had been made in terms of mathematical modelling to predict the structure of turbulence in a compound channel incorporating the mass and momentum transfer over the interface region. A number of numerical models as that of Keller and Rodi (1988), Pasche et al. (1985), and the 3D algebraic stress model of Krishnappan and Lau (1986) has been undertaken along with many experimental work coming in between from Myers (1978) Rajaratnam and Ahmadi (1981), Knight and Demetriou (1983), Tominaga et al. (1989), Knight, and Abril (1996), and Knight (2006) in order to understand the structure of the flow. A number of empirical formulas are available in literature for the prediction of stage-discharge, velocity distribution and boundary shear stress but the dynamicity of such equation is very limited to very few channels or specific type of channel itself.

However, despite this progress an analytical solution for a compound channel, which will give depth-averaged velocity, boundary shear stress distribution in the transverse direction; together with the stage-discharge curve, has been given by different researchers such as Shiono and Knight (1988 and1991), Ervine et al (2000), Abril and Knight (2004), Omran (2008) Tang and Knight (2009) and Kordi et al. (2015).

Shiono and Knight (1988) gave an analytical solution based on the depth average eddy viscosity approach and momentum equation. The analytical solution is applied to steady and uniform flow in a compound channel and the results displayed confirms the capability of the model for the calculation of certain features of the flow sufficiently accurately for engineering design purposes.

Tominaga et al. (1989) shows that the secondary current produced and transformed due to anisotropy of turbulence, which results from the boundary conditions of the bed, the side wall and the free surfaces, as well as the aspect ratio of the channel and the channel

geometry. The three dimensional structure formed due to the coherent structures modifies the primary mean flow. The longitudinal vorticity equation explains and forms the basis of such a secondary current mechanism in closed and gravity flow. The measurement of coherent flow structure is necessary to understand 3D flow structure, but since the velocity of the secondary current is within a few percent of main channel flow it becomes difficult to measure them. The secondary current structure are very different in pressure and gravity flow. In an open channel flow free surface vortex and the bottom surface vortex are separated and forms the main reason in the dip of maximum velocity position and deceleration of mean velocity near surface. The secondary flow structure in rectangular channel are very much different from the secondary flow structure formed in trapezoidal channel.

Shiono and Knight (1991) again came up with the analytical solution but this time they have considered the secondary flow current denoted by Γ. The calibration of coefficient of viscosity λ, friction factor f and secondary current Γ has been done for the Flood Channel Facility FCF series 01-03 i.e. two stage trapezoidal channel. For the case of overbank flow, the experimental data from the FCF have provided comparable details for the 3D flow structures incorporated into the 2D analytical model through parametrization. The only realistic way of determining the depth-averaged secondary flow term has been shown through magnitude of boundary shear stresses and Reynolds stresses. The comparative intensity of secondary term and its impact on the lateral dissemination of the shear layer, have been shown to be unrelated of the relative depth, $D_r (= (H-h)/H)$. In two-stage channels the point friction factors, $f (=8\tau_b/(\rho U_d^2)$ are nearly uniform, but differ from main channel to floodplain due to varying depth. Dimensionless eddy-viscosity values λ, have been obtained through apparent shear stress, and depth averaged Reynolds stresses. Generally, coefficient of eddy-viscosity is taken as constant in overbank flow but in inbank flow consideration, it plays significant role.

Knight and Abril (1996) presented a philosophy for calibration of a river model through numerical simulation for overbank flow using three coefficients related to local friction factors, eddy viscosities and secondary flow. The numerical simulations of the lateral distributions of depth-mean velocity, boundary and Reynolds shear stresses give some useful insight into the calibration philosophy. The calibration philosophy of the model is found to be sensitive to friction factor f and secondary flow term Γ values, particularly regarding their main channel and floodplain. On the other hand, it has been also shown that

insensitivity to dimensionless eddy viscosity λ ratios, wherein even constant values across the section may give satisfactory results.

Ervine et al. (2000) gave new model by rearranging the terms in lateral gradient of $H(\rho UV)_d$ also called as secondary flow term. They also considered the effect of transverse velocity by considering the ratio of longitudinal and transverse velocity as a new constant k and replacing in the secondary flow term. This constraint k predominantly comprises the secondary cells and their intensity in the two-stage channel. They also showed that the value of k < 0.5% for straight compound channel flows and 2% k < 5% for meandering compound flows at least at the apex cross section. The model proposed has the plus point of being applicable to both straight and meandering two-stage channels by accepting an suitable value of k.

Abril and Knight (2004) gave a finite element model for depth-averaged turbulent flow using three hydraulic constraints governing local bed friction, lateral eddy viscosity and depth-averaged secondary flow for prediction of the rating curve relationship for inundating river. The subsequent lateral distribution of depth-averaged velocity are then integrated to give stage-discharge relationship. The comparison of the river flow model using finite element method with the coherence model of Ackers (1991 1992) in two study cases with homogeneous and heterogeneous roughness distribution helped to develop a calibration approach. It is also observed that from comparison of both models and experimental FCF data with homogeneous roughness, the coherence model yields inaccurate results in the prediction, which can be easily improved by using a higher value of the secondary flow term at low relative depths.

Knight et al. (2007) modelled depth-averaged velocity and boundary shear stress in trapezoidal channels with secondary flows incorporating some key 3D flow features into a lateral distribution model for streamwise motion. They suggested that the SKM is based on using a constant value of secondary flow term Γ, commensurate with the lateral gradient of term $H (\rho UV)_d$ and therefore each time sense of the secondary flow term Γ changes, an additional panel is required. Therefore, separate four panels are essential for modelling secondary current flows in symmetric half of a simple trapezoidal channel. Aspect ratio b/H plays a significant role in determining the number of secondary flow cells. Although, accurate depth-averaged velocity distribution prediction, the corresponding boundary shear

stress does not always match the experimental data due to poor modelling of secondary current cells.

Omran (2008) justified that the SKM can account for 3D flow in simple and two-stage channels, is an easy method to program and can produce useful information required by river engineers, such as the stage-discharge relationship and lateral distribution of depth-averaged velocity and boundary shear stress. He also depicted that the accurate prediction of depth-averaged velocity not necessarily obtain the corresponding predicted boundary shear stress as precise as experimental data mainly due to poor modelling of the secondary current cells. The advantage such analytical model is that when no experimental data are available for the ungauged reach, the user can still model the reach through just allocating the roughness value because λ and Γ are automatically determined across the channel via sense of semi-empirical equations.

Tang and Knight (2008) showed the application of the analytical solution to the depth-integrated Reynolds-averaged Navier-Stokes equation with an extra term encompassed to counter the effect of drag due to vegetation. An additional term drag force is used in the momentum equation to model the problem involving vegetation. The approach embraces the effects of bed friction, drag force, lateral turbulence and secondary flow via four coefficients f, C_D, λ, Γ respectively. The new analytical scheme applied to the lateral dissemination of streamwise depth-averaged velocity in a vegetated channel has been employed to symmetric two-stage channel with fractional roughness at the floodplain/ main channel edge, i.e. a single line of trees. It is illustrated in their work that the density of the vegetation affects the shear layer formation over the vegetated and non-vegetated region. In fact, a strong shear layer is generated over the rough surface and the transfer of momentum over interface enhances due to high density of vegetation.

Tang and Knight (2009) presented different analytical models of the depth-averaged Navier-Stokes equations applied to the gravity flow and validated those results with the experimental datasets. The models developed by Shiono and Knight (1988, 1991) are contrasted with those by Ervine et al. (2000) and Castanedo et al. (2005) by means of mathematical experiments on both simple and two-stage channels. All the three analytical solution are similar and approximately similar since they contain similar hydraulic constraints signifying boundary resistance via the bed friction factor f, lateral shear via dimensionless eddy viscosity λ, and the depth-averaged secondary flow via parameter Γ or

K. They also demonstrated the significance of the secondary flow term by comparing results of those models where secondary flow term are not considered with the experimental data. The shortcomings with the assumptions of K model are also discussed. The coefficient K is arguably considered always positive even though the K-value can be either positive or negative, contingent on the rotation of secondary cell. The extended λ method with Γ included, produced reasonably good results even though this model is found sensitive to λ-values.

Omran and Knight (2010) modelled the boundary shear stress distribution using depth-averaged Shiono Knight Method and shown that the poor modelling of secondary flow leads to the inaccurate results. To improve modelling by capturing the secondary current cell effects were analysed through the perturbation in experimental boundary shear stress dissemination. They indicated the poor modelling of the secondary flow term to be an important shortcoming in the prediction of boundary shear stress. The perturbation of the boundary shear stress distribution trend is visible in the aspect ratio larger than one, which in turn can be used as to decide the number, position and rotational direction of secondary current cells. They suggested that in rectangular channel, half the channel counted for modelling should be distributed into four panels to counter the effects of secondary current cells.

Azevedo et al. (2012) used the 2D Laser Doppler Velocimeter in an experimental compound channel to obtain the streamwise and vertical velocity component. They showed that the 3D behaviour of the flow is more noticeable. The results obtained are examined by comparing with the universal laws drawn for isotropic turbulent 2D fully developed open channel flow. They showed that the validity of the universal laws for 2D fully developed open channel flows in the upper interface and floodplain, although the coefficient has to be increased due to increase in turbulent intensity. The non-validity of the universal law in the lower interface or the main channel is mostly due to the strong secondary currents even if their coefficients are changed.

Al-Khatib et al. (2012) used the separate channel division methods in asymmetric two-stage channels with erratic floodplain widths and step heights. Three different interfaces, namely horizontal, vertical and diagonal is selected between the main channel and floodplain subsection. Then the discharge value in each subsection is evaluated in every interfaces together with the whole cross section. From the experimental results, it is observed remarked

that, none of the distinct channel approaches used assessed the calculated discharges correctly for the different ratio of depths in floodplain to main channel.

Zeng et al. (2012) presented different approaches to quantify the friction factor f and eddy viscosity coefficient λ for the application of the analytical solution and to improve the accuracy of the prediction of the lateral depth-averaged velocity in the trapezoidal compound channel flow. In their results, it is quite evident that the friction factor affects the accuracy of the solution. The coefficient of the eddy viscosity can be determined empirically since the precision of the solution has been less dependent on the effects of dimensionless eddy viscosity. Over the interface zone the difficulties to simulate the turbulent flow characteristics multiplies. The main cause of such challenging simulation is the discontinuity of the parameters especially in the interface zone and the channels is divided into different panels considering the cross section of the geometry rather than the internal structure of the turbulence.

Conway et al. (2012) offered a better technique for operating 3D computational fluid dynamics models to guesstimate the stage discharge and velocity distribution of straight open channel flow. In their approach, they used eddy viscosity k-ϵ turbulence closure model since in commonly used analytical solution model the coefficients are calculated through empiricism and vary with different flow conditions. The momentum transfer over the interface may or may not be taken into account, which potentially overestimate the conveyance capacity of the compound channels. The proposed approach is based on inputting (rather than calibrating) physically realistic resistance value and iteratively adjusting the downstream water depths until uniform flow conditions within a specified tolerance are established. They also suggested that the increase in relative depth of flow increases the momentum transfer due to difference in flow depth and velocity in the main channel and floodplain, which in turn over predict the flow ratio. Also, increasing depth increases the overestimation, which is more pronounced in roughened floodplain case.

Liu et al. (2013) presented an approach to model the depth-averaged velocity and boundary shear stress in a submerged and emerged both types of vegetation. In their study, they calibrated an extra coefficient to tackle the drag force due to the vegetation called coefficient of drag C_d. The analytical solution for the transverse variation of depth-averaged velocity is presented through the Shiono Knight Method (1991). Beside the calculation of an extra coefficient, secondary flow cells and eddy viscosity terms are also analysed and their effects

on the solution for the compound channel is presented. For dealing with the secondary flow term, the modified equation of Ervine et al. (2000) model is considered where coefficient K is taken into account. In their study, the most significant factor in the modelling approach is found to be secondary flow parameter K and also its sign, absolute value being determined by the rotational direction and the intensity of secondary flow cell plays an important role.

Jesson et al. (2013) examined a heterogeneous roughed bed in open channel flow through physical and numerical simulation. Depth-averaged velocity and boundary shear stress are experimentally calculated at four different cross sections by acoustic Doppler velocimeter and Preston tube technique respectively. The roughness aspects governs the behaviour of the flow and act as the source of vorticity, which is primarily established as local boundary shear stress and, in turn, affects imitates the momentum transfer and secondary flow in the channel. The flow field adjusts relatively quickly to the boundary roughness. The dissemination of vertical Reynolds stress is complicated and take longer to adjust over the change in boundary roughness unlike streamwise velocity component. Large fluctuation in the eddy viscosity model can be observed in the numerical simulation for the rough boundary conditions.

Yang et al. (2013) used the depth-averaged equation in a rectangular channel derived using the Newton's second law established on an elemental water body. The analytical solution of the lateral variation of the depth-averaged equation is used which comprises the consequences of lateral momentum transfer and secondary flow in supplement to bed friction. The result shows the significance of the parameters used in the analytical solution and their influence together with boundary conditions used. The friction factor f in each subarea is estimated through the Colebrook-White equation and for a known geometry; secondary flow coefficient Γ may be contemplated as uniform for various relative depths, but varies from the main channel and the floodplain respectively. The momentum transfer effects are prior and influencing in the shear layer region and may be practically overlooked outside the shear layer region.

Chao et al. (2013) conducted the experiments in the compound channel with vegetated floodplains for the investigation of the secondary flow characteristics. The variation in the vegetation in terms of size and shape changes the direction of rotation in the whole cross section. Meanwhile the intensities of the secondary flow current in the floodplain are stronger in comparison to the main channel when the flow depth is less. In the higher flow

depth, intensity of the secondary flow decreases rapidly in the floodplain; however, those in main channel are almost the same and keep weak.

Knight (2013) developed the integrating mathematical modelling with experimental work both in the field and in laboratory and exemplified through the development of a software tool that deals with the primary practical issues related to rivers in flood. He emphasized the practical issues in obtaining data and the theoretical problems in identifying relevant flow parameters for streamwise and planform vorticity, turbulence shear stresses and frictional resistance. He also highlighted the concern regarding the conversion of the data to the theory (or vice-versa), then to practical application, are desired in general terms, beginning with how to develop models as a research tool, testing it against different data sets, through to using the model in practice with the embedded tools.

Liu et al. (2014) established the principal equation of discharge per unit width from continuity equation and momentum equation. The analytical solution of the equation derived, including the effects of bed friction, lateral momentum transfer, drag force, and secondary flows. A simple method for estimated solution of the sub-area discharge and the total discharge is presented. Different coefficients are calculated and their sensitivity in the solution is analysed. They stated that the effects of secondary flow cannot be ignored during calculation and their sensitivity varies from floodplain to main channel differently in vegetation and non-vegetation floodplain.

Proust et al. (2015) studied the turbulent non-uniform flows experimentally in compound channels, with vertical and sloping banks in the main channels. An advective transport of momentum and time-averaged transverse flow occurred until the downstream measuring section. The variation in the water depth reaches equilibrium much more easily than the variation in the velocity distribution between the sub-sections. They demonstrated that the depth-averaged Reynolds stresses rises in expense of the depth-averaged value of apparent shear stress and the lateral Reynolds stresses at floodplain edge and in the main channel. The shear layer turbulence and the flux of depth-averaged Reynolds shear stress are superior by the sloping bank relative to the vertical bank. They have also shown that the dispersive term of spanwise velocity can also be of the same order of magnitude as depth-averaged Reynolds stress $-\rho U_d V_d$ and is dependent on the flow direction. Therefore, 2D depth-averaged model does not account for the vertical dispersion of the velocity may reproduce poorly the actual transverse momentum flux.

Parsaie and Haghiabi (2015) presented the stage-discharge relationship for two-stage channel flow using single channel method, divided channel method, modified divided channel method, and contrasted together with the experimental data. The results for all the empirical methods are same when discharge flows in the main channel, whereas by increasing the discharge and covering the floodplains the results of the different models are different. The effects of momentum and energy correction factor have significant effects on distribution of Froude number and specific energy. The non-uniformity of the flow and velocity distribution increases with the flow depth.

Fernandes et al. (2015) improvised the 1D predictors of stage-discharge curves in two-stage channel. The authors used seven different models and validated with experimental datasets. The models used are traditional single and divided channel method along with the Debord method, coherence method, weighted divided channel method, apparent shear stress method and the exchange discharge method. They concluded that the models, which accounts for the momentum transfer over the interface area produces substantially superior results than the conventional approaches. For higher relative depths, predicted discharges for the model, which count turbulent exchange, are very close to the observed value. In their conclusions, they suggested that the exchange discharge models might be used for symmetric configuration while coherence models are more appropriate for the asymmetrical channels.

Kordi et al. (2015) proposed a new model considering both the dispersion and the transverse convection component. The coefficients quantifying secondary flow terms are calibrated and quantified for the distinct lateral sections, expressed based on the perturbation in dissemination of depth-averaged velocity and boundary shear stress distribution. The poor modelling of the secondary flow cells in SKM (Shiono and Knight 1991) and Ervine et al (2000) K method has ascribed the imprecision in calculation of lateral depth-averaged velocity, particularly adjoining the boundary region. To enhance the depth-averaged velocity calculation, the secondary flow term is expressed as the function of the bed shear stress ($\rho g h S_o$) and the depth averaged streamwise velocity (U_d). The improved SKM method is validated for the natural asymmetrical homogeneous and non-homogeneous boundary condition where it is found that the new method does exceptionally well in both the cases and improved the evaluation of the depth-averaged velocity with average relative error of 5% over the boundary region between the main channel and floodplain area.

2.2 Flood hydrograph and flood routing

McCarthy (1938, 1940) proposed a model originally called as a hydrological flood routing model, which eventually gained wide recognition under the name of Muskingum approach. The hydrological routing is the method, which is parametrised in such a way that the outflow is derived as function of inflow for a particular reach of the channel while considering the lumped number of parameter characterizing geomorphological and hydraulic properties.

Nash (1958) used the cascade model of linear reservoir to derive the instantaneous unit hydrograph. The catchment is assumed to be divided as number identical sub-reservoir each having same storage constant. The output of the first reservoir is considered as the input for the second reservoir and so on. The conceptual cascade of the reservoirs is used to obtain the shape of the outflow hydrograph from each reservoir of the cascade. The outflow hydrograph of the nth reservoir is considered as the instantaneous unit hydrograph of the catchment.

Kalinin and Miljukov (1958) presented the applicability of the cascading non linear reservoir method of the Nash (1958) and later, Liu and Todini (2002, 2004) developed TOPKAPI hydrological model using the cascade of linear reservoir model.

Cunge (1969) continued the extension of Muskingum method to time variable parameters whose value can be obtained as the function of the reference discharge. Cunge in 1969 established the Muskingum method as the first order kinematic approximation of a diffusion wave model. By parabolic approach for the estimation of the parameters, Cunge (1969) took the method one-step ahead. This approximation guaranteed the real diffusion equal to the numerical diffusion.

Chow (1964) and Chow et al. (1988) pointed that the original initial derivation presumes that the prior origin of the Muskingum routing technique is that the storage consist both the "prism' level pool storage and the "wedge" storage that counters the imbalance between the inflow and the outflow. Rather, they suggested that the model could be more profoundly seen as the two parameters "lumped" model at the river reach scale, the storage of which can be expressed at any point in time.

Tang et al. (1999) and Tang and Samuels (1999) and numerous other researchers pointed out the shortcoming of the widely used Muskingum method that the method compromises

the mass balance that to reach the values of 8-10%. Although many researcher (Ponce and Yevjevich, 1978; Koussis, 1983; Ponce and Chaganti, 1994; Perumal et al., 2001) have worked on this problem and tried to solve the inconsistency of the mass balance, a decisive and substantial logic was never confirmed.

Beside the wide applicability of the Muskingum Cunge approach, it is also utilised as the routing element in different disseminated and semi-disseminated hydrological models, in which case the conservation of the mass balance is an indispensable attribute. Furthermore, numerous software packages are accessible today to solve the full Saint Venant equations like Stelling and Duinmeijer (2003) and Stelling and Verwey (2005) SOBEK, MIKE 11-DHI Water & Environment (2000), HEC-RAS- US Army Corps of Engineers (2005) and many others. The lack of data of the river reach and cross-section make Muskingum Cunge method more applicable by disregarding the practise of more complicated routing methods. Another reason for its use is that it can be certainly coded at virtually no cost.

Perumal et al. (2007) came up with a new model called variable parameter Muskingum stage hydrographs routing technique for the elaboration of the standard rating curves at an ungauged river location. In their model, stage is used as the routing variable, and this can be justified by the sensitivity of the stage variable with respect to the local variation of the cross sectional flow area of the river reach. This model encompasses a technique to evaluate quantitatively the corresponding prismatic channel section of the reach employing two bounded natural channel cross sections of the reach.

Todini (2007) presented a new model based on the Muskingum Cunge method since several variable parameter Muskingum Cunge flood routing method, mutually with numerous modifications suggested in the literature, does not completely conserve the mass balance, mostly in the mild slopes. Furthermore, he showed that beside the inconsistency of the mas balance another important inconsistency of different variable parameter methods are that the storage inconsistency. If one substitutes back into the Muskingum equations, the parameters derived using Cunge approach, two different and inconsistent values for the water volume stored in the channel is obtained. The effect of pressure term is also tested for the new model, which improved the model dynamics when compared to the solution of full Saint Venant equations, without any adverse effects on the mass balance and compliance with the Muskingum equations. He also claimed that his proposed method would also be

useful for routing waves in channel as well as natural channels with bed slope of range 10^{-3} to 10^{-4} where the flood crest subsidence is one of the dominant phenomena.

Perumal et al. (2009) analysed the multilinear stage-hydrograph routing grounded on the time dissemination system. The nonlinear dynamics of the flood wave transmission by adjusting the model constraints at every routing time step are implicitly solved in the proposed method. The proposed model is verified by the experimental datasets and even in the Tiber River of central Italy. The outline of the proposed model is based on the Muskingum-type routing method, which is used as a linear sub model. The input stage hydrograph is divided into block of constant duration equal to the routing time interval, each of which is routed by Muskingum sub model. The form of the input stage hydrograph is considered as the series of pulses (uniform blocks of duration) and the routed output by this model is sampled at discrete time intervals. The model gave good results and conveniently applied to the real world flood routing problem. The stage-hydrograph produced for the purpose of flood forecasting is reliable when applied to the prismatic section and to the automatic operations of canals.

Perumal et al. (2010) presented a method for accuracy enhancement of the variable Muskingum stage hydrograph routing technique suggested by the Perumal et al. (2007) for rating curve prediction of the ungauged river sites having irregular section. The method enhanced for routing the prismatic channel reaches are used for the application to a natural river reach. It involves rough calculation of the real river reach section at the extreme ends of the reach to an comparable prismatic section with one-to-one correlation recognised among water level of the real section of a given flow area with the corresponding water level of the prismatic channel section of the same flow area. It is conclude from the analysis that the technique of determining the comparable prismatic channel section for a given river reach using real channel section and vice-versa are conveniently applicable method for the flood routing method.

Perumal and Price (2013) presented the hydraulic derivation of a fully conservative, variable parameter MaCarthy Muskingum method derived from the full Saint Venant equation for routing flood wave in prismatic channel using Manning's friction law. The model justified the heuristic assumption of the MaCarthy (1938) theoretically, in which he expressed storage as the prism (i.e. level pool storage) and the wedge storage. The approach used in the model also fulfil the conservation of mass problem which is associated with variable

parameter Muskingum routing method, which has been major issue in past three decades. The model exhibited is used to obtain the stage-hydrograph corresponding to a given inflow or routed discharge hydrograph. In the model the parameter travel time is derived in a same way that of Todini (2007) and Price (2009), but the parameter weighting factor is different from that of Todini (2007) and Price (2009) method. They validated their model with Todini (2009) model with and without using; the diffusion correction advocated by the Cappelaere (1997). The results reveal that the proposed model provides better insight into the rationale behind the Muskingum method, and additionally it enables the stage hydrograph corresponding to the routed discharge hydrograph.

Bhabagrahi et al. (2014) presented the application of the simplified discharge routing method and estimated the stage-hydrograph simultaneously in channel with floodplains. They showed that the performance of the variable parameter of Muskingum discharge hydrograph model and its capability of accurately routing the discharge hydrograph, corresponding stage hydrograph and synthesizing the normal rating curves at the downstream of ungauged river site which is not affected by the downstream effect. They also suggested that the variable parameter of Muskingum discharge hydrograph model should not be used for very mid slopes, which are subjected to backwater effects. This model is best used when no lateral inflow is considered in the river reach. Their study can be used as the base for the planning and management of river water resources in both the diagnostic and prognostic modes, which can be incorporated in the meso- and macro- scale basin models, and land surface schemes of the climate change models.

2.3 Critical Review

There are number of past studies regarding the flow modelling for both inbank and outbank flows, but these tend to examine flow where secondary flow terms are either neglected or included beside considering the computational time and resource requirement to model the flow. Bousmar and Zech (1999) showed that the models where secondary flow terms are not included there overestimation of depth averaged velocity is very common and thus significant modelling of these coherent structures plays a vital role for the prediction. In this study, total five methods are used to justify the importance of the parameters like secondary flow term and mass transfer effect over the interface region which when ignored, affect the results adversely. Again, computational resources required for the analytical solution of RANSE model is comparably very less and robust for field engineers. Review of past

researchers model are done together with the analysis of the effects of secondary flow terms given by Shiono and Knigth (1989, 1991), Ervine et al. (2000), and Kordi et al. (2015) model. Using k-ϵ model gives an extra edge to compare the numerical model with the analytical model solution technique and also validates the computational resource and time required by these two different approaches.

Later half of the study aims at the stage hydrograph and flood routing techniques by constant parameter MC method. Todini (2007) showed that the loss of mass identified by many researchers and authors are very common in this method. However, no one seems to estimate the storage in the reach using two equations derived through the mass balance equation and storage equation given by heuristic assumption of prism and wedge storage by McCarthy (1938).

Chapter 3

THEORETICAL BACKGROUND

3.1   Introduction

This chapter aims to give an outline of the previous study done in the field of open channel hydraulics. A review of the flow features and energy transfer mechanisms is specified with the evaluation of different modelling techniques.

3.2   Flow mechanism

It is fundamental to comprehend the flow behaviour and physics related to it before engaging in any type of modelling either it can be analytical or numerical. The structure of flow affects the velocity distribution, boundary shear stress, resistance of flow and therefore the total conveyance (Knight 2001).

The structure of flow can be classed as the energy transfer mechanisms which cascade energy from one form to another via growth of eddies over different length scale and time scale (Kolmogarov 1942). Vortices can be created due to the turbulence over the boundary shear, vertical and horizontal interface shear, transverse current and coherent structures. Beside that, it can be also created from the geometry of the channel, depth of flow and the nature of flow. (Tominaga et al.1989).

3.3 Boundary shear and turbulence

Flow may be measured as being laminar, transitional or turbulent and open channel flow is no exemption. In case of laminar flow there are no turbulent variations with respect to time, within the transition zone there are turbulent 'bursts' and within the turbulent zone there are recurrent, random turbulent variations. Vortices can induce by either boundary shear, bursting phenomena or combination of both.

The boundary shear because of surface roughness may be the reason formation of vortices (Nezu & Nakagawa, 1993). The term smooth turbulent flow can be defined when the streamlines adjacent to the bed run parallel to it and so the separation will occur. When

roughness elements enters outwards from the viscous sub layer, the boundary vortices adjacent to the bed tend to accelerate over the asymmetries and come to a standstill between roughness elements which results in flow separation as the velocity is reduced to zero (McGahey, 2006). This flow condition is present in most rivers, which is termed as "Hydraulically rough" turbulent flow.

If the boundary is subjected by sequences of events such as ejections and sweeps, which is a second type of boundary turbulence known as "bursting phenomena" (Nezu & Nakagawa, 1984). This condition will occur on smooth and rough bed and due to local uplift of fluid in the area of flow velocity parallel to the channel bed, sudden oscillations, bursting and ejection occurs randomly (Kline et al., 1967). When high velocities flow move closer to the boundary, it builds up near wall vortices by lateral lenghtwise stretch generating new vortices, which is successively transported away by the ejections (McGahey, 2006).

Turbulence has many definitions, attempted in many ways by many researchers. In this manner, thus an outline will be given of possible definitions of turbulence and some background to behaviour induced by turbulence. If the reader wishes to develop these ideas, they should consult one of the many works on turbulence.

Chow (1959) explains it, as "…flow is turbulent if the viscous forces are weak relative to the inertial forces. In turbulent flow, the water particles move in irregular paths which are neither smooth nor fixed but which in the aggregate still represent the forward motion of the entire stream." Whereas others, such as Johansson & Alfredsson, (1986), prefer not to define it and simply state "Existing theories are unable to give detailed and quantitative explanations of the mechanism of turbulence generation…" Similarly Munson et al. (2002) state "…turbulent flow is a very complicated process. Various researchers have dedicated substantial attempt in trying to appreciate the variation of inexplicable attributes of turbulence. Even though an extensive work on the topic has been done, still the subject of turbulent flow remains the least understood area of fluid mechanics." They go on to say that "A unsophisticated means of considering the turbulent flow is to think of it as a series of random, three-dimensional eddy type motions…These vortices varies in size from very small diameter (on the order of size of a fluid particle) to fairly large diameter (on the order of the size of the object or flow geometry considered). They travel arbitrarily, carrying mass…promotes mixing and increases the transport of momentum".

It is known that turbulent flows show unsteady, irregular and random behaviour and contain eddies of irregular motion. The Reynolds number (Re) is utilized when the fluid changes from laminar flow to turbulent while defining the approximate location. For example in a pipe flow, the fluid with a Re value of less than 2000 is considered laminar whereas when it is in excess of 4000 it is considered to be fully turbulent. Similarly on plate flows, the transition between laminar and turbulence begins when Re is approximately 500,000. The Reynolds number is the effect of viscosity relative to inertia and is defined as Eq.3.1 for pipe flow.

$$\text{Re} = \frac{UD}{\vartheta} \tag{3.1}$$

Where, U is the mean velocity, D is the pipe diameter and ϑ the kinematic viscosity. However, in open channel flows, it is taken that D= $4R\left[R = \frac{A}{P} = \frac{\pi D^2}{4\pi D}\right]$, where R is the hydraulic radius, A is the cross-sectional area and P the wetted perimeter hence Eq. 3.2 is applicable.

$$\text{Re} = \frac{4UR}{\vartheta} \tag{3.2}$$

In open channel flow, if Re<500 the flow is generally laminar flow and if Re>12,500 it is turbulent flow. It should be noted that these are estimated guidelines, even if the transition is usually taken as 2000. Generally in open channel flow the viscosity is low subsequent in a large Reynolds number, therefore, most open channel flows are not within the laminar region.

In turbulent flows, the tumultuous behaviour is predominant in velocity, pressure and shear stress and is categorized by random three-dimensional eddies. Sum of the mean velocity (U) and the fluctuating portion of the velocity, u' is the instantaneous velocity (u) which is the time varying part of the velocity in turbulent flow, which varies from the average value.

A transfer of the momentum generated by shear stresses is due to the fluctuation of velocity. These turbulent shear stresses are mentioned as Reynolds stresses and as they only occur in turbulent flow, they result in increased shear stresses from those found in laminar flow.

3.3.1 Vertical and horizontal interfacial shear

Because of shear velocity, gradients at the main channel and floodplain interface the vertical and horizontal vortices may be persuaded in straight channels for overbank flow. Vortices

persuaded by vertical interfacial shear tend to be small scale, with the eddy structures being smallest at the floodplain bed and gradually expanding the water surface.

Two flow when acting in different direction generally happen in case of meandering, skewed channel flow, or lateral inflow induces horizontal interfacial shear. At lower relative depths (e.g. D_r=0.15), the floodplain flow or overbank flow tend to trail the main channel flow direction. Meanwhile in higher relative depths (e.g. D_r=0.25), the overbank flow usually flows parallel to the floodplain (Shiono and Muto 1998).

3.3.2 Transverse (secondary) currents

The anisotropic of turbulence causes secondary currents to be generated and modified. This anisotropic is initiated by the boundary conditions of the bed, sidewall, the free surface along with the aspect ratio and channel geometry (Tominaga et al. 1989). These secondary currents are about only 2-3% of the mean streamwise velocity, which makes it exceptionally challenging to quantify.

The free surface influences the pattern of secondary currents and in rectangular prismatic channels, the free surface causes the secondary currents to flow toward the side wall along the horizontal plane at about y/H=0.6 (Tominaga et al. 1989) where 'y' is the lateral distance of channel and 'H' is height of the channel. Due to the horizontal plane a pair of separated vortices is generated near the sidewall, hence, the upper vortex is termed the "free surface vortex" and the lower side vortex is called the "bottom vortex". At large aspect ratios, the spanwise scale of the free surface vortex increase and reach about 2H. The bottom vortex is confined to less than about *H* in open channel flows. In open channels to closed conduit flows, the pattern of different vortices can be seen in Chlebeck (2009).

The pattern of secondary flows cells is very different from that of rectangular channel flows from the trapezoidal channels; Tominaga et al. (1989) discovered that the patterns of longitudinal vortices depend on the angle of the sidewall. They considered the pattern of these vortices in three trapezoidal channels with varying side slopes of 60^0, 40^0 and 32^0, the results of which suggests the direction and size of the vortices varies with cross section of the channel. Here they named the vortices A, B and C that correspond to the bottom vortex, the longitudinal vortex and the free surface vortex respectively. As the side slope angle reduces from 90^0, vortex B is generated, vortex C is weaker and vortex A develops into the depth-scale vortex Fig. 7. In trapezoidal channels, the maximum value of the secondary currents is of the similar extent as that in rectangular channels, although the pattern differs.
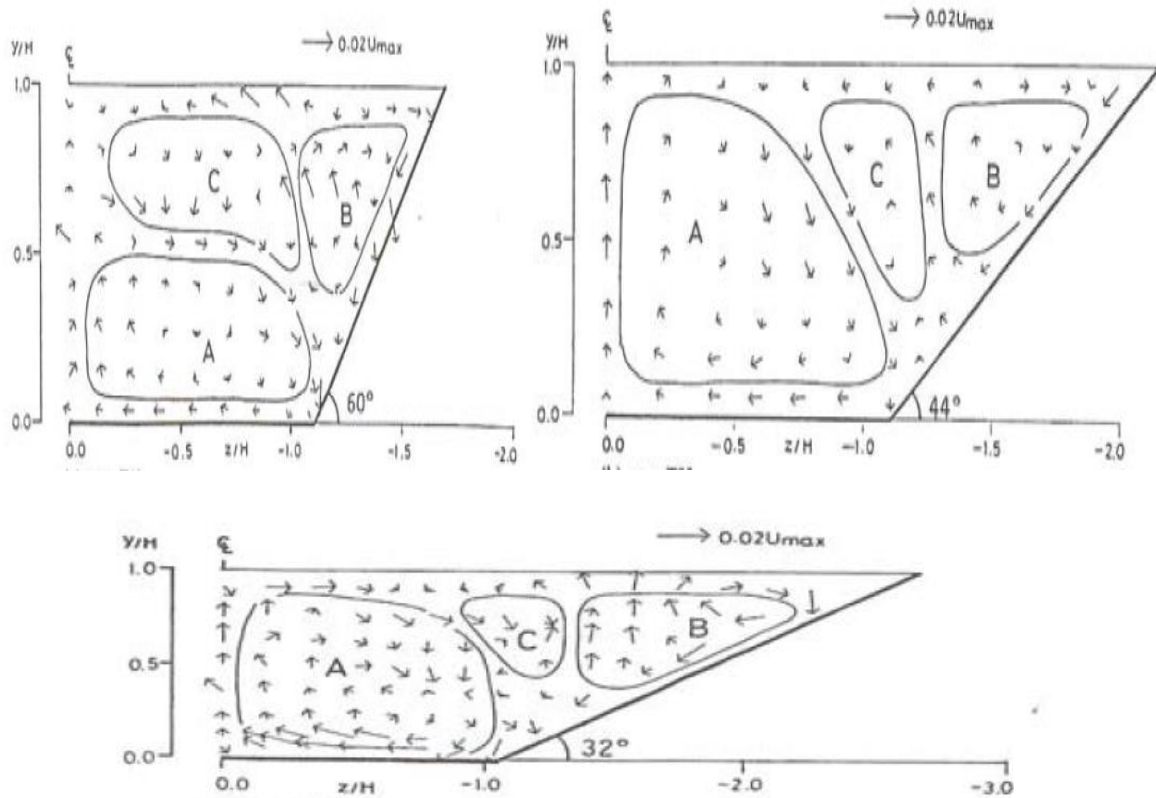
Figure 7 Secondary current vectors in trapezoidal smooth channels (Tominaga et al. 1989)

3.3.3 Coherent structure

Coherent structures, also known as large planform eddies, where there is high velocity gradient it causes the shear instability in regions, for example, at the interface of the main channel and floodplain (Ikeda &Kuga, 1997). Ikeda et al. (2001) conducted a series of laboratory experiments for compound channels of varying relative depth.

Elliott & Sellin (1990), observed in skewed compound channels the slower moving flow on the narrowing floodplain moves over the main channel flow in a different flow direction, which resulted in helical secondary currents developing adjacent to the centreline of the main channel. The increasing floodplain experienced increased velocity due to the faster moving main channel flow entering this region. When it was compared to the equivalent straight channel case, the overall effect was a reduction in the transmission.

Richardson (1992) précises the pattern of the breaking up of eddies as "…big whorls have little whorls, which feed on their velocity; and little whorls have lesser whorls, and so on to viscosity".

3.3.4 Other causes of vortices in channels

Vortices can also be induced due to the natural form of the channel or by man-made obstructions. These include:

- As the floodplain effects only the side of the main channel, the irregular channels have different channel circulations.

- Berms affect the structure of secondary flows and their orientation with depth.

- Braided channels often have a common floodplain; this possibly result in the floodplain flow structures interacting causing further uncertainty and flow separation.

- Natural channels tend to encompass larger width to depth ratios which results in non-homogeneous turbulence, hence the stream is affected by minor wall turbulence (scaled by depth) and free turbulence from the extensive eddy structures which ensures horizontal freedom (Ikeda, 1999).

- Vegetation may cut down or eliminate the vertical interfacial turbulent exchange as it acts as a stream wise barrier between the main channel and floodplain,

- Structures such as bridges and weirs may generate a "vortex street" which may affect the downstream reach.

3.4 Boundary shear stress

Numerous researches are carried in boundary shear stress, as it is a significant factor in flow structure in open channels. Factors including the channels geometry (both cross-sectional and longitudinal), the variation of roughness and sediment concentration all effects the boundary shear stress distribution.

For calculating the boundary shear stress, a simple method was given by Preston (1954) which comprises the placement of a Pitot tube against a boundary and a second static tube placed in the centre of the channel. Initially it was established by using a Pitot tube touching the bottom surface for smooth boundaries in a turbulent boundary layer. This method assumes the boundary shear stress is related to the velocity distribution near the wall (law of the wall). Evaluation of the velocity distribution near the wall is empirically inferred from the differential pressure of the Pitot tube and the static pressure.

The Preston tube technique has a few limitations however; Patel (1965) found that the Preston tube overvalues the surface drag in critical favourable and adverse pressure gradients. It has also been found that in order to take a precise reading of static pressure none of the fluid's kinetic energy can be transformed to a pressure energy at the point of measurement indicative of rise in tube. Therefore, an even hole with no flaws must be used and no additional pressure should be applied to rather tube. In case of both the static and dynamic tubes a great care must be taken in the lateral positioning as slight deviation in arrangement will yield a non-symmetrical flow field, which can induce errors. It is unlikely in practice that the tube positioning will be directly into the flow, however yaw angles of between 12^0 to 20^0 (depending on the specific probe design) give typical errors of less than 1% from the straight aligned values. In order to assist the user, direction finding static Pitot tubes are available which have 3 small holes drilled into a small circular cylinder, one in the centre and one either side which are coupled to three pressure transducer. The cylinder is revolved until the two side holes comes to same pressure value, with the central tap measuring the pressure (Munson et al. 2002). In the skewed channel, the Pitot tube was aligned parallel to the centreline of the main channel and near the walls of the floodplain.

Pursuing Patel's standardization, several researchers have examined boundary shear stress dissemination in separate channel geometries by means of the Preston tube. Myers and Elsawy (1975) investigated boundary shear stress dissemination in two-stage channels with a single floodplain and observed distorted boundary shear stress distributions. Myers (1978) studied momentum transfer mechanisms and found the apparent shear stresses were appreciably larger in comparison to those employed on a compact boundary or floodplain wall at the interface. McKee et al. (1985) substantiated Myers momentum balance methodology by means of the Laser Doppler Anemometry (LDA) method.

Rajaratnam & Ahmadi (1981) exhibited that the boundary shear stress decreases from the centres of the main channel in the direction of the bank of the main channel and floodplain where it grows suddenly. They also find that the boundary shear stress distribution levels off along the main channel before reducing at the walls. They also concluded that in the main channel due to the slower moving floodplain flow the effect of floodplain reduces the boundary shear stress.

Nikuradse in 1926 observed alteration in isotach (lines of equal velocity) patterns in turbulent flow but it was Prandtl (1926) who suggested that turbulent velocity fluctuations in regions of isotach curvature causes secondary flow (Gessener, 1973). However, it was work carried out by Knight and Patel in the 1980's which suggested a link between the agitations in shear stress and the location of secondary cells and also that the number of cells increased with aspect ratio.

Tominaga et al. (1989) and Knight & Demetriou (1983) stated that the shear stress distribution is significantly affected by secondary currents flow towards the wall and reduces when they move in direction opposite to the wall. In addition, Rhodes & Knight (1994) proposed that at the border of the main channel and floodplains of the bank slope has significantly effect on boundary shear distributions.

Hence, by using a model, which is able to replicate the boundary shear stress distribution across the channel, river engineers will be able to accurately determine sediment transport, bank erosion and river morphology.

Flow resistance was classified into four components by Rouse (1965);

i. Surface or skin friction
ii. Form resistance or drag
iii. Wave resistance from free surface distortion
iv. Resistance associated with local acceleration or flow unsteadiness

3.5 Modelling techniques

With advancing technology, there are increasing complex methods of flow, velocity and shear stress calculation tools. This section examines a number of common techniques ranging from simple one-dimensional equation to complex two- and three-dimensional models. The models and methods reviewed herein is not a complete list, but gives an indication to the variety of methods available.

3.5.1 Single channel method (SCM)

This scheme considers the channel as an individual cross-section, irrespective of geometry or flow resistance constraints. These uncomplicated manual computations are generally centered on the Chezy or Manning's equations (the latter is in common use in the UK and is given below in Eq. 3.3).

$$Q = \frac{AR^{2/3}}{n}\sqrt{S_0} \tag{3.3}$$

However, in real time scenario, boundary roughness varies through the channel interface as a result of change in bed material, vegetation or flow obstructions as well as depth. In addition, in immensely vegetated channels the roughness varies with vegetation characteristics (McGahey, 2006). Therefore, different techniques are presented in past literature to evaluate effective roughness such as Pavlovskii (1931), Horton (1933) and Lotter (1933).

A SCM can give a crude approximation to discharge in a channel, but implies that the boundary shear stress is not varying through wetted perimeter, which is not true. The total conveyance in the flume may also be overrated as the model cannot for secondary flow cells, coherent structures or lateral shearing. Myers and Bernnan (1990) shown that this method have significant errors at low overbank flow due to the sudden decrease in hydraulic radius just above bankfull level. Divided channel method was a try to overcome such problem associated with SCM.

3.5.2 Divided channel method (DCM)

Divided channel methods try to overcome some of the limitations of the single channel method, but are often uses the Manning's formula and quickly evaluate manually. As shown in Fig. 8, DCM segregate the channel into different zones depending on their flow behaviour. These lines dividing the channels into zones usually coincide with physical boundaries and can be horizontal, vertical or inclined. The overall summation of the individual discharge obtained for individual zones are estimated using the Manning or Chezy's equations. Since the momentum exchange between the divisions is not accounted for this method also overestimates the total flow within the channel.

Where there are vertical partitions (which resembles to the bank periphery), the perpendicular boundaries are part of the wetted perimeter of the main channel but omitted from the floodplain-wetted perimeter. This compensate the overbank flow retardation due to variation of flow velocity from main channel to floodplain and the interfacial shearing. This concept is not well suited in case of the low relative depth since overall effect of overbank retardation and interfacial shear is so small that it hardly affect the calculations.
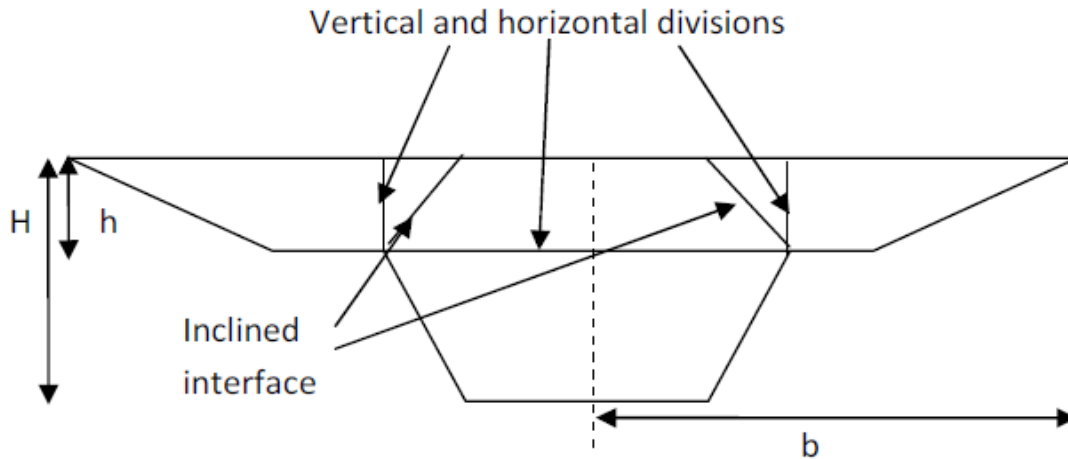
Figure 8 Possible division lines (both horizontal, vertical and inclined) for divided channel method (Chlebeck 2009)

Inclined divisions are based on lines of zero shear stress (Yen & Overton, 1973), i.e., where the velocity gradients and hence momentum exchange is minimum. Typically, these division lines start at the top of the bank and extend out towards the surface at 45^0.

The weighted DCM (Lambert & Myers, 1998) uses both horizontal and vertical partition lines and utilizes a weighting factor for each zone. The empiricism used in this method to estimate the factor is able model the two-stage channels with varying roughness, but its usage limits to prismatic channels only.

The coherent method (COHM) is applicable to two-stage and irregular rough channel flow, which is a manual calculation proposed by Ackers. This method calculates the flow based on both SCM and DCM methods and the coherence is determined as a ratio of them (i.e. Q_{SCM}, Q_{DCM}), as shown in Eq. 3.4.

$$COH = \frac{\Sigma_i^n A_i \sqrt{\left[\frac{\Sigma_i^n A_i}{\Sigma_i^n fP_i}\right]}}{\Sigma_i^n \left[A_i \sqrt{\frac{A_i}{f_i P_i}}\right]}$$

(3.4)

It is assumed that the shear stresses among the assumed interfaces in the DCM will be trivial when contrasted by the boundary stresses and are ignored in the model. The coherence is always less than unity and a discharge adjustment factor is applied to each zonal flow. The method identifies four distinct regions as follows:

Region 1-Low relative flow depths, interaction increasing with depth

Region 2- Moderate relative flow depths, interaction decreases

Region 3-At high relative flow depths a further interaction occurs

Region 4-Compound channel behaves like a single channel

A total of 22 equations for different scenarios have prevented this method being widely adopted.

DCMs require highly idealised and simplified geometries to compute flow within the channel. These methods are generally only applicable to prismatic channels or mildly skewed channels, but cannot be applied to meandering channels. It is taken that the flow is homogeneous and most methods cannot compute discharge in heterogeneously roughened channels.

3.5.3 Exchange discharge model (EDM)

Bousmar & Zech (1999) recommended the exchange discharge model (EDM), which measures transfer of momentum over the interface of the main channel and prismatic or non-prismatic floodplains in one-dimensional model. This model is based on two physical concepts:

- Turbulence exchange due to shear layer development
- Geometrical transfer due to cross-sectional changes

The standardization of turbulent and geometric exchange parameter are important aspect of this model. In addition, realistic cross-sectional geometry is compulsory and is not applicable to meandering channels.

3.5.4 Lateral distribution methods (LDMs)

There are many of such models, which are established on the depth averaged Reynolds Averaged Navier-Stokes equations (RANSE), Eq. 3.5.

$$\frac{\partial u}{\partial t} + U\frac{\partial u}{\partial x} + V\frac{\partial u}{\partial y} + W\frac{\partial u}{\partial z} = -\frac{1}{\rho}\frac{\partial p}{\partial x} + \frac{\mu}{\rho}\left[\frac{\partial^2 u}{\partial x^2} + \frac{\partial^2 u}{\partial y^2} + \frac{\partial^2 u}{\partial z^2}\right] -$$

$$\left[\frac{\partial u'^2}{\partial x} + \frac{\partial u'v'}{\partial y} + \frac{\partial u'w'}{\partial z}\right] \tag{3.5}$$

The physical and theoretical soundness of this model can be expected since these equations are derived from the fundamental fluid flow equations. The basic idea of the method is to

separate the channel into number of "panels" and the unit flow rate (or depth-averaged velocity) is estimated at each zone whose summation give the overall discharge Eq. 3.6.

$$Q = \int_0^B q\,dy = \int_0^B U_d\,dA \qquad\qquad (3.6)$$

These models are not strictly 1-D or 2-D and are perhaps best described as 1-D models with 2-D terms describing 3-D effects. Many methods are classified in this category some of it are flood discharge assessment by Wark et al. (1990), Cunge (1980), Vreugdenhill and Wijbenga (1982), Samuels (1985), Wormleaton (1988), Wark et al. (1991), the k-method by Ervine et al. (2000) and the Shiono-Knight method (Shiono & Knight, 1988 & 1990).

Every other model considers its own assumptions, emphasising the significance of individual constraint, but anyhow each processes end up modelling them in place of evaluating the terms. A comprehensive appraisal of the methods can be found in McGahey (2006). A complete analysis of the Shiono and Knight Method (SKM) is presented in the next section.

3.5.4.1 Shiono and Knight Method (SKM)

The governing RANS equation is derived from fundamental fluid flow equation, which is theoretical as well as physical based equation governing fluid flow. RANS equation for the streamwise motion of a fluid element in an open channel, with a plane bed inclined in the streamwise direction, may be combined with the continuity equation to give

$$\rho\left[\frac{\partial}{\partial x}(UV) + \frac{\partial}{\partial x}(UW)\right] = \rho g S_o + \frac{\delta\tau_{yx}}{\delta y} + \frac{\delta\tau_{zx}}{\delta z} \qquad\qquad (3.7)$$

where {UVW} is the velocity component in the {xyz} directions, x-streamwise parallel to the channel bed, y lateral and z normal to the bed, ρ is fluid density, g is gravitational acceleration, S_o is the channel bed slope, and $\{\tau_{yx}, \tau_{zx}\}$ is the Reynolds stresses on the plane perpendicular to the y and z directions, respectively. Thus Eq. (3.7) can be expressed physically as Secondary flows = weight force + gradient of (lateral + vertical) Reynolds stresses.

Shiono and Knight (1991) gave an analytical solution for prediction of depth-averaged velocity and boundary shear stress by integrating Eq. (3.7) over the flow depth H, to give

$$\rho g S_o - \rho\frac{f}{8}U^2\sqrt{1 + \frac{1}{s^2}} + \frac{\partial}{\partial}\left\{\rho\lambda H^2\left(\frac{f}{8}\right)^{\frac{1}{2}}U\frac{\partial U}{\partial y}\right\} = \frac{\partial}{\partial y}\{H(\overline{\rho U V})_d\} = \Gamma \qquad (3.8)$$

where f is the Darcy-Weishbach friction factor; λ is dimensionless eddy viscosity; s is channel side slope of banks (1:s, vertical: horizontal); Γ is the lateral gradient of the secondary flow force per unit length of the channel and U_d is the depth-averaged velocity given by

$$U_d = \frac{1}{H}\int_0^H U \, dz\,; \quad \tau_b = \left(\frac{f}{8}\right)\rho U_d^2\,; \quad \bar{\tau}_{yx} = \rho\bar{\varepsilon}_{yx}\frac{\partial U_d}{\partial y}\,; \quad \bar{\varepsilon}_{yx} = \lambda U_* H \tag{3.9}$$

where $U_* = (\tau_b/\rho)^{1/2}$ = shear velocity. Shiono and knight (1989) gave the analytical solution to the Eq. (2) while neglecting secondary flow parameters.

$$\rho g S_o - \rho\frac{f}{8}U^2\sqrt{1+\frac{1}{s^2}} + \frac{\partial}{\partial}\left\{\rho\lambda H^2\left(\frac{f}{8}\right)^{\frac{1}{2}}U\frac{\partial U}{\partial y}\right\} = 0 \quad (i.e\ \Gamma=0) \tag{3.10}$$

Equation (3.8) thus includes both vortices about vertical and horizontal axes, and their effects are very significant in the overbank flow where flow moves over the interface and enters floodplain. The analytical solution to Eq. (3.8) may then be expressed for a constant depth, H, domain as

$$U_d = [A_1 e^{\Upsilon y} + A_2 e^{-\Upsilon y} + 8gS_o H f]^{\frac{1}{2}} \tag{3.11}$$

and for a linear side slope domain as

$$U_d = [A_1\xi^\alpha + A_2\xi^{-\alpha-1} + \omega\xi]^{\frac{1}{2}} \tag{3.12}$$

$$\Upsilon = \left(\frac{2}{\lambda}\right)^{\frac{1}{2}}\left(\frac{f}{8}\right)^{\frac{1}{4}}\frac{1}{H}\,; \quad \alpha = -\frac{1}{2} + \frac{1}{2}\left\{1 + \frac{s\sqrt{1+s^2}}{\lambda}\sqrt{8f}\right\}^{\frac{1}{2}}\,; \omega = \frac{gS_o}{\frac{\sqrt{1+s^2}}{s}\frac{f}{8} - \frac{\lambda}{s^2}\sqrt{\frac{f}{8}}}\,; \xi = H-\left(\frac{y-b}{s}\right) \tag{3.13}$$

Equation (3.13) can be used for the analytical solution of the Eq. (3.10) without considering secondary flow term. Solution to Eq. (3.8) is expressed as Eq. (3.14) and (3.15) for constant depth flow and linearly varying side slope respectively.

$$U_d = [A_1 e^{\alpha y} + A_2 e^{-\alpha y} + 8gS_o H f(1-\beta)]^{\frac{1}{2}} \tag{3.14}$$

$$U_d = [A_1\xi^\alpha + A_2\xi^{-\alpha-1} + \omega\xi + \eta]^{\frac{1}{2}} \tag{3.15}$$

$$\alpha = \left(\frac{2}{\lambda}\right)^{\frac{1}{2}}\left(\frac{f}{8}\right)^{\frac{1}{4}}\frac{1}{H}\,; \quad \beta = \frac{\Gamma}{\rho g S_o H}\,; \quad = -\frac{1}{2} + \frac{1}{2}\left\{1 + \frac{s\sqrt{1+s^2}}{\lambda}\sqrt{8f}\right\}^{\frac{1}{2}}\,;$$

$$\omega = \frac{gS_o}{\frac{\sqrt{1+s^2}}{s}\frac{f}{8} - \frac{\lambda}{s^2}\sqrt{\frac{f}{8}}} \; ; \; \xi = H\text{-}\left(\frac{y-b}{s}\right); \; \eta = \text{-}\frac{\Gamma}{\frac{\sqrt{1+s^2}}{s}\rho\frac{F}{8}} \tag{3.16}$$

where A_1 to A_4 are unknown constants, and the local depth is given by $\xi = H\text{-}(y\text{-}b)/s$ (for $y>0$) and $\xi = H + (y+b)/s$ (for $y<0$).

The calibration of constraints f, λ, Γ have been done considerably for distinct cases by Shiono and Knight (1991), Knight and Shiono (1996) Knight and Abril (1996), Abril and Knight (2004), Tominaga and Knight (2004), Chlebeck and Knight (2006) and Tang and Knight (2008). For overbank flow, eddy viscosity coefficient is less significant in comparison to inbank flow. Even constant values for f, λ, Γ gives a good approximation for specific sections or panels (a group of panels). McGahey (2006) and McGahey et al. (2006) illustrate the real time illustration of this model to natural rivers.

3.5.4.2 K-method

Ervine et al. (2000) assumed that the temporal mean velocity components on the right hand side of Eq. (3.8) are a fraction of the depth-averaged velocity as follows:

$$\overline{U} = K_1 U_d; \; \overline{V} = K_2 U_d \tag{3.17}$$

and therefore $\overline{UV} = K\,U_d^2$ (3.18)

in which K = empirical coefficient that varies with geometry and roughness of the boundaries. The term $K\,U_d^2$ completely takes over the complex three-dimensional mixing process, which not only includes a horizontal shear layer due to mass exchange in and out of the main channel but also takes care of expansion and contraction losses. This method is referred as K-method here for simplicity.

$$\rho g S_o - \rho\frac{f}{8}U^2\sqrt{1+\frac{1}{s^2}} + \frac{\partial}{\partial}\left\{\rho\lambda H^2\left(\frac{f}{8}\right)^{\frac{1}{2}}U\frac{\partial U}{\partial y}\right\} = \frac{\partial}{\partial y}\{H\rho K U_d^2\} \tag{3.19}$$

The analytical solution of Eq. (3.19) is

$$U_d = [A_1 e^{Y_1 y} + A_2 e^{-Y_2 y} + G]^{\frac{1}{2}} \tag{3.20}$$

for a domain of constant depth while for a domain with linearly varying side bed (1: s)

$$U_d = [A_1 \xi^{\alpha 1} + A_2 \xi^{-\alpha 2} + \omega\xi]^{\frac{1}{2}} \tag{3.21}$$

where

$$G = \frac{8gS_{oH}}{f} \; ; \; Y_1 = \left(\frac{1}{H\lambda}\sqrt{\frac{8}{f}}\right)\left(K + \sqrt{K^2 + 2\lambda(\frac{f}{8})^{\frac{3}{2}}}\right) \; ; \; Y2 = \left(\frac{1}{H\lambda}\sqrt{\frac{8}{f}}\right)[2K] - Y_1$$

$$\alpha_1 = -\frac{1}{2}[(1 + 2K\mathbb{Q}) - \{(1 + 2K\mathbb{Q})^2 + \mathbb{Q}(f\sqrt{(1 + s^2)} - 8K)\}^{\frac{1}{2}}]$$

$$\alpha_2 = -[(1 + 2K\,\mathbb{Q}) + \alpha_1]; \; \mathbb{Q} = \frac{s}{\lambda}\sqrt{\frac{8}{f}} \; ; \; \omega = \frac{gS_o}{\frac{\sqrt{1+s^2}}{s}\frac{f}{8} - \frac{\lambda}{s^2}\sqrt{\frac{f}{8} - 2\frac{K}{s}}} \tag{3.22}$$

When secondary flow is ignored, i.e. $K = 0$, the solutions of Eq. (3.20) and (3.21) by the K-method becomes equal to that of U_d solution by the SKM method, namely Eq. (3.10).

3.5.4.3 Extended SKM model

The two-dimensional Saint-Venant equations streamwise multiplied by ρH can be written as follows (Yulistianto 1997):

$$\frac{\partial H}{\partial t} + \frac{\partial}{\partial x}UH + \frac{\partial}{\partial y}VH = 0 \tag{3.23}$$

$$\rho H\frac{\partial U}{\partial t} + \rho UH\frac{\partial U}{\partial x} + \rho VH\frac{\partial U}{\partial y} + \rho g H\frac{\partial H}{\partial x} = \rho g H\,S_{ox} + \frac{\partial}{\partial y}H\tau_{xy} + \frac{\partial}{\partial x}H\tau_{xx} - \rho g HS_{fx} -$$

$$\rho\frac{\partial}{\partial x}\int_{zb}^{zw}(\bar{u} - U)^2 dz - \rho\frac{\partial}{\partial y}\int_{zb}^{zw}(\bar{u} - U)(\bar{v} - V)dz \tag{3.24}$$

For a uniform flow, Eq. (3.24) reduces to Eq. (3.25) which is analogous to the conventional lateral distribution model:

Secondary current term Γ

Γ1   Γ2

$$\rho g HS_{ox} + \frac{\partial}{\partial y}H\tau_{xy} - \rho g HS_{fx} = \rho\frac{\partial}{\partial y}\int_{zb}^{zw}(\bar{u} - U)(\bar{v} - V)dz + \rho VH\frac{\partial U}{\partial y} \tag{3.25}$$

Dispersion term Secondary-current term, Γ   Transverse convection term
(Shiono and Knight 1990)   (mass-transfer effect)

This Eq. (3.25) show that the secondary current term Γ can be split into the dispersion term due to helical secondary currents, called Γ1 here, and the transverse convection term (or mass transfer between subsections), Γ2, where the velocity transverse component V does not equal zero. Shiono and Knight (1990) showed that the term Γ1 can appear as a ratio of

the bed shear stresses that is verified by Shiono and Knight (1991). The term Γ2 can be calibrated by K- model. The extended can be rewritten as Eq. (3.26).

$$\rho g S_o - \rho \frac{f}{8} U^2 \sqrt{1 + \frac{1}{s^2}} + \frac{\partial}{\partial} \left\{ \rho \lambda H^2 \left(\frac{f}{8}\right)^{\frac{1}{2}} U \frac{\partial U}{\partial y} \right\} = \underbrace{\frac{\partial}{\partial y} \{ H(\overline{\rho U \bar{V}})_d \}}_{\Gamma 1} + \underbrace{\frac{\partial}{\partial y} \{ H \rho K U_d^2 \}}_{\Gamma 2}$$
(3.26)

Bousmar (2002) stated that the secondary flow term Γ1 has no significant effect over floodplains, displays less influence in the main channel, contrasted to the mass-transfer term Γ2 since the difference in momentum can be observed easily over the main channel and floodplain, and their initial velocities are not same. He also showed that lateral inflow has the most significant effect over momentum while the outflow effect is implicitly considered in the kinetic head variation. This asymmetry in the inflow and outflow effect over main channel to floodplain and vice-versa is consequently due to transfer of mass due to turbulence, which persist even if the mean mass transfer is equal to zero.

3.5.4.4 Eddy viscosity model

The most famous eddy viscosity model can be found in most of the CFD software packages like ANSYS-FLUENT or CFX. The highly used two-equation empirical turbulence closure model like k- ε or k-ω are used widely because of their ability to perform wel in fully turbulent flow and near wall problems respectively. The basic ideologies of these models is to counter the small high-frequency fluctuation through time averaging which gives additional term. These additional terms are calculated through empiricism and are stated as quantifiable terms for closure model. This approximation leads to the semi-empirical model based on the transport equations for turbulent kinetic energy 'k' and its dissipation rate 'ε'. This can be expressed as the following expression Eq. 3.27:

$$\underbrace{\frac{\partial k}{\partial t}}_{\substack{\text{Rate of}\\\text{change}\\\text{of k}}} + \underbrace{U_i \frac{\partial k}{\partial x_i}}_{\substack{\text{Convective}\\\text{transport of}\\\text{k}}} = -\underbrace{\frac{\partial}{\partial x_i}\left[\acute{u}_i \left(\frac{\acute{u}_j \acute{u}_j}{2} + \frac{\acute{p}}{\rho} \right) \right]}_{\substack{\text{Turbulent transport}\\\text{of k}}} - \underbrace{\overline{\acute{u}_i \acute{u}_j} \frac{\partial U_i}{\partial x_j}}_{\substack{\text{P=turbulence}\\\text{production}}} - \underbrace{\nu \overline{\frac{\partial \acute{u}_i}{\partial x_j} \frac{\partial \acute{u}_i}{\partial x_j}}}_{\substack{\text{E=rate of}\\\text{dissipation}\\\text{of k}}}$$
(3.27)

Beside all the possible approximation, the transport k-equations derived are of no use because new unknown correlations emerges in term of turbulent transport and dissipation terms. These problems can be resolved through following assumptions. Postulating that the turbulent transport of k is proportional to the gradient of k (Rodi 1993).

$$\overline{\acute{u}_i \left(\frac{\acute{u}_j \acute{u}_j}{2} + \frac{\acute{p}}{\rho} \right)} = \frac{\nu_t}{\sigma_k} \frac{\partial k}{\partial x_i}$$
(3.28)

Tominaga and Stathopoulos (2007) gave an empirical value for turbulent Schmidt number denoted as σ_k. In their studies it ranges from 0.2-1.3, the selected values of σ_k has a significant effects on the results. They acclaimed that σ_k value should be evaluated accounting the domineering coherent structures for every case. Though, σ_k usually taken as 1.0 (*e.g.* Nezu and Nakagawa 1993, Pope 2000, Rodi 1993).

Reynolds stress tensor can be correlated to average flow velocity through:

$$-\acute{u}_i\acute{u}_j = \nu_t\left[\frac{\partial U_i}{\partial x_i} + \frac{\partial U_i}{\partial x_i}\right] - \frac{2}{3}k\delta_{ij} \tag{3.29}$$

where ν_t is the eddy viscosity, δ_{ij} is the kronecker delta (δ_{ij}=1 for i=j; and δ_{ij}=0 for i≠j); and k is the turbulent kinetic energy, defined as k=$\acute{u}_i\acute{u}_i/2$.

Using Eq. (3.27), (3.28) and (3.29)

$$\underbrace{\frac{\partial \varepsilon}{\partial t}}_{\substack{\text{Rate of}\\\text{change}\\\text{of }\varepsilon}} + \underbrace{U_i\frac{\partial \varepsilon}{\partial x_i}}_{\substack{\text{Rate of}\\\text{change}\\\text{of }\varepsilon}} = \underbrace{\frac{\varepsilon}{k}(C_{\varepsilon 1}P - C_{\varepsilon 2}\varepsilon)}_{\substack{\text{Production and}\\\text{dissipation rate}\\\text{of }\varepsilon}} + \underbrace{\frac{\partial}{\partial x_i}(\frac{\nu_t}{\sigma_t}\frac{\partial k}{\partial x_i})}_{\substack{\text{Turbulent}\\\text{transport of }\varepsilon}} \tag{3.30}$$

where the eddy viscosity can be substituted as:

$$\nu_t = C_\mu k^2/\epsilon \tag{3.31}$$

Total five empirical constants are found in k-ε method table 2, whose standard value for open channel flow are dependent on the model to contemplate the logarithmic distribution near the wall in channel flow with Von-karman k=0.4 (Nezu and Nakagawa 1993).

Table 2 Values of the constants in the k-ε model for open-channel flows

C_μ	$C_{\varepsilon 1}$	$C_{\varepsilon 2}$	σ_k	σ_ε
0.09	1.44	1.92	1.2	1.2

3.6 The Muskingum-Cunge (MC) method

The biggest advantage of the MC method is parameterization, which does not depend on the flow data availability. This notion is still functional when field flow data are accessible, but compromising over certainty (Tewolde, 2005). Tewolde (2005) also mentioned that the

MC constraints are estimated on the ground of flow and channel features. Boroughs et al. (2002) used the finite difference method for solving MC equation, while the parameters are estimated through the spacing between grids in finite differences scheme and the channel geometry features. The MC can be solved on two different sets of formulation, which can be differentiated based on the routing coefficients of the mathematical solution. They include:

3.6.1 Constant coefficient method

In this approach, reference discharge is used to estimate the routing coefficients. These coefficients have a commanding role in the solution of the routing equation. The reference discharge could be the average of the peak flow and base flow or the peak flow itself. The basic idea behind this approach is that the volume remains constant throughout the reach (i.e. volume is conserved between upstream and downstream end). This approach is counted as an efficient direct solution technique (Merkel, 2002).

3.6.2 Variable coefficient method

The routing constants in such type of approach is time dependent and vary at every time interval to manifest the flow features mainly wave celerity, friction slope, and top width variation of the increasing and decreasing flood wave. The explicit approach at every time step helps to incorporate the difference in the velocity of flow and the changing top width at each cross section of main channel and floodplain. This provides a robust computation of the real outflow covering most of the variables in the routing coefficient calculation. The three points direct and four points iterative procedure for solving the finite difference scheme. In the three point direct solution, routing coefficients are resultant of the known discharges (inflow at the first and second time steps and outflow at the first time step). The four point iterative technique calculates the outflow at the second time step based on the three known discharges. The iterative solution to such routing technique should converge to the resulting discharge depending upon error tolerance (Merkel, 2002).

3.6.3 Selection of routing time and distance steps

The variation in time step Δt and space step Δx in MC constant parameter method is used for characterizing the simulation outflow hydrograph on the basis of time and space step parameters. This study have been performed by Ponce (1981) and he exhibited in his study

that MC produces reliable results, within a practical range of Δt and Δx. This method select Δx on the basis of Eq. (3.32).

$$\Delta x \leq \frac{1}{2} \{c\Delta t + \frac{Q_o}{BS_o c}\} \tag{3.32}$$

Where, c is the wave celerity in (m/s), Q_o is the reference discharge in (m³/s), B is the top width of channel in (m), and S_o is the bed slope.

1. Single step reach is that reach where Δx is more than the length of the reach L.
2. The reach is divided into steps only when the length of reach L is more than 3/2 times the Δx. If number of steps considered is two then the routing will be done for two reach in place of one whole reach. In this case, the outflow of the first reach will be the inflow data for the next reach. In another word, the routing calculations are done for the upstream section of the reach and the solution for outflow hydrograph is obtained by routing the next downstream half of the reach (Merkel, 2002).

Garbrecht and Brunner (1991) illustrated that the discrete value of time step produces better results in routing flood hydrograph. The range of Δt should be one day to five minutes. The routing time interval can be selected based on equality $\frac{\Delta x}{c\Delta t}$ < value of the curve derived from X value in Cunge curve. For having good temporal resolution, Δt must be selected such that there is at least minimum five discrete points on the rising part of inflow hydrograph.

3.6.4 Derivation of the Muskingum-Cunge (MC) equation

Cunge (1969) used the diffusive effect by transforming the original Muskingum equation into proper diffusive model. The kinematic routing model considered:

$$\frac{\partial Q}{\partial t} + c \frac{\partial Q}{\partial x} = 0 \tag{3.33}$$

where Q is the discharge in (m³/s), x is the longitudinal coordinates in m, t is the time coordinates in s and c is the wave celerity in (m/s).

Cunge discretized the respective finite difference weighted approximation for the partial derivative on a four-point scheme:

$$\frac{\partial Q}{\partial t} \approx (X\left(Q^{i+1}_{\ j} - Q^i_{\ j}\right) + (1-X)\left(Q^{i+1}_{\ j+1} - Q^i_{\ j+1}\right))/\Delta t \tag{3.34}$$

$$\frac{\partial Q}{\partial t} \approx (\beta \left(Q^{i+1}_{j+1} - Q^{i+1}_{j} \right) + (1 - \beta) \left(Q^{i}_{j+1} - Q^{i}_{j} \right))/\Delta x \tag{3.35}$$

where, $Q^{i+1}_{j+1}= Q((i+1)\,\Delta t, (j+1)\,\Delta x)$, $Q^{i+1}_{j}= Q((i+1)\,\Delta t, j\Delta x)$, $Q^{i}_{j+1}= Q(i\Delta t, (j+1)\,\Delta x)$

$Q^{i}_{j}=Q(i\Delta t, j\Delta x)$.

$X(0 \leq X \leq 1)$ is the space weightage factor and $\beta\,(0 \leq \beta \leq 1)$ is the time weightage factor. After rearranging the approximation Eq. (3.33), leads to the following first order kinematic wave equation as:

$$\frac{[X\left(Q^{i+1}_{j}-Q^{i}_{j}\right)+(1-X)\left(Q^{i+1}_{j+1}-Q^{i}_{j+1}\right)]}{\Delta t} + c\,\frac{[\beta\left(Q^{i+1}_{j+1}-Q^{i+1}_{j}\right)+(1-\beta)\left(Q^{i}_{j+1}-Q^{i}_{j}\right)]}{\Delta x} = 0 \tag{3.36}$$

In a more formal way, it can be rewritten as:

$$\frac{[X\left(Q((i+1)\Delta t,j\Delta x)-Q(i\Delta t,j\Delta x)\right)+(1-X)\left(Q((i+1)\Delta t,(j+1)\Delta x)-Q(i\Delta t,(j+1)\Delta x)\right)]}{\Delta t} +$$

$$c\,\frac{[\beta\left(Q((i+1)\Delta t,(j+1)\Delta x)-Q((i+1)\Delta t,j\Delta x)\right)+(1-\beta)(Q(i\Delta t,(j+1)\Delta x)-Q(i\Delta t,j\Delta x))]}{\Delta x} = 0 \tag{3.37}$$

By assuming $\beta = \frac{1}{2}$ i.e. time centred scheme. Eq. (3.36) can be rearranged as Eq. (3.38) after some algebraic calculation.

$$Q^{i+1}_{j+1} = C_{o}\,Q^{i+1}_{j}+ C_{1}Q^{i}_{j} + C_{2}Q^{i}_{j+1} \tag{3.38}$$

Where,

$$C_{o} = \frac{2\Delta x\,X+ c\Delta t}{2\Delta x(1-X)+c\Delta t} \tag{3.39}$$

$$C_{1} = \frac{-2\Delta x\,X+ c\Delta t}{2\Delta x(1-X)+c\Delta t} \tag{3.40}$$

$$C_{2} = \frac{2\Delta x\,(1-X)- c\Delta t}{2\Delta x(1-X)+c\Delta t} \tag{3.41}$$

The main difference between the original Muskingum method and the MC method is that the original Muskingum solution is derived from ordinary differential equation after integration of the continuity of mass equation in space while in another case its partial derivative solution of diffusion wave model.

A variable constraint can be formulated from the discretization of any explicit parabolic and hyperbolic scheme, by using the Taylor series expansion for the discharge Q. Cunge (1969) showed that the Eq. (3.38) is first order approximation, with second order residual equal to zero, of the kinematic model given in Eq. (3.33). By using Taylor series expansion for discharge Q one can write:

$$\frac{\partial Q}{\partial t} + c\frac{\partial Q}{\partial x} - \frac{Q_o}{2BS_o}\frac{\partial^2 Q}{\partial x^2} = 0 \tag{3.42}$$

with numerical diffusion, given by:

$$R = \frac{c\Delta x}{2}(1 - 2X)\frac{\partial^2 Q}{\partial x^2} + \cdots \tag{3.43}$$

In Eq. (3.42), B is the surface width in m; S_o is the bed slope in (m/m).

Eq. (3.37) can also be interpreted as the solution of the parabolic Eq. (3.42), providing the following relation holds:

$$\frac{c\Delta x}{2}(1 - 2X) = \frac{Q_o}{2BS_o} \tag{3.44}$$

Cunge (1969) obtained an equation for X by imposing a condition where numerical diffusion equated to the physical one.

$$X = \frac{1}{2}\left(1 - \frac{Q_o}{c\Delta xBS_o}\right) \tag{3.45}$$

Where X denotes the weighting factor whose value differs in between 0.0 to 0.5 (dimensionless). Q_o is defined as the reference discharge in (m³/s), S_o is the bed slope in (m/m), c is the kinematic wave celerity in (m/s), Δx is the routing reach or sub-reach length in m and B is the top width of water surface in m.

Tewolde (2005) shown the reference discharge as:

$$Q_o = Q_b + 0.5 (Q_p - Q_b) \tag{3.46}$$

Where,

Q_o is the reference discharge in (m³/s), Q_b is the base flow in (m³/s) taken from the inflow hydrograph and Q_p is the peak discharge of inflow in (m³/s). The base flow is defined as

the minimum inflow mostly composed of the groundwater or infiltrated water (Tewolde and Smithers, 2006).

K is defined as the storage time constant in s, which has same analogy to that of wave travel time within the river reach and calculated approximately as:

$$K = \Delta x / c \tag{3.47}$$

Ponce and Yevjevich (1978) presented the following expression for the C_o, C_1, C_2 as:

$$C_o = \frac{-1+C+D}{1+C+D} \tag{3.48}$$

$$C_1 = \frac{1+C-D}{1+C+D} \tag{3.49}$$

$$C_2 = \frac{1-C+D}{1+C+D} \tag{3.50}$$

The ratio of physical and numerical diffusivities is derived in terms of the dimensionless "Courant number" (C); and "cell Reynolds number" (D), as;

$$C = \frac{c\Delta t}{\Delta x} \tag{3.51}$$

$$D = \frac{Q_o}{c\Delta x B S_o} \tag{3.52}$$

In case of VPMC method, parameters C and D varies at each time interval, as a function of the reference discharge Q_o relevant to each computational section in which river reach will be divided. By comparing Eq. (3.39) to (3.41) with the Eq. (3.48) – (3.50), the original parameters of the Muskingum can be expressed as:

$$K = \frac{\Delta t}{c} \tag{3.53}$$

$$X = \frac{1-D}{2} \tag{3.54}$$

Todini(2007) used these parameters to define the VPMC method by estimating parameters Eq. (3.53) and (3.54) at every length and time steps.

For ease, the value of courant number and cell Reynolds number is substituted in the Eq. (3.48) to (3.50) to derive a final expression for the routing coefficients C_o, C_1, C_2 as:

$$C_o = \frac{\frac{\Delta t}{K} - 2X}{\frac{\Delta t}{K} + 2\,(1-X)} \tag{3.48}$$

$$C_1 = \frac{\frac{\Delta t}{K} + 2\,X}{\frac{\Delta t}{K} + 2\,(1-X)} \tag{3.49}$$

$$C_2 = \frac{-\frac{\Delta t}{K} + 2\,(1-X}{\frac{\Delta t}{K} + 2\,(1-X)} \tag{3.50}$$

3.6.5 Range of "X" parameter

Heatherman (2008) showed that the range for parameter X might vary from 0 to 0.5. However, a positive value of this parameter in the MC method produces a lower limit of size of distance step. Ponce and Theurer (1982) for time and distance step confirmed that the negative value of X in practical manner triggered no computational problem. Beside the negative value of X a better computational simulation of the problem is possible. A negative value of the X is indicative factor showing that the outflow contribution in storage is higher in comparison to the inflow contribution. This is possible when the backwater is significantly conceivable (Reid, 2009). Heatherman (2008) also reported that weighting parameter is insignificant in the MC and even the negative value for X sometimes tend to procure stable and more accurate solution.

3.6.6 Limitation of the Muskingum-Cunge (MC) method

Even though the applicability of the MC is very extensive it does has many limitation and foremost one is the inability of the method to account for the backwater effects, in a very similar way that of original Muskingum method. Beside this, no lateral inflow is considered while routing through the channel or reservoir, which makes it incomplete even though results produced are quite admissible.

Although, constant coefficient method works well for very long reaches and large drainage areas, more work still need to be conducted for small reaches having very small bed slope channel, which is found in real time scenario. In variable parameter Musingum-Cunge method, mass conservation and balance is the most appearing defect where volume of water upstream does not come equal to volume of water downstream disregarding mass conservation (Todini, 2007; Perumal et al. 2009).

In usual circumstances, computational stability may deferred when the wave travels time is less than the computational interval Δt. The stability condition for optimise solution is when the courant number is more than one. This in turn shows the relation between the Δt and Δx which can be presented as $\Delta t = \Delta x / C$ (Johnson, 1999). Where Δt and Δx are the temporal and spatial weightage factor and C is the Courant number.

The deciding standards for the routing models is affected by the features such as accuracy required, availability and type of data, computational facility availability, computational time and cost availability, and the extent of flood wave information desired. The analysis of the data taken from Elbashir (2011) is done in the next part followed by HEC-RAS and MIKE 11 analysis of same data.

3.7 River Analysis System, HEC-RAS

The HEC-RAS software code and authorization are released to public domain by the Hydrologic Engineering Center for the U.S. Army Corps of Engineers. This software package provides their users to perform one-dimensional steady flow, unsteady flow, and sediment transport problems. The Hydrologic Engineering Center's develops the HEC-RAS as a part of "Next Generation" (NexGen) of hydrologic engineering software. This project named NexGen project incorporates different aspects of hydrologic engineering, mainly comprising river hydraulics; real-time river forecasting for reservoir operations; rainfall-runoff analysis; reservoir system simulation; flood damage analysis. The following steps are used to model the problem.

3.7.1 Geometric Data

The very first step includes geometric data input which can be selected from the main program window. This will trigger the Geometric Data Editor and exhibits the river system. The river name is entered and the upstream is denoted as "Upper Reach". Total eight cross sections are defined, with cross section eight being the upstream cross section and the first being the downstream cross section. The following method of identifying the highest number being the upstream section is used in the program for placing the cross sections in numerical order is the only cross section identifier. The Cross section Data Editor is used for entering cross sectional data, which pops up when Cross Section icon on the Geometric Data Editor. The X-Y coordinates for the eight cross sections are entered in the editor window. Four or more coordinates are required to be entered for defining the cross section.

The geometric consideration, which is made according to cross section identifier, illustrates the spacing between the cross section as 1000 m apart. The elevation difference between the 8000 km long reach (i.e. between upstream and downstream) is approximately 3.76m. Consequently, the slope obtained from this is around 0.00047 m/m, which is fairly milder slope. Other geometric data that is considered in this is Manning's n values of 0.04 in the left overbank (LOB), main channel, and right overbank (ROB), respectively. Before saving, the geometry data as the file name "Brosna Geometry", coefficient of expansion and contraction are given as 0.30 and 0.10 respectively.

3.7.2 Unsteady Flow Data

The Boundary condition and the initial conditions are added for the given set of system at the commencement of the simulation period. Under the edit option, in the main program the Unsteady Flow Data Editor can be found where all the boundary and initial conditions are inserted.

3.7.3 Boundary Conditions

The farthest two points in the geometric data are upstream and downstream cross-section which are also situated in the boundary condition column in Unsteady Flow Data Editor. Moreover, in this particular case user can find River Station 8 on the upstream and River Station 1 on the downstream according to the cross section identifier. Boundary conditions are set by highlighting the adjacent cell under Boundary Condition Type. After cell is highlighted, not all option for boundary conditions are available. The program will automatically gray out all irrelevant boundary condition types. Under the option "Add Boundary Condition Location", Internal boundary conditions may be added according to the problem statement.

3.7.4 Upstream Boundary Condition

For River Brosna flow hydrograph is selected by highlighting the cell and pressing the Flow Hydrograph button. In this particular example, the inflow hydrograph is manually inserted in the respective Enter Table radio button. The radio button use Simulation time is selected after Data Time Interval is set to 15 minutes. Another option for the user is to read hydrograph data from a DSS file. The DSS file and path option is when selected, a screen will pop-up. In this window, the user has to select the desired DSS file by browsing it in the

memory. Once the DSS file is selected, a list of all of the DSS pathnames within that file will be displayed in the table. Pathnames filter are provided to reduce the number of pathnames. After the chosen DSS pathnames are found, the user can close the window and the filenames and pathnames are found to be logged in the Flow Hydrograph Window.

3.7.5 Downstream Boundary Condition

The downstream river station (i.e. identified as 1 river station) are given normal depth as a boundary condition. Similarly, as in the above upstream boundary condition case, here also the cell corresponding to the river station is highlighted and the normal depth button is emphasized. The window, which pops-up after selecting the normal depth option, acquires the value of slope as 0.00047. This indicates that the user has to enter the friction slope for the reach near the boundary condition thus usually slope of the bed is taken a good estimate in place of friction slope.

3.7.6 Initial Conditions

Flow and stage information at every cross sections, as well as the elevation input at any storage area for the given system is considered as the Initial conditions. The initial condition tab in the Unsteady Flow Data Editor is used to establish the initial condition for the system.

For the program, to perform a steady-flow backwater run to compute the corresponding stage at every cross section requires flow data of the reach. The upstream initial flow of 53.633 m^3/s, corresponding the baseflow of the hydrograph is entered at the upstream boundary condition. In addition to the flow data, Initial elevation for each storage area is required. Finally, data in the editor window are saved and closed.

3.7.7 Unsteady Flow Analysis

An unsteady flow analysis can be initiated after all the geometry and unsteady flow data are inserted. Under Run menu within the main program window one can find unsteady flow analysis. After selecting aforementioned option, a window will display for Unsteady Flow Analysis. After selecting the geometry file "Brosna Geometry" and the Unsteady Flow File "Unsteady Flow" in the plan window, save the plan selected and title it as "Brosna Plan". A short identifier is entered as "Brosna" and then the plan is saved.

3.7.8 Simulation Time Window

In the Simulation Time Window, start and end dates and times for the flood events are mandatory. The format for entering date and time are as follows: either 01Jan1990 or 01/01/1990 while considering the time field 24 hours system is maintained (i.e. 1 p.m. is entered as 1300). For this application, the simulation time began and ended at 0800.After saving the date and time in the given particular format the simulation time window is closed.

3.7.9 Computation Settings

Within the Unsteady Flow analysis editor window, several computational settings are possible such as the computational interval; hydrograph output interval; instantaneous profiles interval; and the name and path of the output DSS file.

In this case, the computational interval is kept at 2 minutes, which is small enough to accurately counter the rise and fall of the flood wave. The simulation time depends on the computational interval hence it should be kept as low as possible considering the computational time requirement. The output hydrographs are set to interval of 15 minutes. This defines the relation of the output computed stage and the flow hydrographs written in HEC-DSS. The detailed output interval was set at 6 hours, which justifies the interval over which hydraulic output are computed within the post processor. The amount of post processing time depend on the detailed output interval hence it should be fairly large to reduce the time and storage. The path selected for the output to DSS was "C:\HEC\RAS\Unsteady\Brosna.dss."

3.7.10 Location of Stage and Flow Hydrographs

There are options for denoting position to obtain the processed hydrographs and presented for display. The operator may choose different cross sections, group of cross sections, or entire reach from the option menu in the Unsteady Flow Analysis Window. For particular instance, "All Reaches" are chosen. This selection will compute hydrographs throughout the cross section selected. If the operator is operating on extremely large data set, computation time and data storage can be cut down by only picking the most crucial cross sections for output. Fig. 9 shows the results obtained through above procedure in HEC-RAS.
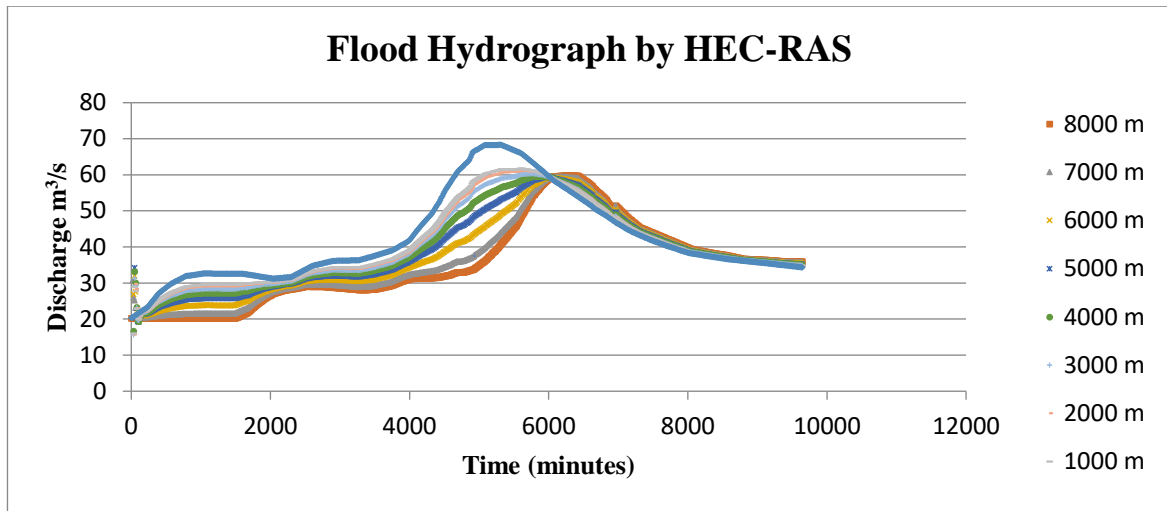
Figure 9 Flood event Nov-Dec 1994 Brosna River using HEC-RAS

3.8 About Mike 11 Software

MIKE 11 simulation software product has been presented by the DHI (Danish Hydraulic Institute) which is compatible to perform Hydrodynamics, Rainfall-Runoff, Structure Operation, Dam Break, Advection Dispersion, and Water Quality model simulation. In a network of open channel flow, which is mostly unsteady and non-uniform, can be simulated using the implicit finite difference model i.e. Hydrodynamic Module (HD) in MIKE 11. The HD simulations comprises of the time series of water depth/levels and discharges associated with it. The one dimensional St. Venant equations (1D) continuity and momentum equations are used in MIKE 11 for open channel flow analysis.

MIKE 11 software are based on the following assumptions, which are:

1. Water is incompressible and homogeneous,

2. Bottom slope is small,

3. Flow everywhere is parallel to the bottom (i.e. wave lengths are large compared with water depths).

The flow is described according to the number of terms used in momentum equations.

1. Dynamic wave (full Saint Venant equations)

2. Diffusive wave (backwater analysis) and

3. Kinematic wave (relatively steep rivers without backwater effects).
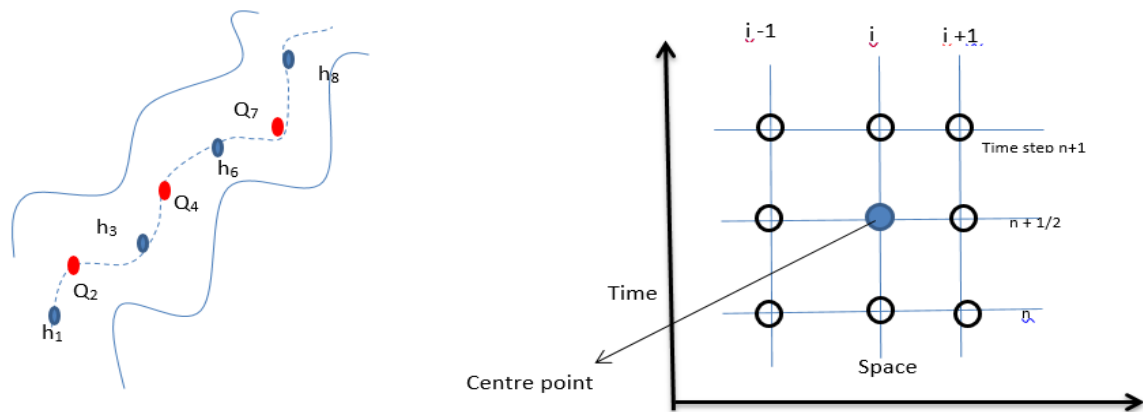
Figure 10 Six (6) Point Abbott-Ionesco schemes and implicit scheme used in Mike 11

In MIKE 11, implicit finite difference scheme is used for computing discharge Q and flow depth H at every time step consecutively. The solution scheme used here i.e. implicit finite difference convert the partial difference equation into implicit finite difference equations, which are solved over computational grid swapping Q and H points. Abbott-Ionescu six-point numerical scheme is coupled in the software for grid generation shown in Fig 10.

3.8.1 Boundary conditions

The concept of boundary condition (BC) in the MIKE 11 software is segregated as external boundary condition and internal boundary condition. The external BC looks for the upstream and the downstream condition of the river reach. Meanwhile, internal BC takes care of hydraulic structures where St. Venant equations are not applicable. Some of the typical upstream BC and downstream BC for analysis are inflow hydrograph for specific event upstream and constant water level time series in downstream with reliable rating curves respectively.

3.8.2 Initial condition

Initially time is assumed to be zero as initial condition.

3.8.3 River Branches

In the HD module of MIKE 11, the river branches are discretized and denoted as reach node. The actual stream flow and the concept of discretization of stream corridor is shown in Fig. 11.

3.8.4 Representation of cross sections

The coordinate system used to represent the river cross sections is X & Z coordinate system shown in Fig. 12. The abscissa denotes the width of river while z coordinate signify the vertical distance of x coordinates. To define the flow characteristic like bed slope, flow changes, shape, flow resistance etc. properly in MIKE 11, river cross section should be represented accurately.
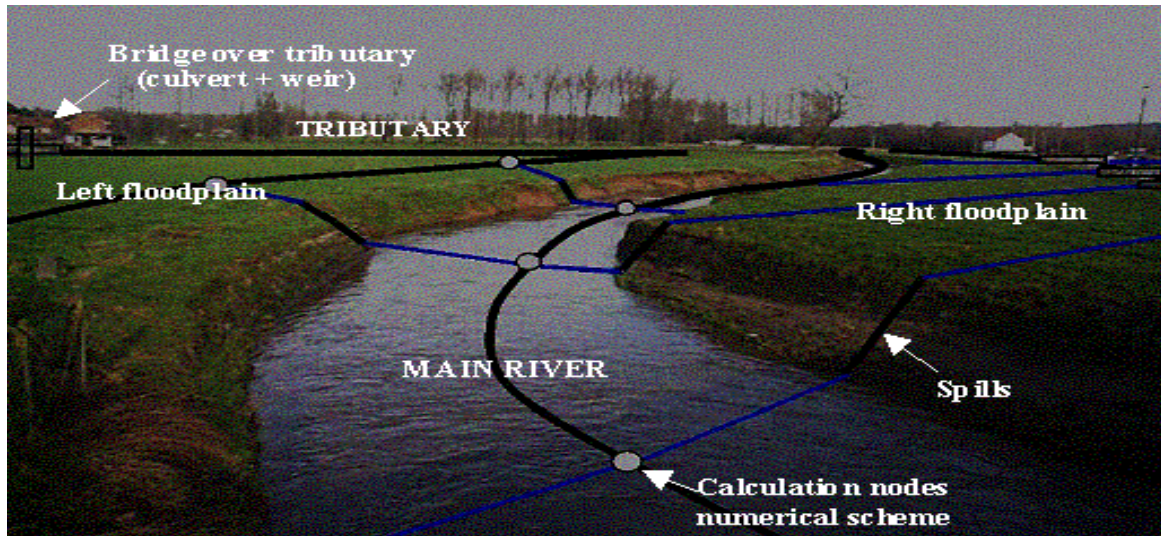

Figure 11 Discretization of river branch in the Mike 11 hydrodynamic model
(Source: https://bwk.kuleuven.be/hydr/Research/urban-river/River)

3.8.5 Equations used

To determine the backwater profile across the bridge or the discharge, energy equation can be utilized as it takes into account the friction loss and the contraction/expansion losses. Total four cross sections are required out of which all one is the river cross section and other are randomly expressed in the cross section editor.

Ideally, the distance within the bridge and the up- and downstream cross-sections is maintained within the order of b, where b is the bridge opening width. Lastly, the streamlines are confirmed to be parallel at section one and four.

The equation solved from section *i* to *i*-1 reads

$h_{i-1} + h_{v(i-1)} = h_i + h_{vi} + h_{f(i, i-1)} + h_{e(i, i-1)}$ (3.51)

where h and h_v are water level and velocity head at cross section (i denotes the subsection) and h_f and h_e are the friction and expansion losses respectively between two sections i and i-1 in Eq. (3.51).
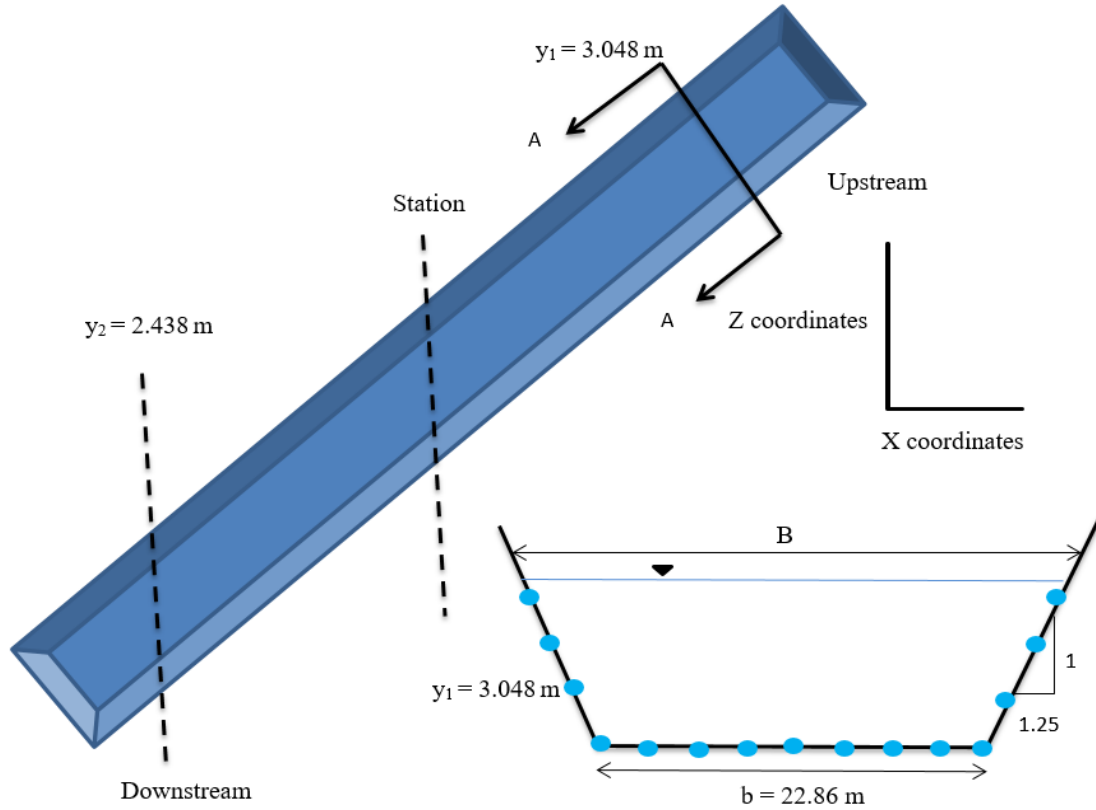

Figure 12 Discretization of cross section of river in the Mike 11 and illustration of both the lateral profile and the cross-section for the Brosna Offaly river reach

The velocity head is defined as

$$h_v = \frac{\alpha \, Q^2}{2g \, A^2} \tag{3.52}$$

where discharge is calculated through manning's equation i.e. conveyance k times the square root of bed slope

$$k_i = \frac{a_i \, r_i^{\frac{2}{3}}}{n_i}; \quad K = \sum_1^N k_i; \quad A = \sum_1^N a_i \tag{3.53}$$

Where

$Q = Discharge$ at the section.

V = velocity distribution coefficient.

k = *Subsection* conveyance.

a = *Subsection* area.

K = *Total* cross section conveyance.

A = Total cross section area.

r= *Hydraulic* radius.

n= *Manning's* roughness coefficient.

N =Number of subsections

The friction loss between cross-section i and i-1 can be estimated by Eq. (3.54).

$$h_{f(i,\ i-1)} = \frac{L_{i,i-1}\,Q^2}{k_i k_{i-1}}$$ (3.54)

where $L_{i,i-1}$ is the flow length in the approach reach.

Expansion or contraction between two sections can be expressed as Eq. (3.55)

$$h_{e(i,i-1)} = C\left|\frac{a_i vi^2}{2g} - \frac{a_{i-1}v_{i-1}{}^2}{2g}\right|$$ (3.55)

where C is the contraction or expansion coefficient. This coefficient is dependent upon the channel shape and size while the default values for contraction and expansion are 0.3 and 0.5 respectively indicating that the losses due to expansion are typically larger than losses due to contraction.

3.8.6 Solution method

The assumption considered in the energy equation method is that the flow through reach is sub-critical. Further, iteration technique is used for obtaining solution. The bridges are pre-estimated grounded on a series of water level upstream and downstream value. As a result discharge is calculated depending upon each series of water level. The algorithm for determining the discharge has the following steps:

1. Trial discharge estimation.
2. Calculation for backwater from section 3 to section 4.

3. Calculation for backwater from section 3 to section 2 established through the result from step 2.

4. Calculation for backwater from section 2 to 1 established through the result from step 3.

5. Comparison of the flow depth determined through step 4 and actual flow depth at section 1.

6. The modification of discharge is based on the comparison in step 5. And if the deviation is within the limit, algorithm terminates there itself or return to step 2.

All the way through the calculations, the outcomes are matched with critical flow. Code by default considers the critical flow at the location either if the solution found is below the critical flow depth or if the step 2-4 do not converge. Further, code by default take critical flow at section one if valid solution is not obtained after reaching maximum number of iterations (default 50).

3.8.7 Working procedure and simulation

This annex describes basic methodologies of the following work items of MIKE11 modelling, referring to a simple sample model with eight cross sections. These items are listed in order of the actual procedure of modelling.

1. Preparing time series file (**.dfs0)
2. Preparing network file (**.nwk11)
3. Preparing cross section file (**.xns11)
4. Preparing HD (hydrodynamic) file (**.hd11)
5. Preparing boundary file (Empty file) (**.bnd11)
6. Preparing simulation file (**.sim11)
7. Inputting boundary data (**.bnd11)
8. Simulation (**.sim11)
9. Viewing result file (**.res11)

3.8.7.1 STEP-1(Preparing Time Series File)

File extension of this file is *.dfs0, since MIKE 11 does not take excel file directly it is important to make time series file of given extension file. Inflow discharge data of Brosna Offaly River at upstream and downstream of 8km reach is known. An excel file is first made

for time and discharge and then copied to the time series file in MIKE zero. In file properties give general information of the river like name or reach length etc. and then select equidistant calendar axis in our case we have selected flood events of 4/11-11/11 1994. In item information select discharge save **.dfs0 file in an appropriate folder.

3.8.7.2 STEP-2 (Preparing Network File)

The following network file is of *.nwk11 file extension. Major information to be included for network files are river name, coordinates of cross section locations and chainage (i.e. distances of cross sections from the upstream end). Either prepare excel file or text file for cross sectional coordinates and input other necessary data on nwk11 file on the basis of topographic survey results or directly input the data if the dimensions are uniform and not complex as in our case where cross section is uniform throughout i.e. trapezoidal for 8000 m reach length. The network data consists of coordinates of each station on the river, branch name and the distance between each station. After importing, file data to ntwk11 file and input other necessary data on nwk11 file save the file to appropriate folder.

3.8.7.3 STEP-3(Preparing Cross-Section File)

The file extension of this particular file is *.xns11 containing major information of the cross section of each station also including information of river name, cross section ID, chainage, cross sectional shapes (X, Y), and roughness coefficient. Provide cross sectional data of the stations in x and y coordinates which is depicted in each station of the network file. Chainage shows the number of the station on the network for example first chainage is named as zero i.e the upstream of the river where inflow hydrograph data is known. Save this file in appropriate folder.

3.8.7.4 STEP 4 (Preparing HD (Hydrodynamic) File)

This file takes the initial conditions with the file extension as *.hd11. Major information contained in a hydrodynamic file are initial conditions and additional output files. Input necessary information and check water depth, Froude number, wind input, sedimentation data or other morphological data if available. Also, save this file in appropriate folder.

3.8.7.5 STEP-5(Preparing Simulation File)

Simulation file having file extension *.sim11 have major information such as directories and names of input files, simulation time step and period and directories and names of a

result file. Make a .sim11 file by specifying directories and names of input files, input simulation and result information.

3.8.7.6 STEP-6(Inputting Boundary Data)

Boundary data determined by the boundary file with file extension as *.bnd11 are chainage (location) and time series of boundary inflow/ water level, upstream boundary of the demo model i.e. inflow discharge and downstream boundary of the demo model. Open network editor through .sim11 file and input boundary data. After that open "Start" page of the sim11 file and start the simulation, which will take some time depending upon the time step and complexity of the model.

3.8.7.7 RESULT

Use application called MIKE VIEW to open the result file of extension *.res11 Fig. 13.
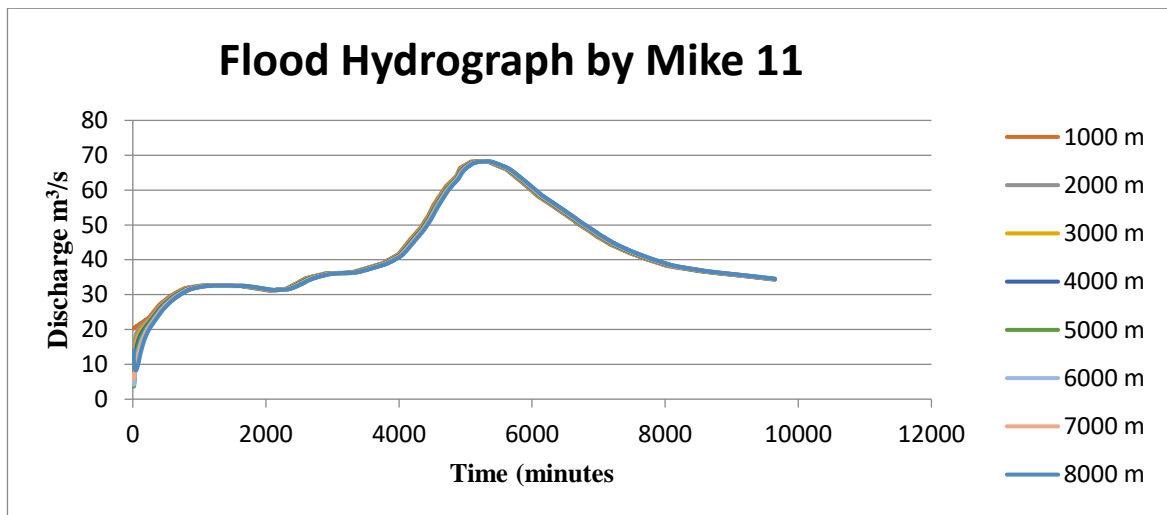
Figure 13 Flood event Nov-Dec 1994 Brosna River using MIKE 11

Chapter 4
RESULTS & DISCUSSIONS

4.1 General

This section deal with the calculation, solution and the discussions of the different models and their application analogy. Different models used for the stage discharge prediction and flood routing techniques are presented in the previous chapter while their working and principles are also stated above with the clarity that the user can apply these methods to produce the results for different channels. In this section, more of the application analogy and their working will be discussed together with the discussion of the model on the basis of their performance. For stage discharge prediction, the models are reviewed and presented for a compound channel from Flood Channel Facility (FCF) phase A series 02 and 03 at different relative depths. The systematic outcomes from discussed models are contrasted to each other and with experimental data from compound trapezoidal channel tests. All the data related to compound channel FCF phase A series 02 and 03 may be found at www.flowdata.bham.ac.uk. Fig. 14 shows the symmetric compound channel with side slope 's' equals to one, while 'b' is half of bed width equals to 0.75 m (constant for both channel dimensions with B/b ratio as 2.2 and 4.2 respectively), 'B' is the length from centerline to start of the side slope in floodplain area, 'h' is the height of the main channel 0.15m fixed, 'H' is the depth of water and bed slope S_o is equal to 0.001027.
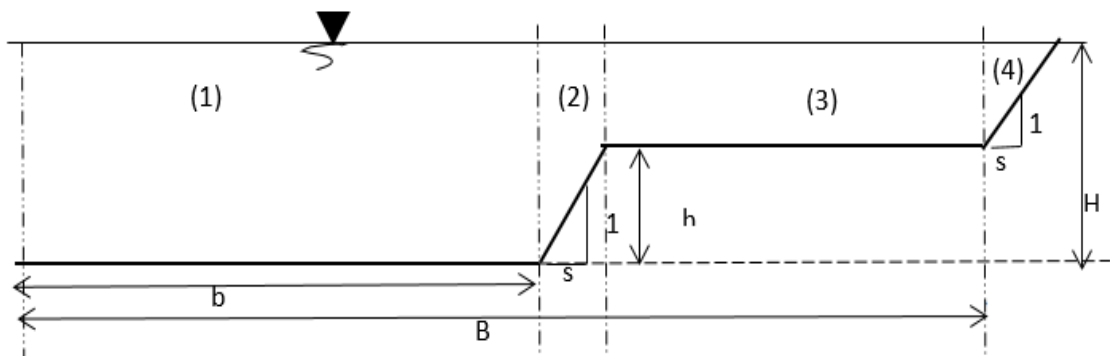

Figure 14 Symmetric compound channel with side slope s=1

Flood routing has been done on the river Brosna Offaly of Ireland whose dataset can be found in the Elbashir (2011) thesis. The river dimension are as follows total length of the

river reach considered is of 8 Kms while main channel is having trapezoidal cross section with bed width 'b' equals to 22.86m, side slope 's' equals to 1.25 and depth of water at upstream and downstream are 3.048m and 2.4384m respectively . Data of flood event Nov-Dec 1994 is considered since its hydrograph obtained is more or less have familiar shape as discussed in the theoretical background (i.e. prominent rising limb, crest area and the recession limb). Other reason of choosing this data set is the prominent nature (i.e. attenuation and lag) displayed by the inflow and outflow hydrograph obtained is very much visible. Table 3 represents the reach characteristics of river Brosna while Fig. 15 illustrates the cross section of the river reach.

Table 3 River Brosna reach characteristics

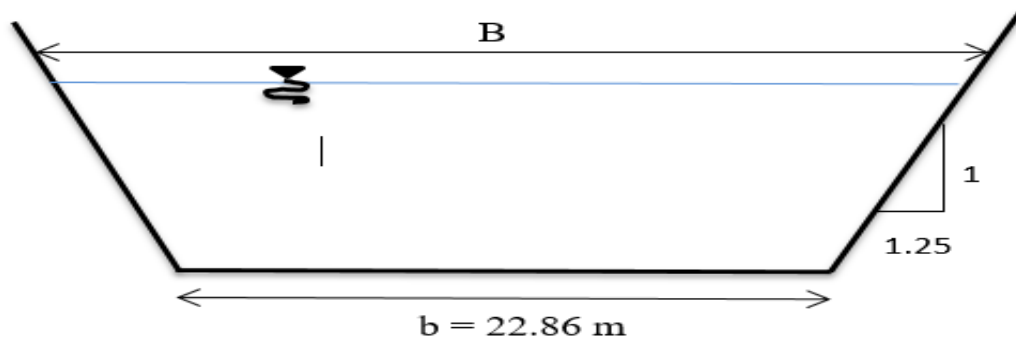| Length (Kms)	Bed width (m)	Side slope	Water depth (m)	Average bed slope (m/m)	Manning's roughness $(m^{1/}3/s)$
8	22.86	1.25	3.048 Upstream 2.4384 Downstream	0.00047	0.04

Figure 15 Cross section of the river reach

4.2 Discussion of SKM, K method, Extended SKM

Tang and Knight (2009) stated that at the side edge $(UV)_d = 0$ (i.e. the depth averaged secondary current cell) since $V=0$ at this location. A viable assumption to be made is that $(UV)_d$ is zero at the edge of the secondary cell and it enhances either taking positive or negative value towards centerline of the cell, influenced by the sense of cell rotation. The convention for rotational cell of $(UV)_d$ is considered positive for clockwise cell and vice-

versa for anti-clockwise cell, as shown by Chlebeck and Knight (2006) and Knight et al. (2007), same convention adopted herein. The value of Γ is then depends on the lateral gradient of $(UV)_d$ for each half of the cells. The thinking behind SKM is that the panels are preferred with an understanding of the configuration of the secondary flow cells, which tend to ascribe the constant value of Γ to each panel.

4.2.1 Discussion on K-method

Complex behavior of fluid flow across the floodplain varies with the water depth over the floodplain. It is questionable whether the secondary cell component expressed by Eq. (11) varies linearly with depth-averaged velocity U_d. Lorena (1992) exhibited that for a given geometry the fraction of transverse to longitudinal component $\bar{V}/\bar{U}$ varies in the range of 2-4% for straight compound channels. Tang and Knight (2009) stated that the assumption that K is constant does not hold true rather it varies laterally, unlike Γ, which remains constant throughout the panel. Transverse component can either be negative which makes assumption taken by Ervine et al. (2000) again debatable since value of K can also be negative as well. This indicates that the proposition by Ervine et al. (2000) that K is positive is not always true.

4.2.2 Discussion on Extended SKM

Kordi et al. (2015) showed that the significance of dispersion term corresponding to Eq. (3.25) Γ1 is comparatively less over floodplain than mass-transfer term Γ2. The momentum transfer secondary current term Γ2 appears at the interface of the subsection and its consequences proliferates into the floodplains. In the improved, model both dispersion and the assumptions made by Shiono and Knight (1991) and Ervine et al. (2000) respectively estimate mass-transfer terms. The term Γ1 can be estimated as the ratio of bed shear stresses while the ratio of transverse to longitudinal component K=U/V appears to be an invariable coefficient influenced by the geometry of the channel.

4.3   Boundary conditions for U_d solution

For a symmetric channel, half channel is considered and divided into number of panels depending upon channel geometry and secondary flow cell parameter. In this study FCF phase A channel series 02 and series 03 with B/b ratio of 4.2 and 2.2 is divided into four panels from centerline to side slope of floodplain with either constant depth or linear depth

domains as shown in Fig. 14, the analytical solution for U_d was given using matrix product of matrices formed by coefficients A_1, A_2, A_3, and so on. For every panel two coefficient, A_1 to A_2 or A_3 to A_4 has to be eliminated using proper boundary conditions as:

- The velocity gradient with respect to y at the centre of the main channel is zero because of symmetry i.e. $\frac{\partial U}{\partial Y} = 0 \; at \; y = 0$.

- All joints of domains must satisfy the continuity of the velocity which gives boundary condition as follows i.e. $U_i = U_{i+1}$ & $\frac{\partial U_i}{\partial y} = \frac{\partial U_{i+1}}{\partial y}$

- Finally, the velocity must be zero at the edge of the flood plain side slope (U=0). It therefore follows that seven unknown constants are required in the analytical solution which can be obtained by solving seven linear equations.

- Omran (2005) went on to include a μ factor into the boundary conditions to account for continuity of unit force where *f* and λ are different between panels. For a constant depth domain, Equation holds as $(\mu \frac{\partial U_d}{\partial y})_i = (\mu \frac{\partial U_d}{\partial y})_{i+1}$; $\mu = \lambda \sqrt{\frac{f}{8}}$.

- When the channel is symmetrical, the flow can be modelled for half of the channel and doubled to give the overall discharge. In this case, an extra "boundary" condition is stipulated at the centreline which states: $(\mu \frac{\partial U_d}{\partial y})_i = 0$.

4.4 Application philosophy and calibration of coefficient

The analytical solution of SKM is based on the calibration of three parameters namely friction factor f, eddy viscosity coefficient λ, and secondary flow parameter Γ. Constant parameters for each panel is used to evaluate the coefficients in the matrix which in turn are used for the calculation of U_d. Generally, for simplicity panel junction coincides with the location where flow depth is discontinuous. Thus for modeling a symmetric rectangular compound channel only two panels are more than enough for the half of the channel. If more complex secondary flow cells are present, then further division of the channel into more panels may be required (Knight et al. 2007).

Darcy-Weishbach formula is applied for the calculation of friction factor f for every panel using experimental data using back calculation. Usually, to make the evaluation easier it is recommended that the standard value of λ = 0.067≈ 0.07 is imposed on most of the panels. Note that standard value of λ does not affect the solution for the overbank flow where Γ and
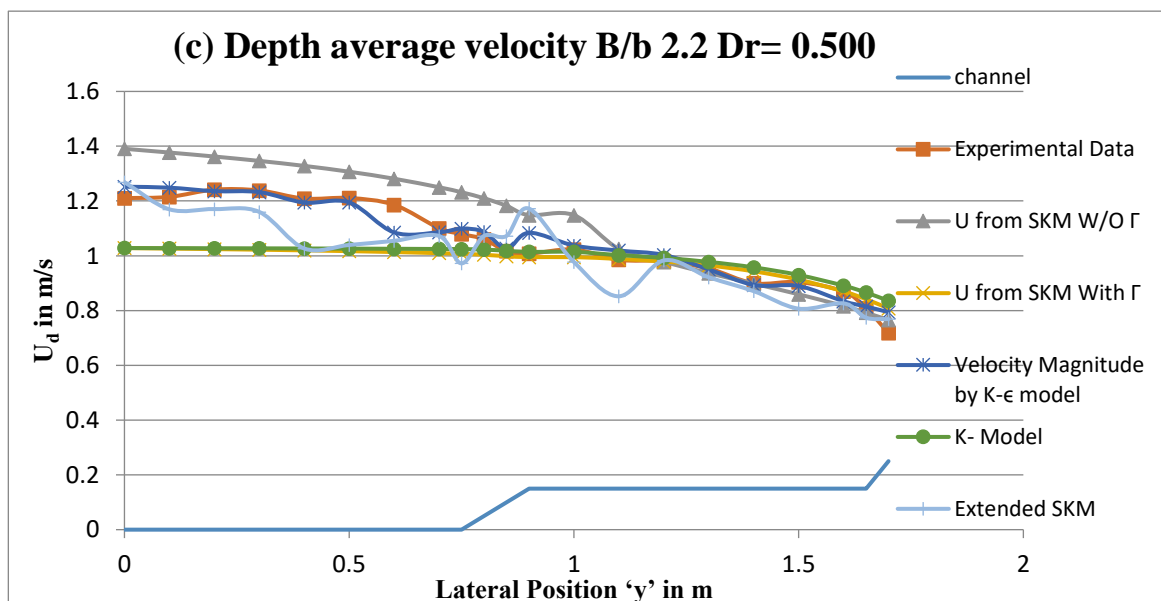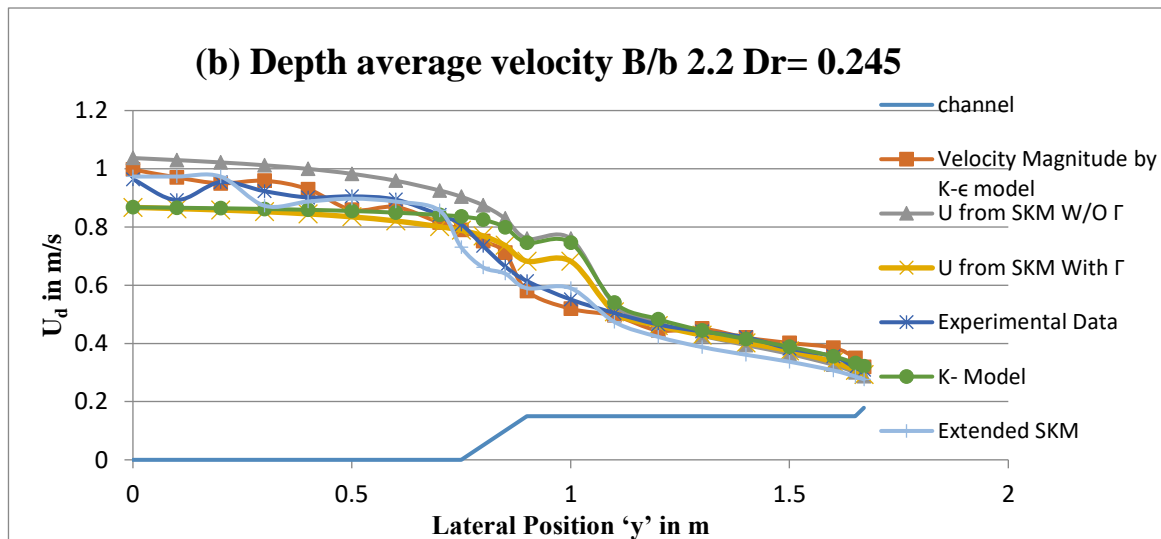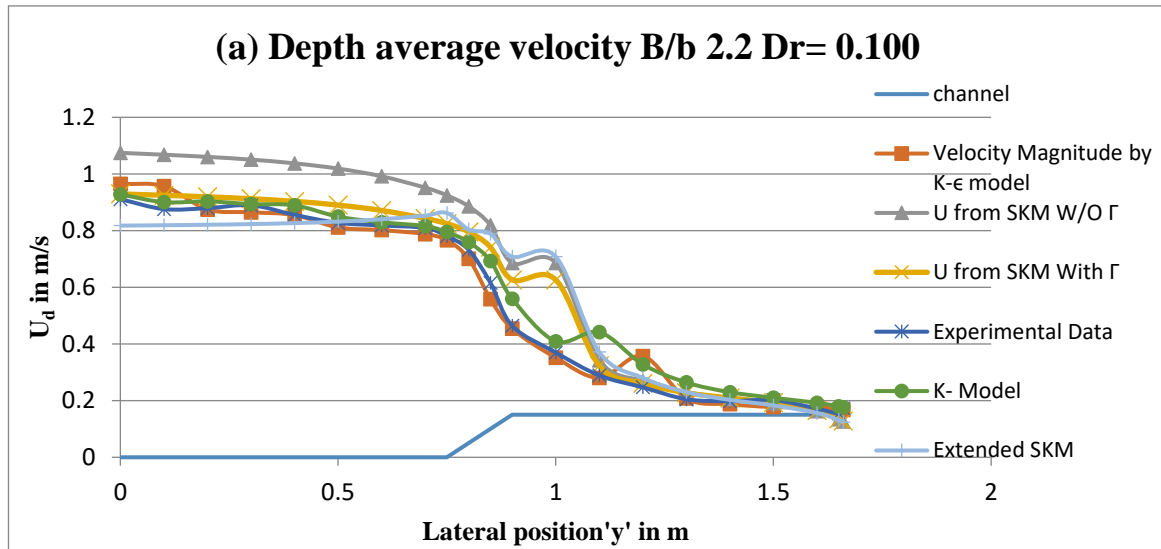
f play important role while in case of inbank flow it has a major effect on the results. Also, note that the sign of Γ can be assumed positive in main channel and negative over floodplain (Shiono and Knight 1991). For the calculation of boundary shear stress U_d evaluated from analytical solution can be used to obtain $\tau_b = \rho f U_d^2 / 8$.

A CFD code ANSYS Fluent is used for the application of k-ϵ model using multiphase flow volume of fluid (VoF) formulation in pressure based solver. This software package is used for the analysis of heat flow and fluid flow in any type of geometry. Finite volume method is adopted as a numerical scheme in which integral form of conservational equations are solved over each control volume and control surface. Surface and volume integrals are approximated using suitable quadrature formulae. In an open channel flow, fluid flow is multiphase governed by force of gravity and inertia. By tracking the volume fraction of two or more immiscible fluid VoF solves single set of momentum equations for each domain. For calculation of pressure term pressure-velocity coupled algorithm called SIMPLE (Patankar 1980) is used. Velocity inlet has been given as an inlet boundary condition while for the walls no slip condition is considered as a boundary condition.

4.4.1 Application to compound channel

To analyze the difference between the various models, data from two symmetric compound channels were chosen: FCF phase A channel (Knight and Sellin 1987; Knight 1992, www.flowdata.bham.ac.uk). These had bed slope of 0.001027and channel width ratio of 2.2 and 4.2 with varying relative depth from $0.1 \leq D_r \leq 0.5$. Due to symmetricity, only half of the channel is modeled with four panels as shown in Fig. 14. The parameter Γ for each panels are considered from the lateral variation of apparent stress and force per unit length due to secondary flows plot from Shiono and Knight (1991). While Abril and Knight (2004) also gave different expression for Γ as $0.05\rho g h S_o$ for inbank flow, $0.15\rho g H_{mc} S_o$ for the main channel during overbank flow, and $-0.25\rho g H_{fp} S_o$ for the floodplain during overbank flow where ρ is the density of fluid, $g = 9.81$ m/s^2 acceleration due to gravity, S_o is the bed slope, and H, H_{mc}, and H_{fp} are the channel depth for main channel and floodplain depths. Kordi et al. (2015) stated that the value of K varies linearly from zero, on the centerline axis of main channel, to maximum amount at the end of panel 1 (see Fig. 14). Similarly, in panel 2 K value decreases linearly from beginning of the floodplain to the end of panel 2. In panel 3 and 4, K is zero Ervine et al. (2000). The predicted lateral distribution of U_d is shown in Fig.

16 along with the experimental data for the channel B/b 2.2 with varying relative depth ratio as 0.1, 0.245, and 0.5.
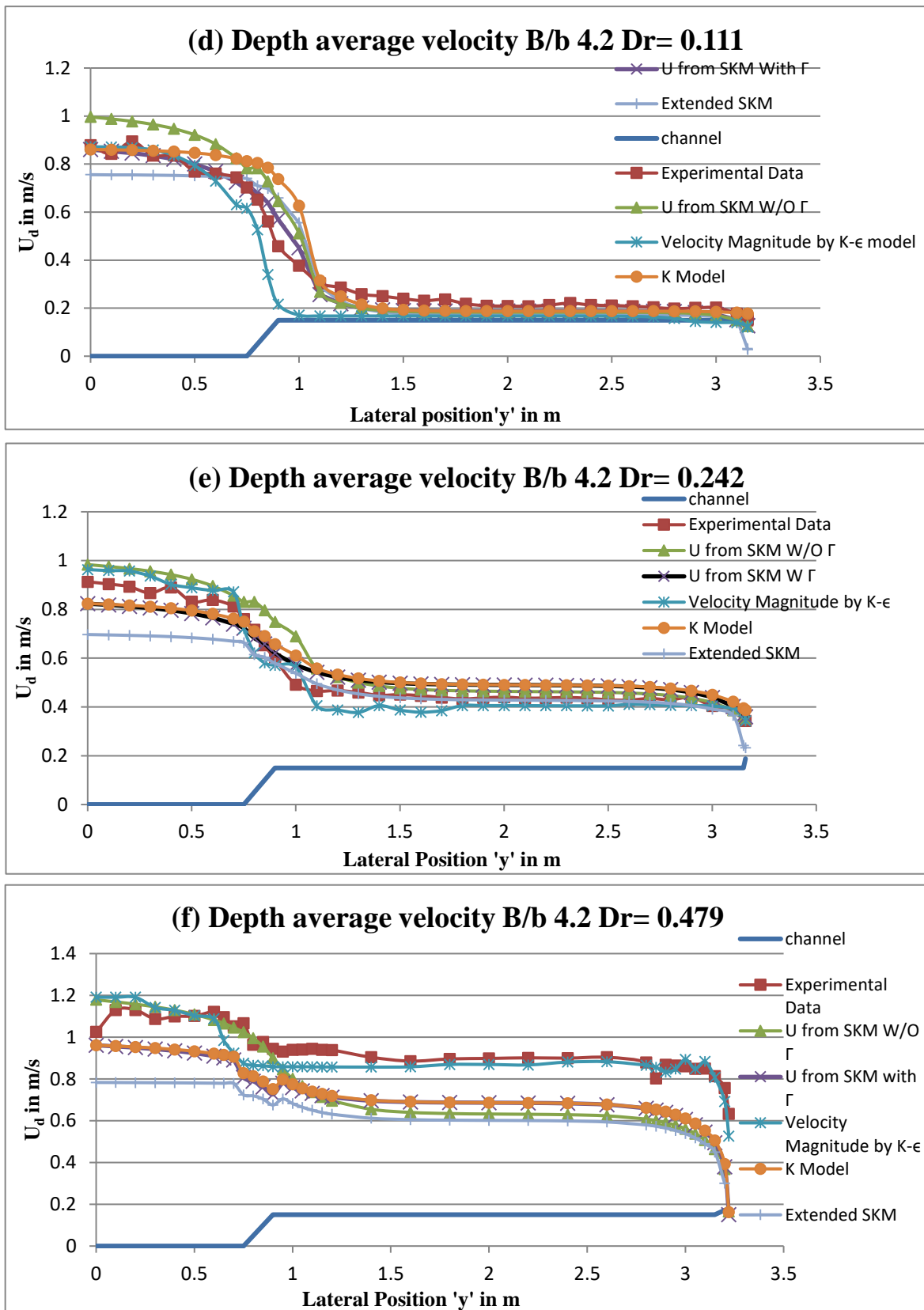
(d) Depth average velocity B/b 4.2 Dr= 0.111

(e) Depth average velocity B/b 4.2 Dr= 0.242
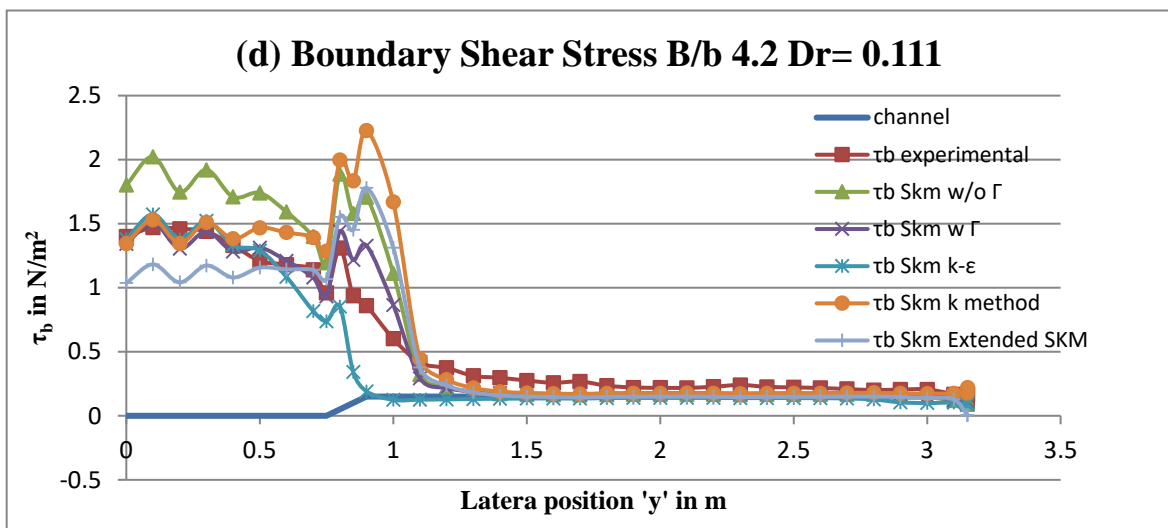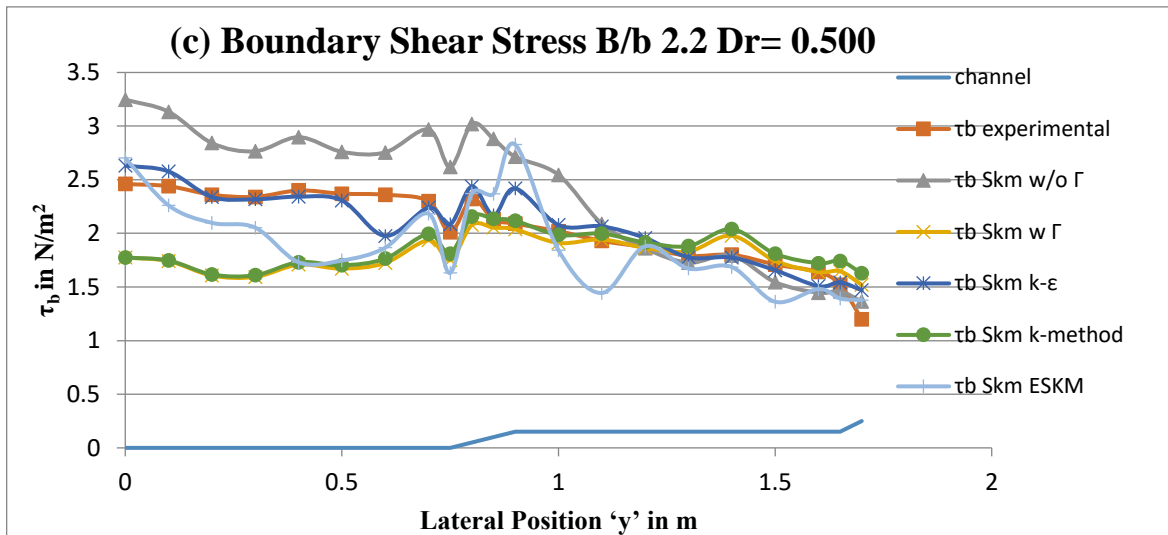

(f) Depth average velocity B/b 4.2 Dr= 0.479

Figure 16 Ud (y)) distribution for experiment FCF phase A series 02 and 03 (a) to (c) B/b 2.2 & (d) to (f) B/b 4.2 for various model with and without inclusion of secondary flow in SKM

4.4.2 *Boundary Shear stress results*

The boundary shear stress distribution is another important parameter for river flow modelling. It is prerequisite while analyzing force balances, or when standardizing a numerical model for flow prediction, which frequently demands the acquaintance of the variation of local resistance coefficients. The calculation of boundary shear stress through analytical solution model is done with help of Darcy weisbach equations for friction factor. From the experimental dataset of FCF channel phase A series 02 and 03 boundary shear stress, depth averaged velocity are known which in turn helped for the estimation of the friction factor as $f = 8\tau_d/\rho U_d{}^2$. By using the estimated depth averaged velocity U_d and friction factor f one can estimate boundary shear stress τ_d by reverse substitution of the parameters in the Darcy weisbach equations. Following Fig. 17 represents the lateral boundary shear stress distribution τ_d using different methods.

(c) Boundary Shear Stress B/b 2.2 Dr= 0.500

(d) Boundary Shear Stress B/b 4.2 Dr= 0.111
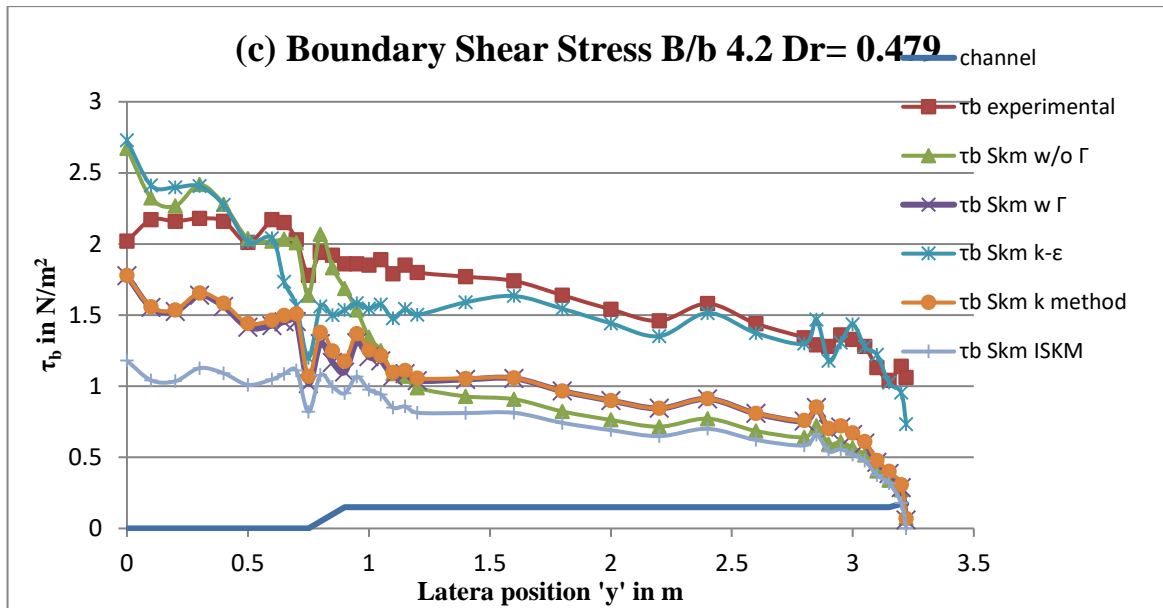

(e) Boundary Shear Stress B/b 4.2 Dr= 0.242
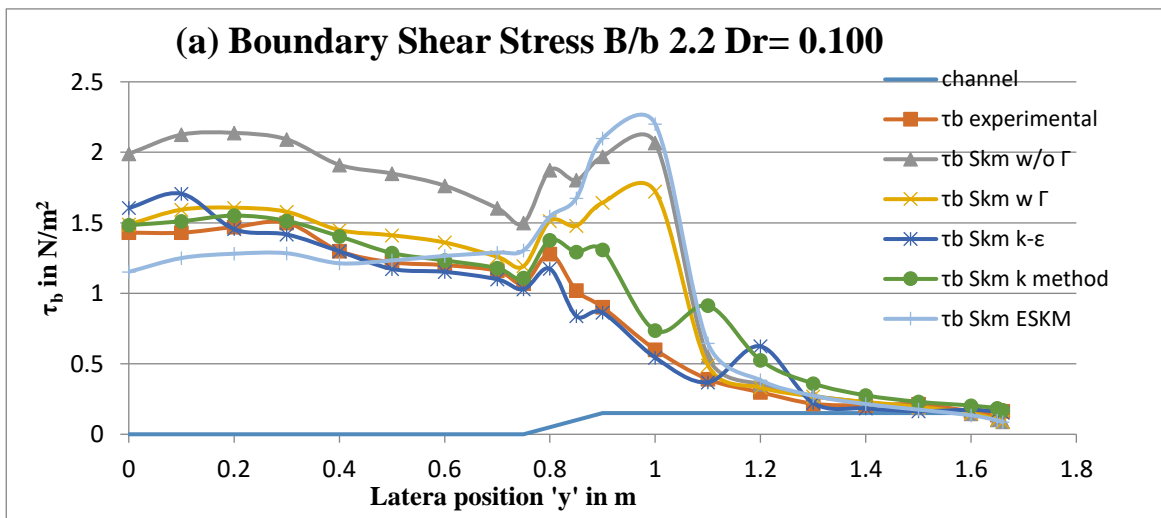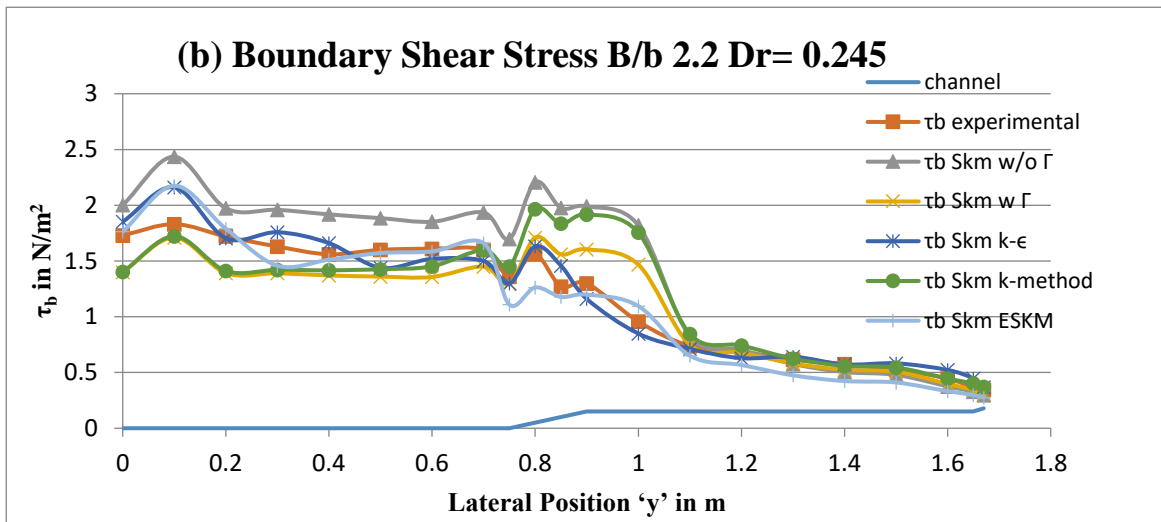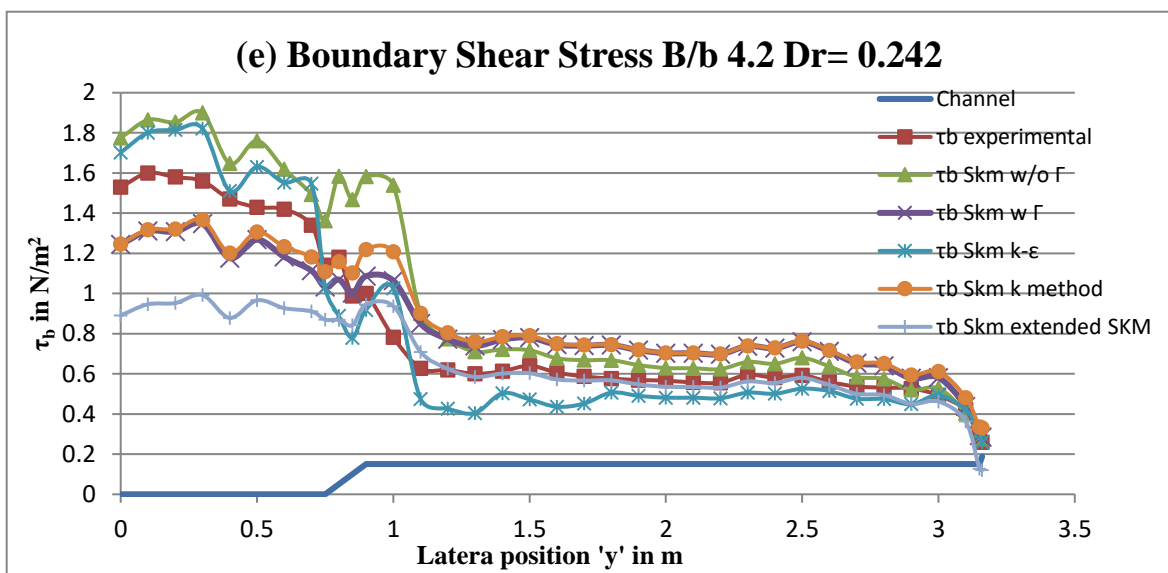
Figure 17 τb (y) distribution for experiment FCF phase A series 02 and 03 (a) to (c) B/b 2.2 & (d) to (f) B/b 4.2for various model with and without inclusion of secondary flow in SKM

4.5   Stage discharge

After calculation of depth-averaged velocity U_d stage discharge at three different relative depths for both channel is estimated at three cross sections. From experimental data, stage discharge is plotted for several cross sections and then the estimated stage discharge of three cross section for both channels are validated with them using different models. Following Fig. 18 shows the stage discharge distribution of both channel and their estimated stage with respect to the flow depth for each relative depth.
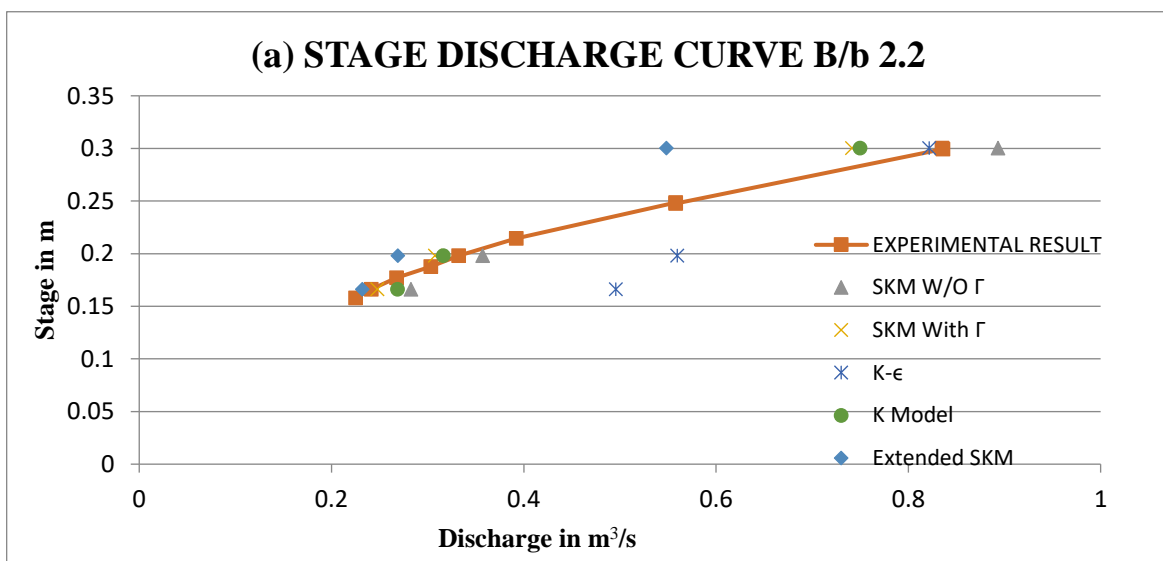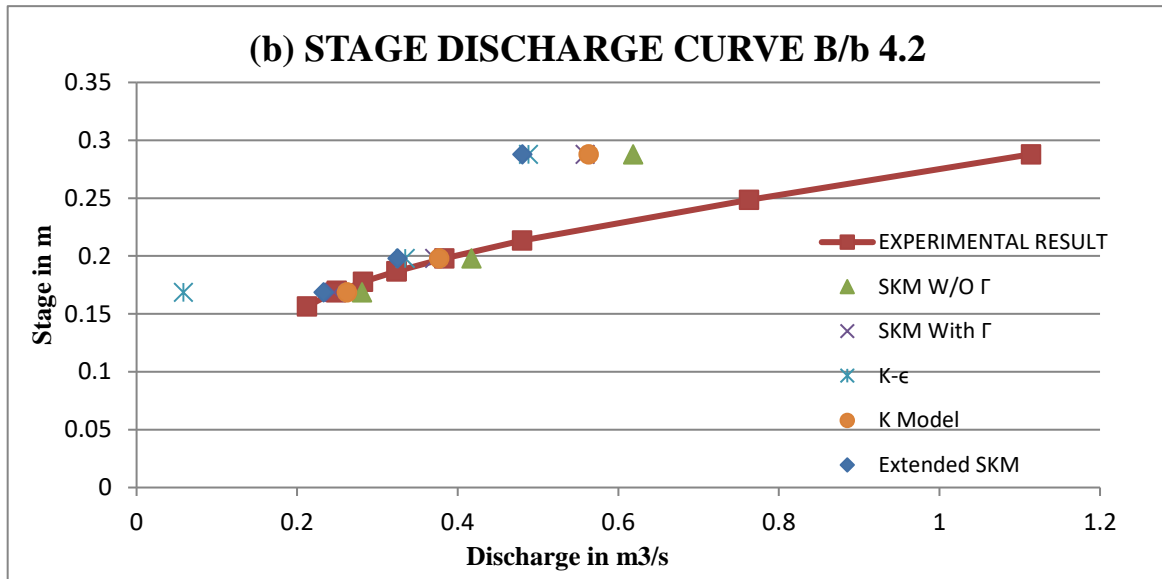
Figure 18 Stage discharge curve for FCF phase A series 02 and 03

4.6 Calibration of Muskingum-Cunge (MC) parameters

As discussed in section 3.6, the MC method is applied where parameters K and X are estimated on the basis of the reach characteristics and the inflow hydrographs. From the dataset of flood event 1994 it is clear that the time to reach the peak discharge is 87.25 hours. The time increment Δt can be estimated based on Eq. 3.32, which yields Δt as less than 12.1 hours.

According to the relation given in section 3.6.3 increment in Δt is selected as 0.25 hours. The reference discharge can be calculated based on the relationship given in Eq. 3.46.

Base flow discharge is either estimated from the base flow separation method or filtering discussed in 1.5.1. Using the same procedure base flow Q_b is estimated as 16.3508 m^3/s. Meanwhile peak discharge is also selected from the given data set of flood event Nov-Dec 1994. The reference discharge Q_o is know calculated which is equal to 44.2947 m^3/s. The area of flow can be obtained from given below.

$$A = (b + sy)y \tag{4.1}$$

Using the reach characteristics given area of the cross section is coming out be 50.235 m^2. Mean velocity of the flow in the upstream section is then calculated on the basis of discharge area relationship as V = Q_o/A which is equals to 1.033 m/s. Considering the mean velocity of 1.033 m/s, Froude number is nearly equals to 0.24 which indicates the flow to be gradually varied sub critical and channel to be mild slope. The wave celerity (c) can be

obtained on the relationship mentioned in Table 1, which is coming to be 1.549 m/s. The routing reach length Δx can be estimated by Eq. 3.32 as:

$$\Delta x \leq \frac{1}{2}(1.549 \times 0.25 \times 60 \times 60 + \frac{44.2947}{27.148 \times 0.00047 \times 1.549}) \tag{4.2}$$

Hence, $\Delta x \leq 2308.35$m, which is less than 2/3 the length of the total reach as discussed in section 3.6.3, therefore the reach is divided into eight sub-reaches of equal distance 1000m.

So, Δx = 1000m. Then the value of MC weighting factor can be estimated using Δx value as shown in Eq. 3.45.

$$X = \frac{1}{2}(1 - \frac{44.2947}{27.148 \times 0.00047 \times 1.549 \times 1000}) \tag{4.3}$$

So, X = -0.62 and the travel time K can be estimated as the ratio of the routing reach length to the celerity which is equals to 645.577 sec. This indicates the time required by the wave to reach downstream as (645.577/3600) = 0.18 hours. By substituting the calculated values of K, X, Δt in Eq. 3.48, 3.49 and 3.50, the coefficients C_o, C_1, C_2 of the MC method can be determined as:

$$C_o = \frac{\frac{0.25}{0.18} - 2 \times -0.62}{\frac{0.25}{0.18} + 2\ (1-(-0.62))} = 0.569 \tag{4.4}$$

$$C_1 = \frac{\frac{0.25}{0.18} + 2 \times -0.62}{\frac{0.25}{0.18} + 2\ (1-(-0.62))} = 0.034 \tag{4.5}$$

$$C_2 = \frac{-\frac{0.25}{0.18} + 2\ (1-(-0.62))}{\frac{0.25}{0.18} + 2\ (1-(-0.62))} = 0.398 \tag{4.6}$$

Now, the outflow can be calculated on each routing reach step using the Eq. 3.38.

Table 4 Hydraulic parameters of the cross sectional area of river Brosna for flood event 1994

| Q_o (m^3/s)	B (m)	A (m^2)	V_{avg} (m/s)	C (m/s)
44.2947	27.148	50.235	1.033	1.549

The resulting calculations of characteristic reach parameters such as reference discharge, top width, cross sectional area, the average velocity and the wave celerity are shown in table 4 and resulting routing coefficients calculations are shown in table 5.

Table 5 Coefficients of routing calculation for river Brosna for flood event 1994

Time to peak (h)	Q_o (m^3/s)	Δt (h)	Δx (m)	X	K (h)	C_o	C_1	C_2
87.25	44.2947	0.25	1000	-0.62	0.18	0.569	0.034	0.398

4.7   Results of Muskingum-Cunge (MC) application

The results obtained by the application of the constant parameter MC method have been demonstrated as the hydrograph in Fig.19 This is clear from the figure that the lag in the following outflow hydrograph in each sub-reach is very minute and the smaller time increment Δt used gives results with considerable change in the attenuation of the computed outflow which is remarkably very small for such time increment parameter Δt as 0.25 h.
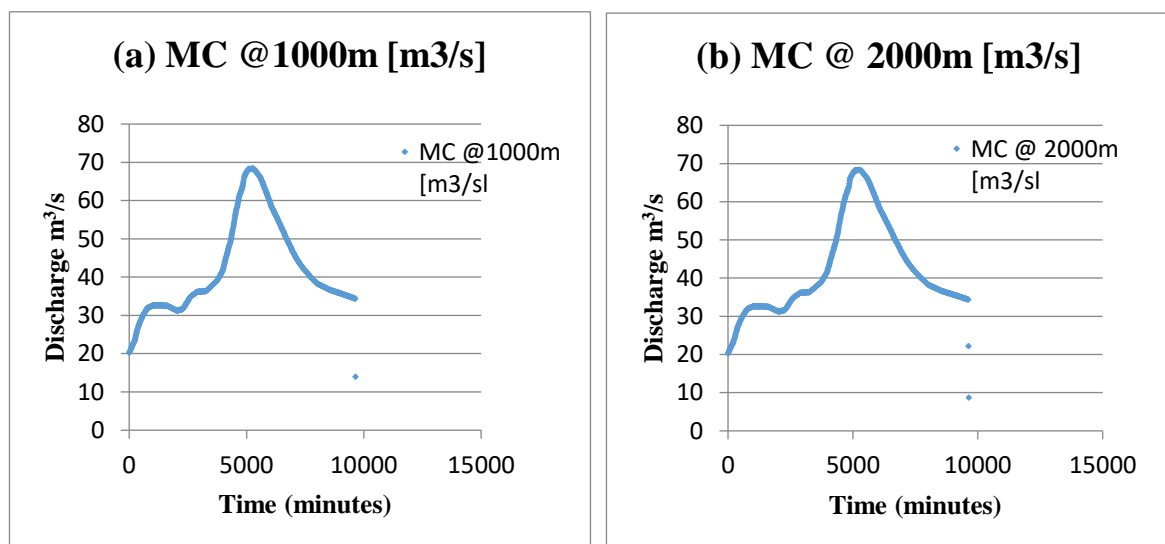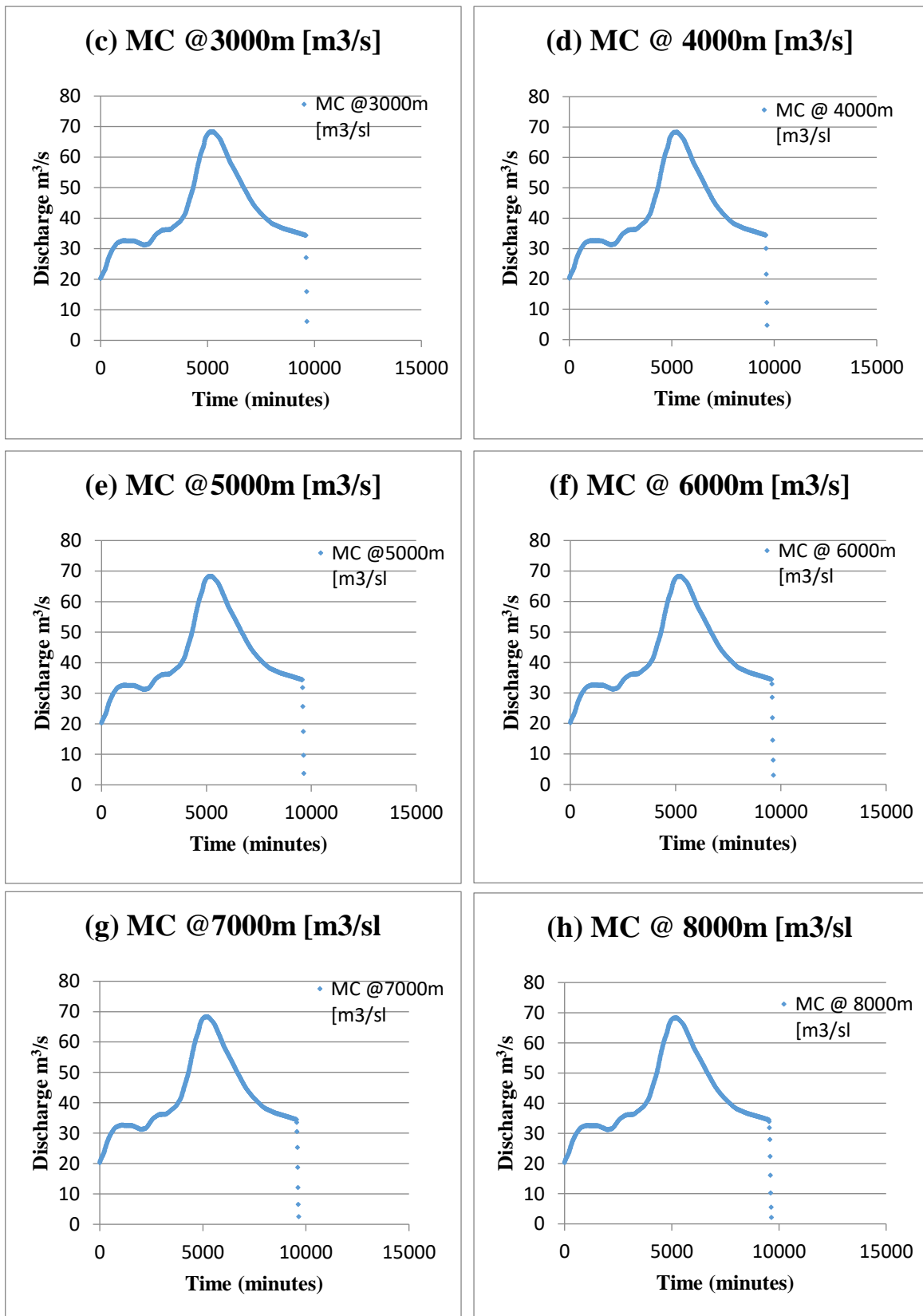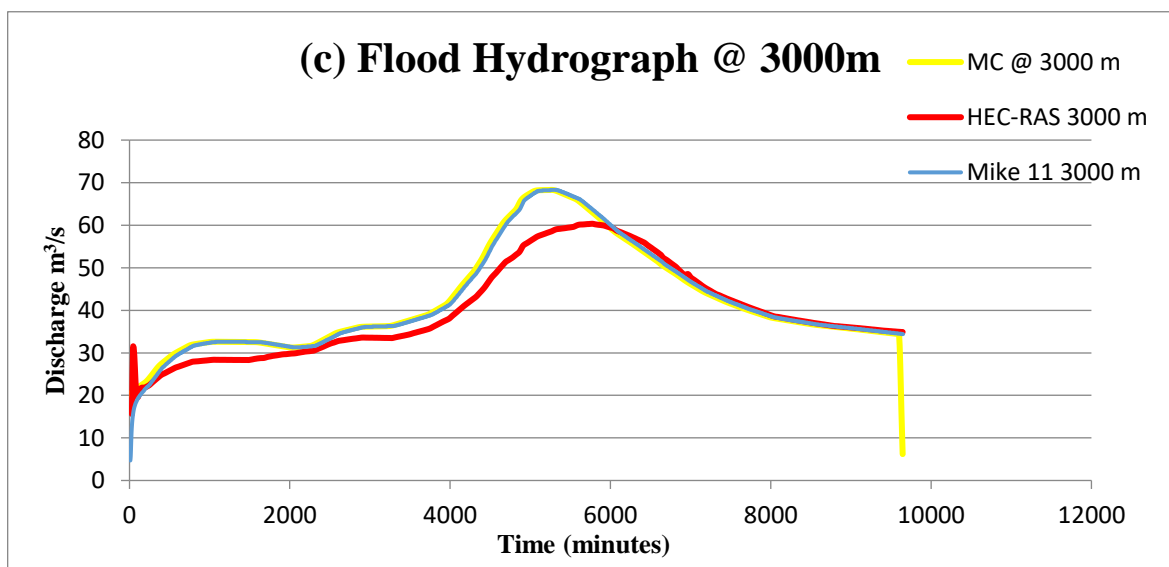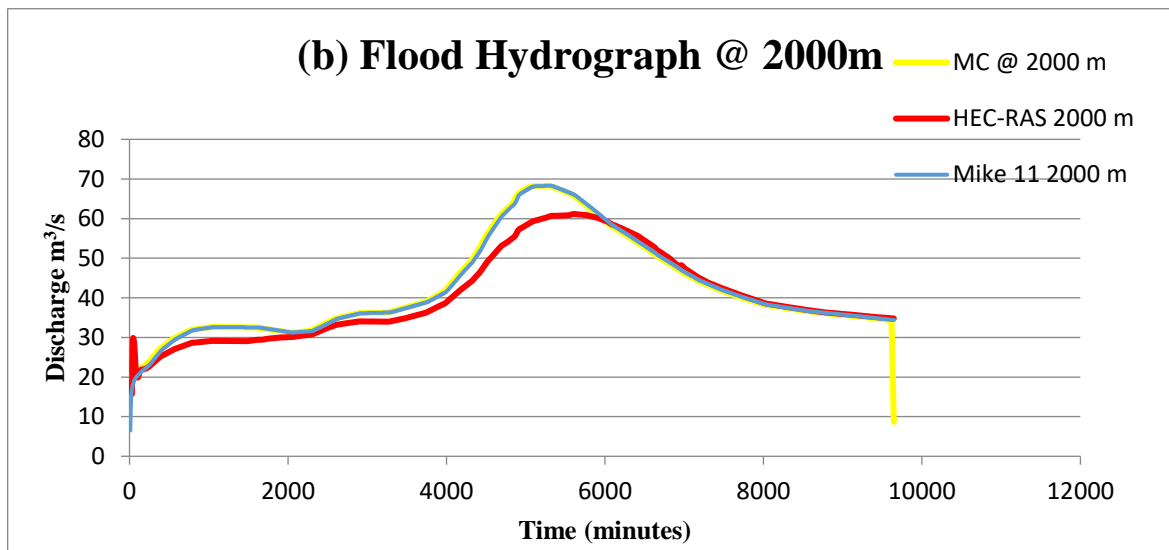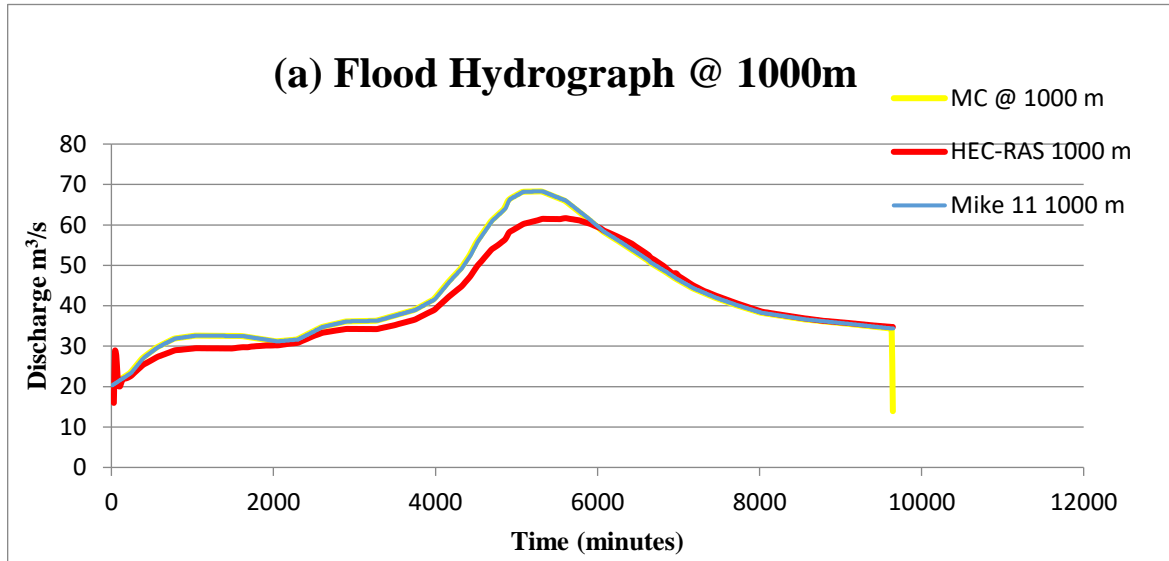
Figure 19 Flood hydrograph at eight sub-reaches of river Brosna for flood event 1994
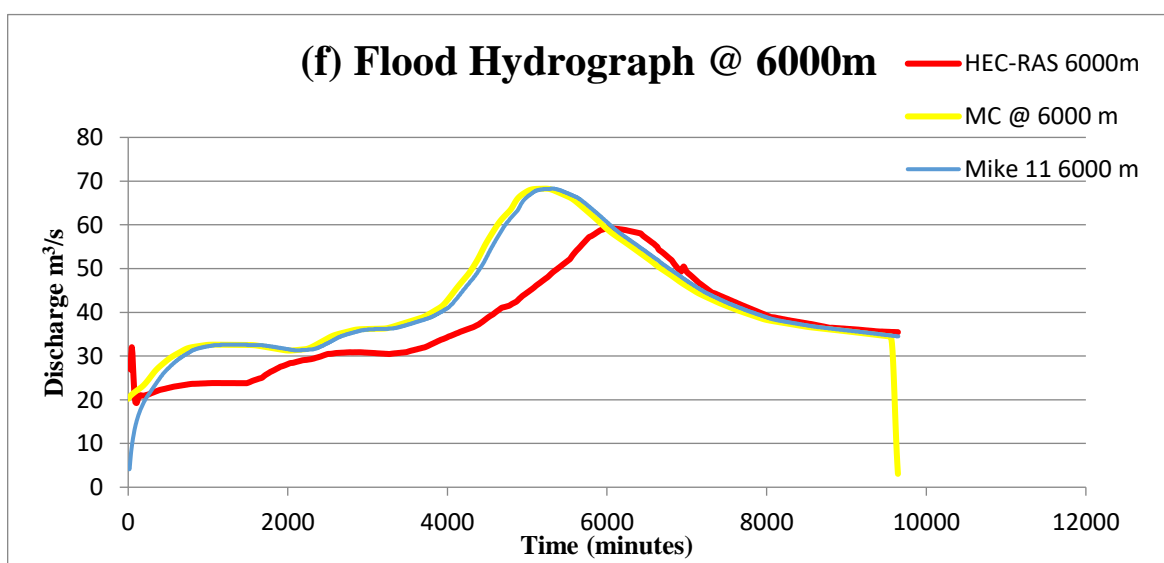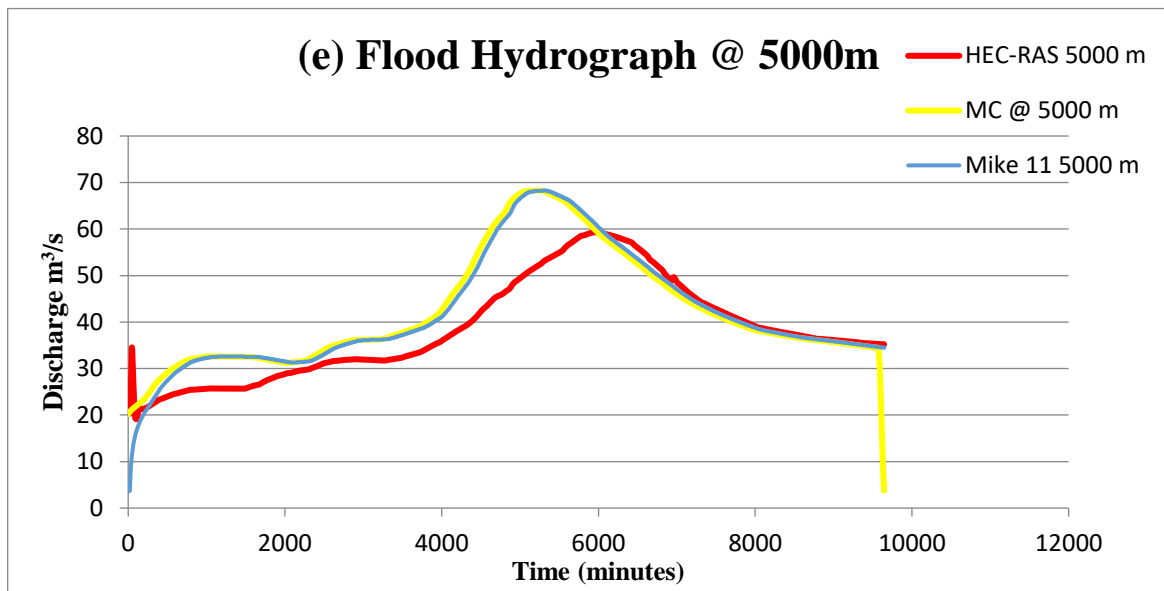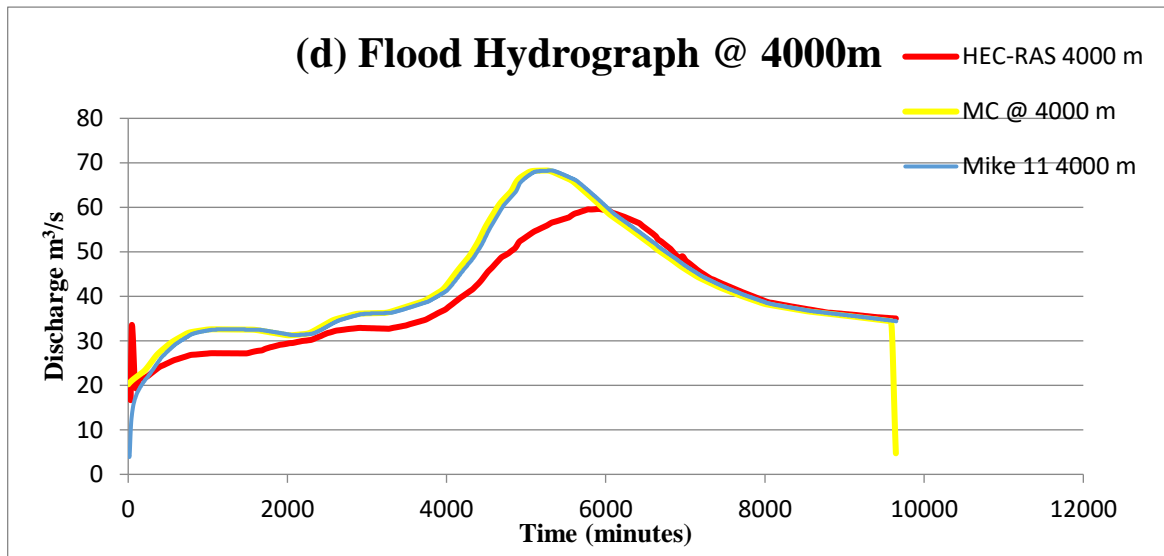
The flood hydrographs of Nov-Dec 1994 is having a good shape as shown in above Fig. 19. Despite this, the model parameters (i.e. K and X) plays a vital role and should be estimated very precisely. Here in this case due to the difference between the actual and the estimated values of these parameters, prediction suffers in cost of poor reproduction of outflow hydrograph at sub-reaches.

The application of constant parameter MC method to the flood event 1994 illustrated in Fig.19 indicates that the outflow computed from time increment 0.25 hour is not even close to the outflow hydrograph predicted from the experimental set ups. Even higher value of time increment step induce dispersion error and thus use of this method merely relates to the actual outflow hydrographs. The inflow and computed outflow reaches their peak value at same time which means that the travel time K is less than Δt.

The validation of the outflow hydrograph obtained from constant parameter MC method is done with the two software packages HEC-RAS and MIKE 11, which is shown in Fig. 20 below. The outflow obtained in both the software package are very different. The variation of the results obtained can be illustrated more clearly on the basis of graphs obtained from all application methodologies. The poor prediction of the MC method is not well trusted here in this case, which gives upper hand to the software approaches because they are easy approach wise and also results obtained in the HEC-RAS are more relatable and acceptable as compared to the Constant parameter MC method. In addition, the input parameters of such software packages are also very much similar to that of the MC method and hence no more parameters are required to work on them.

Despite the fact that more parameters help to define problem completely and more accurately with no compromise over physic of problem.
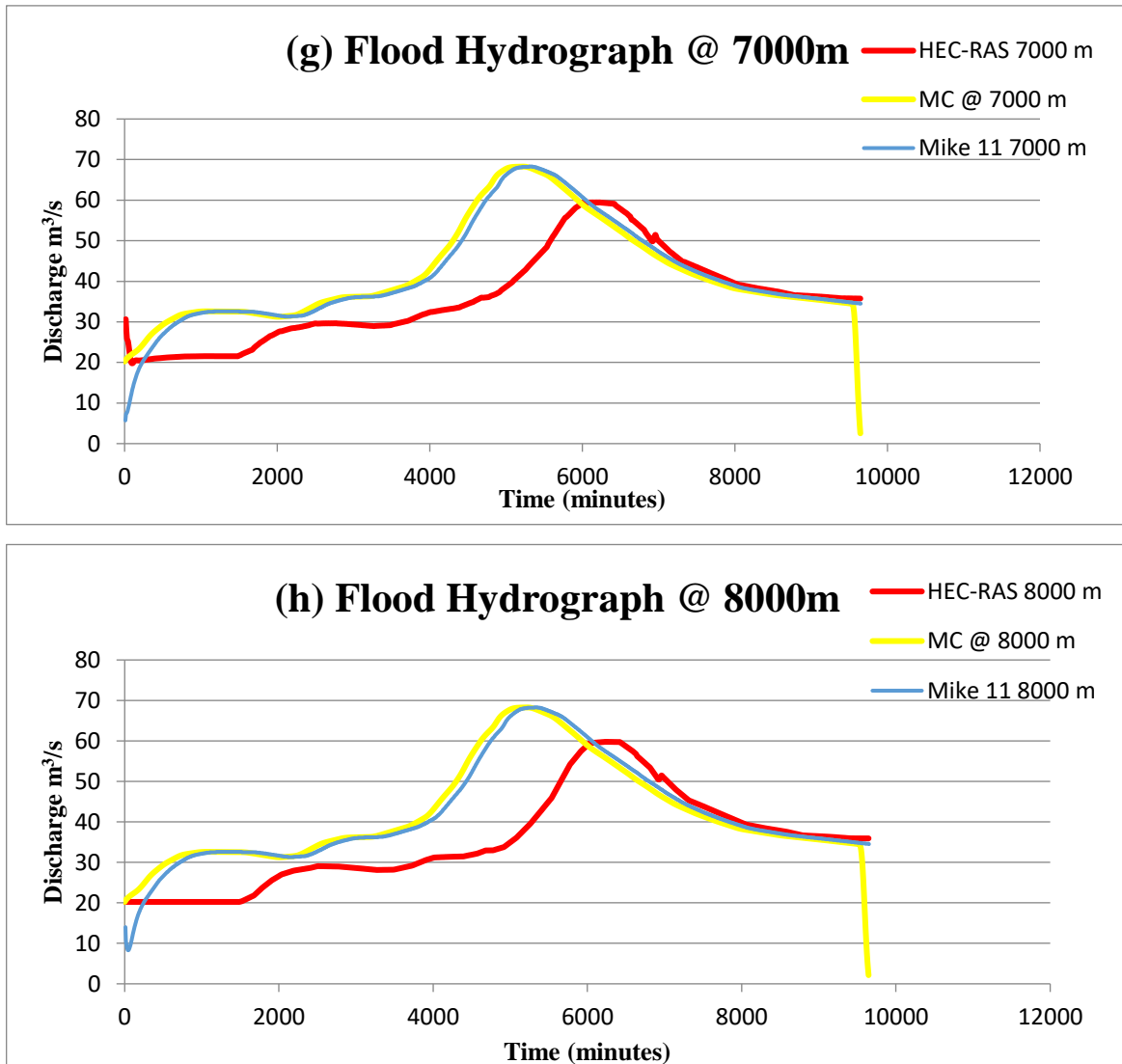
(a) Flood Hydrograph @ 1000m

(b) Flood Hydrograph @ 2000m

(c) Flood Hydrograph @ 3000m

(d) Flood Hydrograph @ 4000m

(e) Flood Hydrograph @ 5000m

(f) Flood Hydrograph @ 6000m

(g) Flood Hydrograph @ 7000m

(h) Flood Hydrograph @ 8000m

Figure 20 Flood hydrograph at eight sub-reaches for river Brosna for flood event 1994 using Muskingum-Cunge, HEC-RAS and MIKE 11

In the above Fig. 20 , the most significant change in terms of attenuation and lag can be found in the HEC-RAS results (also see Fig. 9) while MIKE 11 also shows some of the variation but the peak flow of the computed outflow reaches almost at same time of the inflow hydrograph. Beside the fact that in MIKE 11 the variation of the outflow hydrograph is very trivial but it pronounces when it comes to lower sub-reaches. This can be explained on the basis of the milder slope of the river Brosna considered which makes it difficult to simulate in the MIKE 11 software since significant outputs are not much distinct. MIKE 11 is the software, which is a complete package for flood forecasting, is developed on a small river reach by DHI. Despite the similarity of the river reach considered here in this case, problem is not well simulated.

4.7   Water storage analysis

The MC parameters K and X are two most substantial parameters estimated once for constant parameter MC method and are most widely used in many other methods including VPMC method. Regardless of its wide usage there two discrepancy which are found in the practical use of MC method. The first one is the incompetency of the method to conserve mass even though whole concept of flood routing is based on continuity and conservation of mass equations. Second most profound discrepancy is the unsteady state of storage and difference in the peak value of storage obtained using two different equations derived from continuity and prism & wedge storage equations are very indefinite in nature.

$$S_{t+\Delta t} = S_t + \left(\frac{I_{t+\Delta t} + I_t}{2} - \frac{O_{t+\Delta t} + O_t}{2}\right)\Delta t \tag{4.7}$$

The same storage can also be estimated by discretizing Eq. (4.8) and using the value of K and X determined in the section 4.6.

$$S = KX\,I + K\,(1 - X)O \tag{4.8}$$

$$S_{t+\Delta t} = K\,X\,I_{t+\Delta t} + K(1 - X)O_{t+\Delta t} \tag{4.9}$$

The below Fig.21 illustrates the plot of storage on two different storage Eq. (4.7) and (4.9).
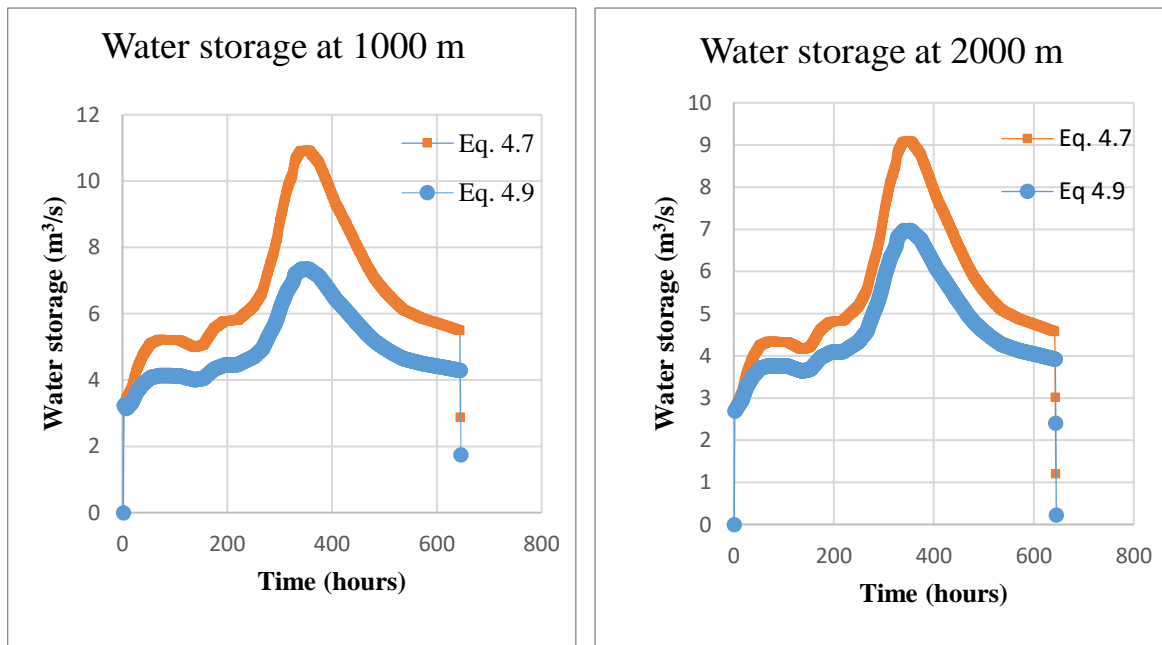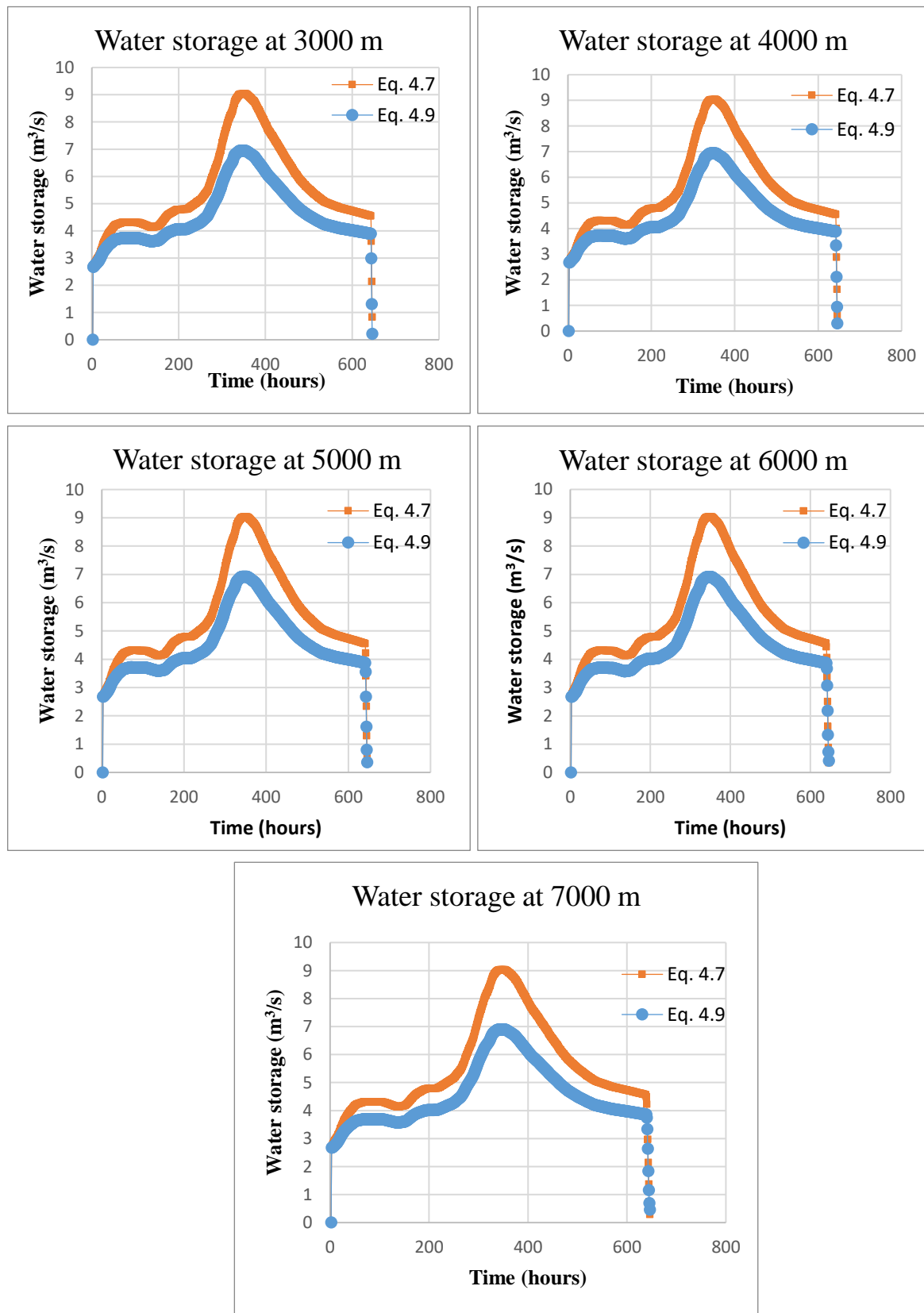
Figure 21 Storage volume computed using eq. (4.7) and (4.9)

The above figure shows the inconsistency of the MC method. Unexpectedly, none of the two equations produces same results for storage in addition to that both equations are found inconsistent to steady state conditions. From the Fig. 21 one can easily notice that both storage plot does not return to the original steady state as the consequence of the aforementioned mass imbalance (in practical experience the water is not lost but rather stored in the channel) and another possible observation is that the Eq. (4.9) always produce storage lower than it should be.

Chapter 5

ERROR ANALYSIS

5.1   Predicted Relative Error for Different Models

An overall comparison of the estimated values of depth-averaged velocity U_d value has been done for different models based on relative error values. A relative error value can be estimated through $\{((U_p - U_m)/U_m) \times 100\}$ where U_p is the predicted depth-averaged velocity and U_m is the measu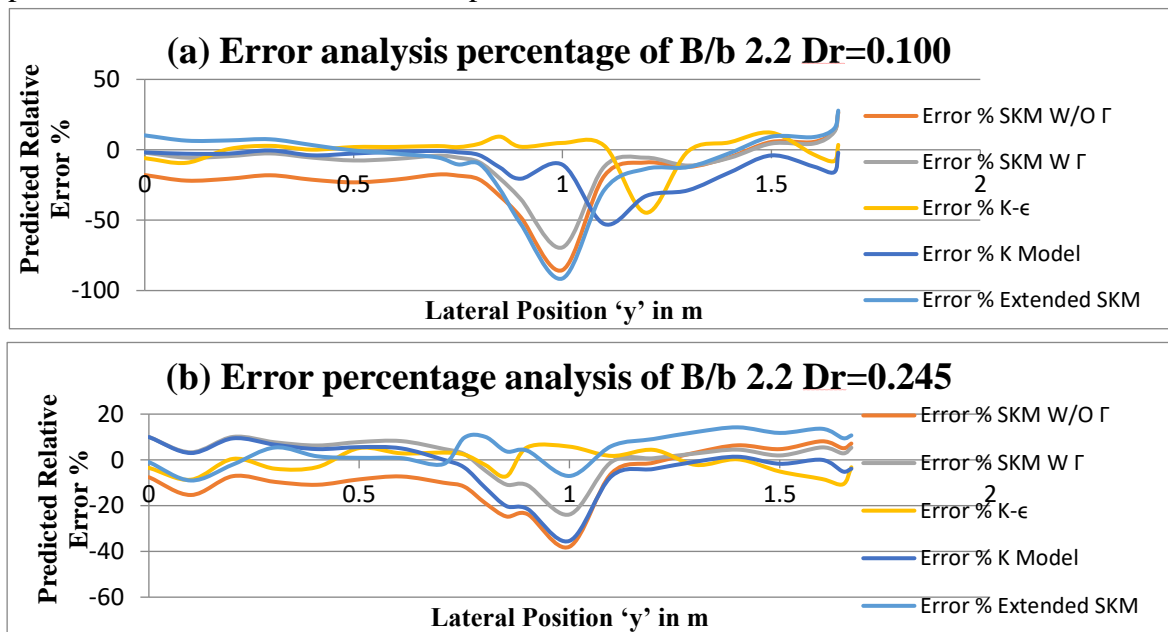red depth-averaged velocity i.e. experimental U_d. The relative errors are plotted against the lateral position of channel and the fluctuation of error is observed for the lateral distribution of depth-averaged velocity. In Fig 22 the relative error distribution over lateral position of the cross section of channel is represented.

The comparison among the measured value and predicted value for different methods are also done on the basis of the line of good agreement. The predicted values of depth-averaged velocity is plotted against the measured value of depth-averaged velocity and the values which are closer to the line drawn at 45° from origin in first quadrant (also known as line of good agreement) is considered to be good prediction. In Fig 23 the comparison of the predicted and measured value are represented.
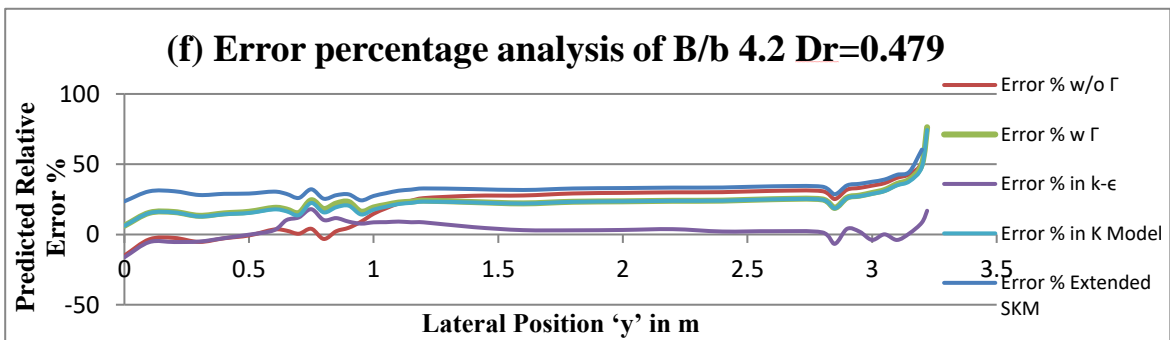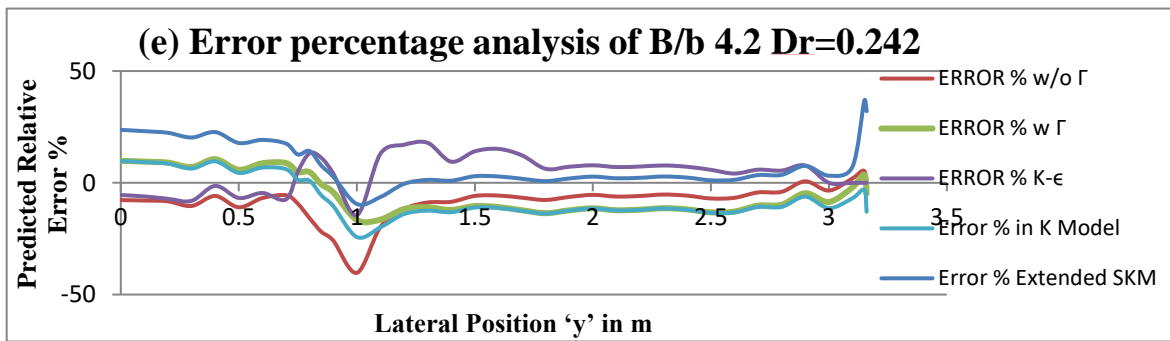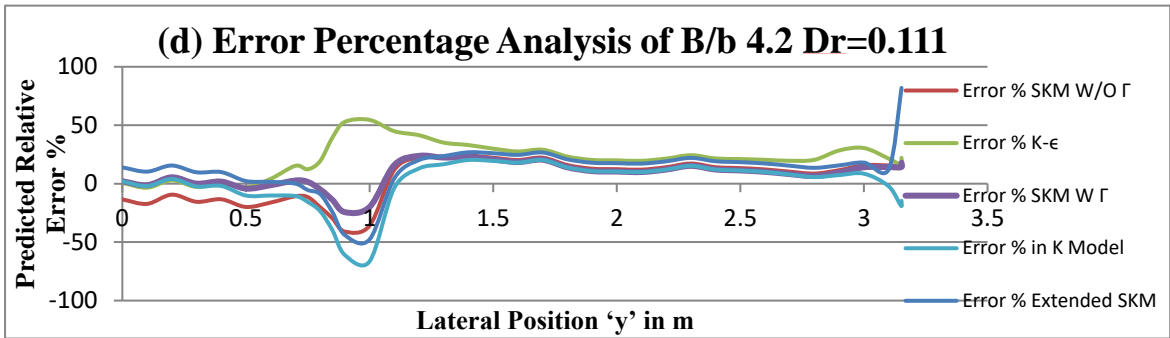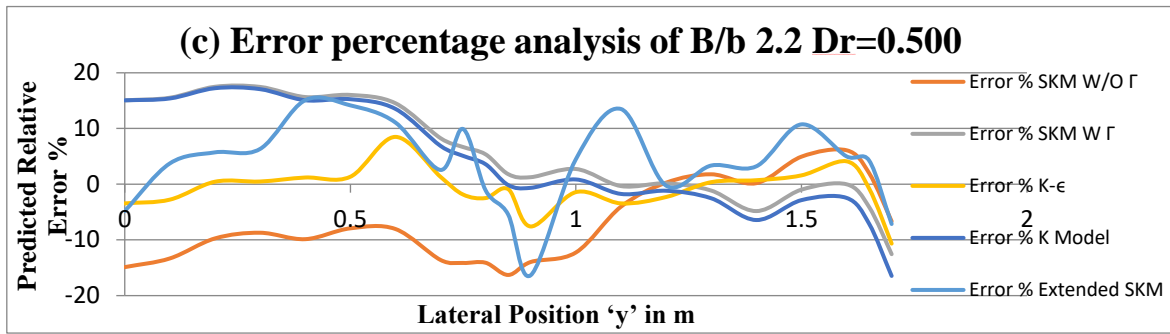
Figure 22 A comparisons among the predicted relative error values by the different models

(a) Error analysis B/b 2.2 Dr= 0.100

(b) Error analysis B/b 2.2 Dr=0.245

(c) Error analysis B/b 2.2 Dr=0.500

(d) Error analysis B/b 4.2 Dr=0.111
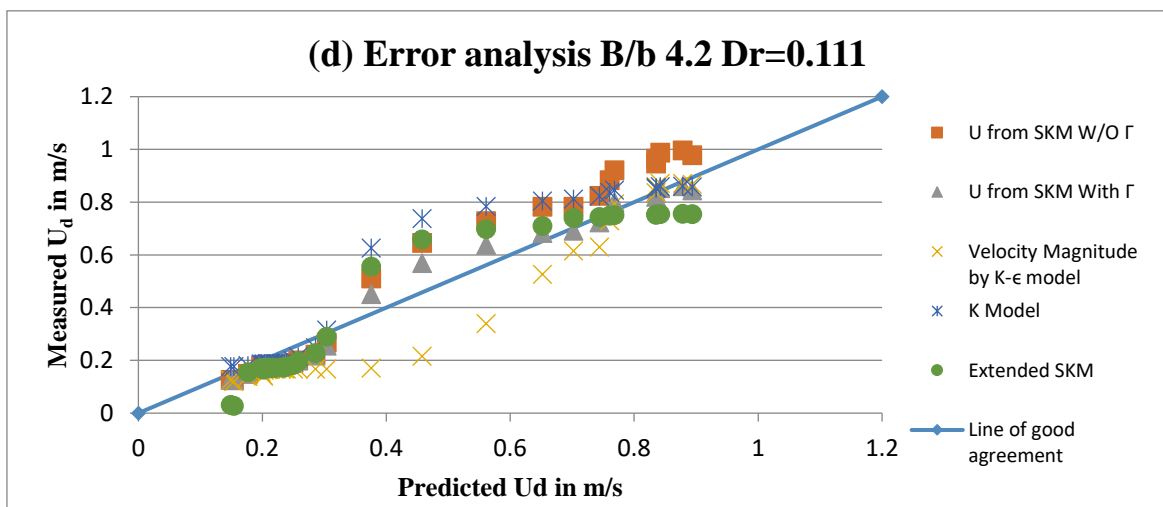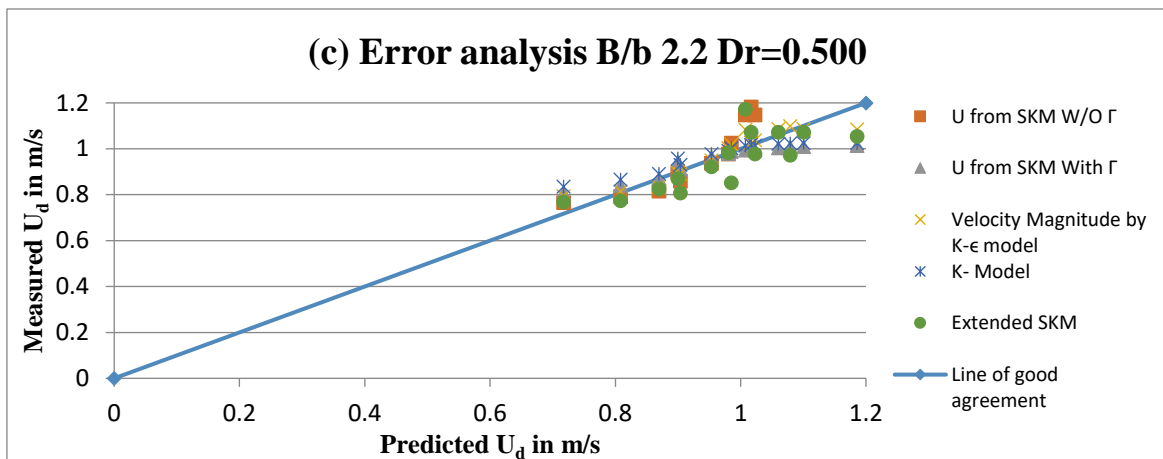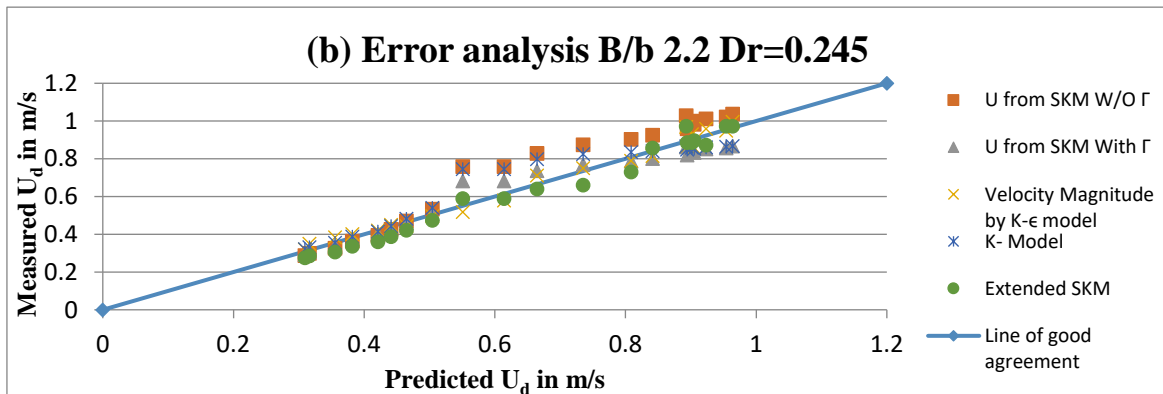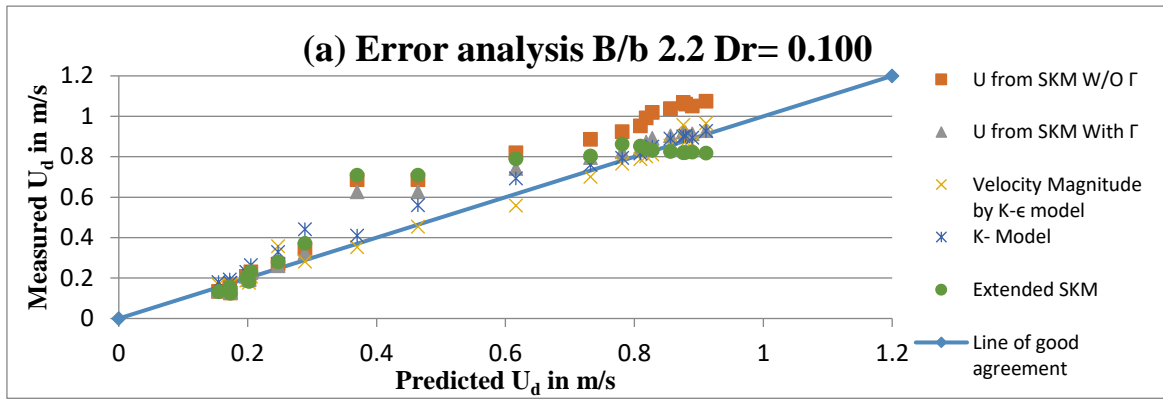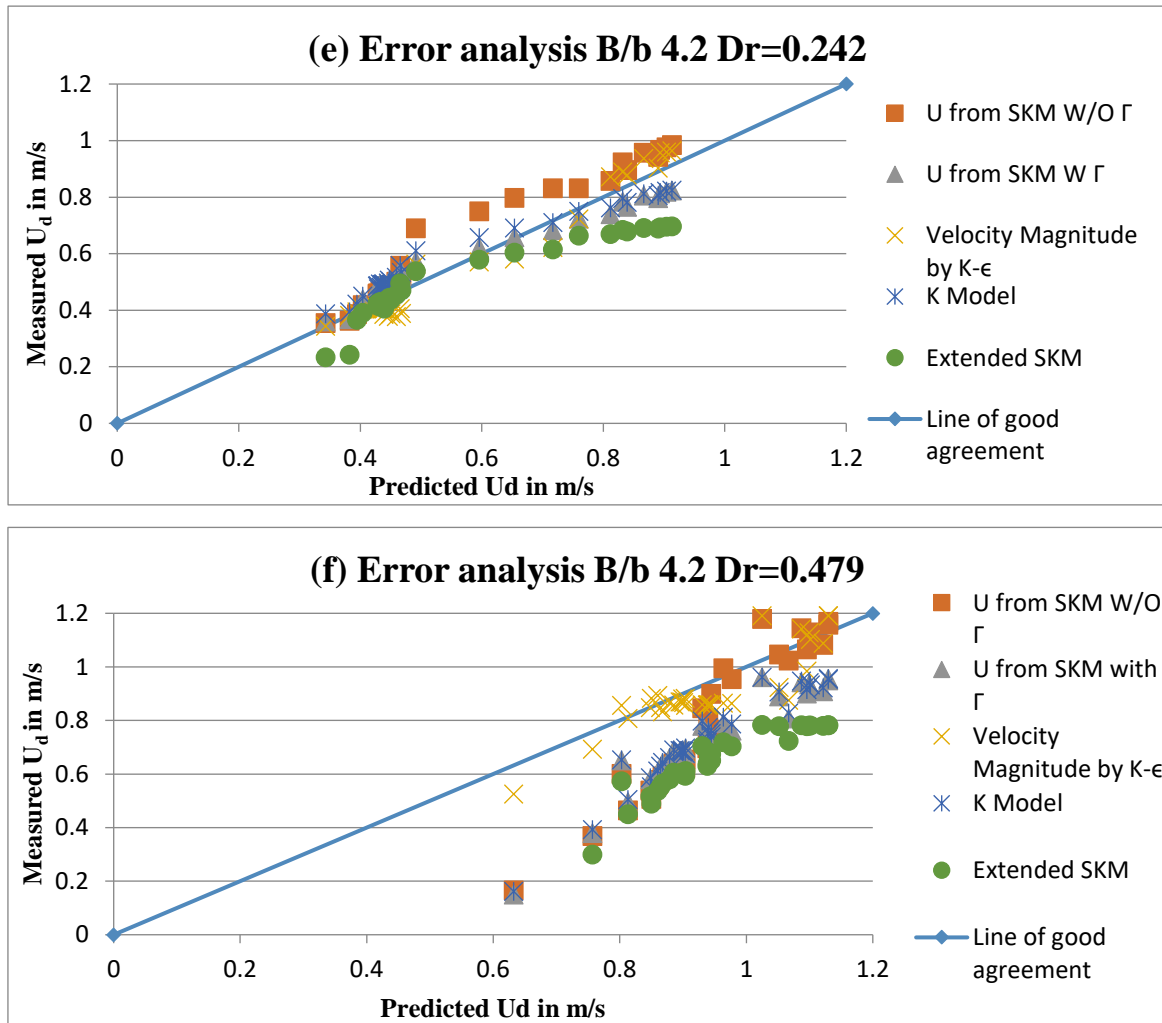
Figure 23 A comparisons among the predicted values and the Measured value of depth-averaged velocity by the different models

5.2   Conservation of Mass Consideration

The percentage error in the volume storage can be estimated through Eq. 4.10.

$$\text{EVOL\%} = \left[\left\{\frac{\sum_{i=1}^{N} Q_{ci}}{\sum_{i=1}^{N} I_i}\right\} - 1\right] \times 100 \tag{4.10}$$

where Q_{ci} is the ith ordinate of the computed discharge hydrograph and I_i is the ith ordinate of inflow hydrograph at the same time level as that of outflow discharge hydrograph. A negative sign of EVOL% indicates that the loss of mass is occurring while positive sign mean that the gain of mass occurred. A value of EVOL% is zero when total mass is conserved.

Following table 6 represent the value of EVOL% for the constant parameter MC method, HEC-RAS, and Mike 11.

Table 6 Conservation of mass consideration EVOL% of every sub-reach of river Brosna flood event 1994

Model	Branch 1000m	Branch 2000m	Branch 3000m	Branch 4000m	Branch 5000m	Branch 6000m	Branch 7000m
Muskingum-Cunge model (Constant parameter)	-0.0479	-0.0463	-0.0419	-0.0386	-0.0365	-0.0350	-0.0603
HEC-RAS	1.5175	3.6312	2.9222	2.2722	1.6670	1.0932	0.5410
MIKE 11	0.1630	-0.1399	-0.1327	-0.1222	-0.1100	-0.0948	-0.0677

Chapter 6

CONCLUSIONS AND SCOPE FOR FUTURE WORK

6.1 Analysis of modelling technique for stage discharge

The results obtained for the lateral distribution of depth-averaged velocity, boundary shear stress and stage-discharge curve for the trapezoidal compound channel using SKM model with/without secondary flow term, K-model, Kordi et al. (2015) model and k-ϵ model are represented in the last section. A number of conclusions drawn from Fig.16, Fig.17 and Fig. 18 can be stated as:

1) In general, all five models shows same trend for the U_d (y) results which agree reasonably well with experimental data in some model while in others there is no such agreement over some part of the channel or the floodplain due to poor calibration of the parameters.

2) In SKM, without Γ model has always over predicted for both U_d (y) and τ_b (y) in floodplain and interface region since in both the region secondary flow cells have significant effect due to mass transfer. No secondary flow consideration means that the only governing parameter is friction factor f since eddy viscosity coefficient λ is taken constant for every model. Meanwhile for main channel it have comparatively shown closer plots with experimental result in both U_d (y) and τ_b (y) prediction.

3) In the SKM with Γ model gives better results in comparison to SKM without Γ over both flood plain and main channel but over interface region its dependability is very much doubtful since it only estimates the dispersion term due to helical secondary current.

4) In the K-method, the value of K has to be positive for floodplain region and negative to the main channel region, which is overruled in the assumption. Despite that, it produces agreeable result over main channel region but in case of floodplain, it has underestimated the results.

5) The extended SKM model does perform well over interface region in all relative depths. However, in higher Dr = 0.500 and 0.479 it underestimate the result over floodplain which can be tackled by considering the sign of coefficient K over the floodplain region.

6) It is clear from the Fig. 17 and Fig. 18 that k-ε performed exceptionally well which tend to indicate the ability of the model to evaluate secondary flow. By increasing, the meshing criteria in the ANSYS fluent one can achieve finer result by compromising computational time.

7) It is also clear from Fig. 17 and 18 that the main differences in the predicted results are over the mixing region where secondary flow is inevitable. As the relative depth, increases the results of various models underestimate the prediction of the depth average velocity except k-ε model.

8) Overall prediction of τ_b (y) for both the channels are showing same trend for SKM with Γ, K method, extended SKM and k-ε method. However, in the SKM without Γ model there is a drastic change in trend over the interface of the main channel and floodplain. This can also be observed for some other models, which indicatively shows poor calibration of coefficients.

9) Beside the good approximation of the U_d (y), prediction of τ_b (y) distribution not necessarily always have good agreement with experimental data, mainly due to poor modelling of secondary current cells. The sign of Γ varies laterally depending upon the sense of secondary flow current and the region of the channel it is formed. Based on the sign of Γ and the number of secondary flow cells, the number and the location of the panels should be determined.

10) All the models do exceptionally well over the main channel region. However, prediction of τ_b (y) over the interface region only k-ε and extended SKM predicted well. In the extended SKM method prediction of both U_d (y) and τ_b (y) can be refined by the good calibration of the coefficients.

11) Stage discharge plot for both the FCF phase A series 02 and 03 have been plotted for different models and they are validated with the experimental data. It is clear from the Fig. 18 that the stage discharge curve has a reasonably good agreement for both the series. Extrapolation can be used to obtain further discharge depth relation since plot obtained are overall satisfactory.

The following points may also be noted from Fig. 22 and Fig. 23:

1) A comparison of the percentage relative error values {((U$_{predicted}$ − U$_{measured}$)/U$_{measured}$)*100} is shown in Fig. 22 for all the models having B/b 2.2 and 4.2 with respect to different relative depth considered. It is quite visible from the plot that the most significant errors are found over the interface area in all the models.

2) The SKM model with and without Γ consideration have overall average percentage error of 8-20 % and 5-10% respectively. Meanwhile least overall average percentage error is of 0-3% in k-ε method whereas 3-8% and up to 10% of overall average percentage error is visible in extended SKM method and K-method respectively.

3) Similarly, in Fig. 23 a comparison of predicted depth-averaged velocity is done with the measured depth-averaged velocity. The plot obtained has a line of good agreement around which the scattered plot is represented. It is clear from the Fig. 23 that the SKM model without Γ consideration falls out of the line of good agreement which illustrates the significance of mass transfer and planform vortices consideration for such models.

4) Best results are obtained in k-ε models in all relative depths. Meanwhile other models such as K-model and extended SKM model do perform well in the lower relative depths but in the Dr = 0.479 plot of B/b 4.2 most of the analytical model fall out from the line of good agreement.

6.2 Analysis of flood routing and flood hydrograph

Flood routing through hydrological technique (i.e. MC method) and two software packages (i.e. HEC-RAS and MIKE 11) are used to obtain the outflow hydrograph at eight sub-reaches for river Bosna offaly of Ireland. The flood hydrograph of flood event Nov-Dec 1994 is considered because of its good shape as shown in Fig. 4. The following outcomes can be obtained from Fig. 19 and Fig. 20.

1. It is clear from the Fig. 19 that constant parameter MC method does not produce noticeable change in the outflow hydrograph shape for the minimum routing time increment of 0.25 hours. The outflow hydrograph computed at every 1000m does not have significant lag and hence are very close to the inflow hydrograph.

2. This same trend is visible for the MIKE 11 meanwhile HEC-RAS Fig. 20 produces a result, which have more lag and are more accurate when compared to the outflow hydrograph obtained experimentally.

3. The inflow and the computed outflow hydrograph reach their peak almost at the same time, which indicates that the routing time increment is greater than the travel time.

4. It is evident from the Fig. 20 that the constant parameter MC method is not capable for producing outflow hydrograph for this instance. This could be explained on the basis of the mild slope of the channel which does not dampen the error in the routing procedure.

This can also be noted from Fig. 21 and Table 6.

1. In the water storage analysis Fig. 21, the steady state of the storage plot is not achievable in the constant parameter MC method even though the inflow and outflow are identical. This can be another indication of the wrong estimation of the travel time parameter.

2. Second most evitable observation is the two-storage plot for the same outflow hydrograph is obtained from Eq. 4.7 and Eq. 4.9. Equation 4.9 obtained from discretizing the storage equation obtained from the assumption of prism & wedge storage always estimates lower storage than it should be.

3. The mass conservation is another big issue of these models despite the fact that the models are developed on the continuity and mass conservation equations. The loss of water is not possible case instead it is stored in the channel reach i.e. water is never lost. This can be possibly due to the milder slope and due to the inaccurate discretization of the diffusion wave model.

4. The loss of mass is estimated through the $\mathrm{EVOL(in\%)} = [\{\sum_{i=1}^{N} Q_{Ci} / \sum_{i=1}^{N} I_i\} - 1] *$ 100 for each method of flood routing considered and illustrated in the table 6. A negative sign indicated the loss of mass and positive sign indicates the gain of mass. Meanwhile $\mathrm{EVOL(in\%)}$ is when zero it indicates that the mass is fully conserved.

5. From table 6 it is clearly evident that no mass is conserved in any of the model. The loss of mass is seen in every sub-reaches of the constant parameters MC method.

6.3 Overall conclusion

The SKM and K-method includes secondary flow term while extended SKM beside the dispersion term it also takes account of mass transfer term. The analytical models have a similar trend because of the similar hydraulic parameters representing boundary resistance

via bed friction factor f, lateral shear via dimensionless eddy viscosity λ, and depth-averaged secondary flow via parameters Γ or K. Beside the similar trend, variation in results is mainly due to poor calibration or modelling of the secondary flow terms in overbank flow. Thus, analytical method accounts for the complex three-dimensional flow in compound channel and can produce useful information to the field engineers. It is demonstrated that the analytical solution of those model, which do not consider secondary flow term, are less dependable in comparison to models considering secondary flow parameters. This in turn necessitate the modelling of secondary flow and also reinforce the importance of including such effects in all open channel flow modelling of velocity and boundary shear stress distribution (via Γ or k). The K-method gives reasonably good results in some cases, but it is dependent on the K-values. Either coefficient K can be negative or positive which is to be considered while solving analytically for U_d. For the extended SKM method, secondary flow term is defined as a function of the bed shear stress and the depth-averaged streamwise velocity. Even though this method gives good results compared to others analytical solution, modelling of secondary flow term becomes a primary issue since a good calibration of secondary flow term can only fetch a good result. Most of the analytical model fails to predict precisely in higher relative depth but k-ε numerical model predicted best out of the various models. Over interface region k-ε predicted closest in most of the result. Results can be more enhanced using grid convergence index and by refining and sizing of the mesh component but due to less computational resource it is compromised in this study. In ANSYS fluent computational time can be optimized by the meshing criteria which can always fetch a fast result in cheap computational resources. Applicability of numerical model is self-justified by the results but analytical models provide easier way in least computation cost. Further experimental work is needed to investigate and model planform and streamwise vorticity in overbank flow to momentum transfer, and how turbulence parameters should be properly represented in RANS models.

The constant parameters MC method is used for the prediction of outflow hydrograph for river Brosna for the flood event 1994. Despite the simplicity and the extensive applicability of the method, their use is narrowed when it comes to mass conservation and milder slope of the channel reach. Most of the channels and rivers have milder slope and hence alternative method is required to facilitate the solution of such flood events discussed above. Software packages are reliable when the hydrologic parameters available to the user are sufficiently correct. The stage-hydrograph and flood routing are significant in terms of flood planning

and management. The overall dependency on stage-discharge and stage-hydrograph is very high which in turns depend on the correctness of the modelling approach. Flood forecasting can also be done on the basis of the methods shown in this study. The methods discussed above are easy and can be used by field engineers for flood studies and management.

6.4 Scope for Future Research Work

Application of the different modelling techniques in stage–discharge are done for the trapezoidal compound channels. It can also be done for the natural river reach using all the five models as discussed above. Calibration of the different parameters like friction factor, eddy viscosity coefficients and secondary flow term in the natural river system will also play a key role for prediction of depth-averaged velocity distribution, boundary shear stress distribution and stage discharge curve.

For the flood routing technique one can go for VPMC method in which parameters like travel time and weighting factor varies at each routing time step. The incapability of the constant parameter MC method in terms of mass conservation and unsteady state of storage can be resolved through proper discretization of the storage equation and also by correcting the travel time parameter. Different channels with different slopes can also be used to check the feasibility of the above-discussed models in steeper slope. Finally, different routing time size can be used to obtain outflow hydrograph and one can check the variation of the results based on the routing time size.

References

Abril, J.B. and Knight, D.W., (2004). "Stage-discharge prediction for rivers in flood applying a depth-averaged model." *Journal of Hydraulic Research*, IAHR, Vol. 42, No. 6, pp 616-629.

Ackers, P. (1992). "Hydraulic design of two-stage channels." Proc. Inst. Civ. Eng. Water Marit. Energy, 96(4), 247–257.

Al-Khatib, I. A., Dweik, A. A., & Gogus, M. (2012). "Evaluation of separate channel methods for discharge computation in asymmetric compound channels." *Flow Measurement and Instrumentation*, 24, 19-25.

Azevedo, R., Rojas-Solórzano, L., & Leal, J. (2012). "Experimental characterization of straight compound-channel turbulent field." 2nd European IAHR Congress; 06/2012.

Boroughs, C., Craig, B. and Zagona, E. (2002). "Daily flow routing with the Muskingum-Cunge method in the Pecos River- RiverWare Model." Proceedings of the Second Federal Interagency Hydrologic Modelling Conference, Las Vegas: NV.

Boroughs, C., Craig, B. and Zagona, E. (2002). "Daily flow routing with the Muskingum-Cunge method in the Pecos River- RiverWare Model." Proceedings of the Second Federal Interagency Hydrologic Modelling Conference, Las Vegas: NV.

Bousmar, D., and Zech, Y. (1999). "Momentum transfer for practical flow computation in compound channels." *J. Hydraul. Eng*., 10.1061/ (ASCE)0733-9429(1999)125:7(696), 696–706.

Bousmar, D., Zech, Y. (2002). "Periodical turbulent structures in compound channels." River Flow 2002, 1, 177–185, D. Bousmar, Y. Zech, eds. A.A. Balkema, Abingdon, UK.

Cappelaere, B. (1997). "Accurate Diffusive Wave Routing." *J. Hydraulic Eng*., ASCE, 123(3),174–181.

Castanedo, S., Medina, M., Mendez, F.J. (2005). "Models for the turbulent diffusion terms of shallow water equations." *J. Hydr. Engng*. 131(3), 217–223.

Chadwick, A., Morfett, J. (1993). "Hydraulics in Civil and Environmental Engineering." *2nd ed., London: E & F N Spon*.

Chao, L. I. U., SHAN, Y. Q., YANG, K. J., & LIU, X. N. (2013). "The characteristics of secondary flows in compound channels with vegetated floodplains." *Journal of Hydrodynamics*, Ser. B, 25(3), 422-429.

Chin, D. (2000). "Water Resources Engineering." New Jersey: Prentice Hall.

Chlebek, J., Knight, D.W. (2006).”A new perspective on sidewall correction procedures, based on SKM modelling.” RiverFlow 2006, Lisbon 1, 135–144, R.M.L. Ferreira, E.C.T.L. Alves, J.G.A.B. Leal, A.H. Cardoso, eds. Taylor & Francis, London.

Chow, V. T. (1964) "Handbook of Applied Hydrology." McGraw-Hill, New York, NY.

Chow, V. T., Maidment, D. R., and Mays, L. W. (1988). "Applied Hydrology." McGraw-Hill, New York, NY.

Chow, V.T., (1959). “Open channel hydraulics.” International Edition, McGraw Hill, New York.

Connected Water, (2006). “Managing the linkages between surface water and ground water.”[Online]Availablefrom:http://www.connectedwater.gov.au/framework/baseflow_separation.php.

Conway, P., O'Sullivan, J. J., & Lambert, M. F. (2012). “Stage–discharge prediction in straight compound channels using 3D numerical models.”

Cunge, J. A. (1969). "On the subject of a flood propagation computation method (Muskingum method)." Delft, The Netherlands, *J. Hydr. Res*., 7(2), 205–230.

Cunge, J. A., Holly, F.M. and Verwey, A., (1980). "Practical aspects of computational river hydraulics." The Pitman Press, Bath, UK.

DHI Water and Environment: MIKE 11 (2000). User Guide and Reference Manual, DHIWater & Environment, Horsholm, Denmark.

Elbashir, S. (2011). “Flood routing in natural channels using Muskingum methods” (Doctoral dissertation, Dublin Institute of Technology).

Elliott, S.C.A. and Sellin, R.H.J., (1990). “SERC flood channel facility: skewed flow experiments.” *Journal of Hydraulic Research*, IAHR, Vol. 28, No. 2, pp 197-214.

Ervine, D. A., Babaeyan-Koopaei, K., and Sellin, R. H. J. (2000). “Twodimensional solution for straight and meandering overbank flows.” *J. Hydraul. Eng*., 10.1061/(ASCE)0733-9429(2000)126:9(653), 653–669.

Fernandes, J. N., Leal, J. B., & Cardoso, A. H. (2015). “Assessment of stage–discharge predictors for compound open-channels.” *Flow Measurement and Instrumentation*, 45, 62-67.

Garbrecht, J., Brunner, G. (1991). “A Muskingum-Cunge Channel Flow Routing Method for Drainage Networks Davis: US Army Corps of Engineers-Hydrologic Engineering Centre.”

Gessner, F.B., (1973). "The origin of secondary flow in turbulent flow along a corner." *Journal of Fluid Mechanics*, Vol. 58, Part 1, pp 1-25.

Graf, W. H. (1991). "Flow resistance over a gravel bed: Its consequence on initial sediment movement." Fluvial hydraulics of mountain regions: Lecture notes in earth sciences, Vol. 37, A. Armanini and G. Di Silvio, eds., Springer, Berlin, Heidelberg, 15–32.

Guo, J. (2006). "Urban Hydrology and Hydraulic Design." Highlands Ranch: Water Resources Publications, LLC.

Guo, J. and Julien, Y., (2005). "Shear stress in smooth rectangular open-channel flows." *Journal of Hydraulic Engineering*, ASCE, Vol. 131, No. 1, January, pp 30-37.

Han, D. (2010). "Concise Hydrology." London: bookboon.com Ltd.

Heatherman,W. (2008). "Flood Routing On Small Streams: A review Of Muskingum-Cunge, cascading Reservoirs, and Full Dynamic Solutions." [Online], Available from: 88 http://stormwater.jocogov.org/Projects/Reports/Heatherman_ku_0099D_10020_DATA_1[1].pdf [Accessed 2 November 2011].

Horton, R.E, (1933). "Separate roughness coefficients for change bottoms and sides." *Engineering News Record*, Vol. 111, No. 22, pp652-653.

Ikeda, S. and Kuga, T., (1997). "Laboratory study on large horizontal vortices in compound open channel flow." *Journal of Hydraulic, Coastal and Environmental Engineering, JSCE*, Vol. 45, pp 493- 498.

Ikeda, S., (1999)."Role of lateral eddies in sediment transport and channel formation." River Sedimentation, Jayawardena, Lee and Wang, eds., Balkema Rotterdam, 195-203.

Ikeda, S., Sano, T., Fukumoto, M. And Kawamura, K., (2001). "Organised horizontal vortices and lateral sediment transport in compound channel flows." *Journal of JSCE*, (accepted).

ISO 1100-2, (1998). "Measurement of liquid flow in open channels - Part 2: Determination of the stage-discharge relation."

Jesson, M., Sterling, M., & Bridgeman, J. (2012). "Modeling flow in an open channel with heterogeneous bed roughness." *Journal of Hydraulic Engineering*, 139(2), 195-204.

Johansson, A.V. and Alfredsson, P.H., (1986). "Structure of turbulent channel flows". Chapter 25, Encyclopedia of Fluid Mechanics, Volume 1-Flow phenomena and measurement, Editor Cheremisinoff, N.P., Gulf Publishing House.

Johnson, D. (1999). "Channel Routing." [Online] available from http://www.comet.ucar.edu/class/hydromet/07_Jan19_1999/html/routing/sld066.html.

Kalinin, G. P. and Miljukov, P. I. (1958). "Approximate methods for computing unsteady flow movement of water masses." Transactions, *Central Forecasting Institute*. Issue 66 (in Russian).

Keller, R.J., and Rodi, W. (1988). "Prediction of flow characteristics in main channel/flood plain flows." *Journal of Hydraulic Research* 26(4): 425–441.

Klein, A., (1981). "Turbulent developing pipe flow." Journal of Fluids Engineering, ASME, Vol. 103, pp. 243–249.

Knight, D. (2013). "Hydraulic problems in flooding: from data to theory and from theory to practice." In *Experimental and computational solutions of hydraulic problems* (pp. 19-52). Springer Berlin Heidelberg.

Knight, D. W. (1981). "Boundary shear in smooth and rough channels." *J. Hydr*. Div., 107, HY7, 839–851.

Knight, D. W., and Abril, B. (1996). "Refined calibration of a depthaveraged model for turbulent flow in a compound channel." Proc. Inst. Civil Eng. Water Marit. Energy, 118(3), 151–159.

Knight, D. W., and Sterling, M. (2000). "Boundary shear in circular pipes running partially full." *J. Hydraul. Eng*., 126(4), 263–275.

Knight, D.W. (1992). SERC Flood Channel Facility experimental data — Phase A. 1-15. SR Rep. No. 314, HR.

Knight, D.W. and Abril C., J.B., (1996). "Refined calibration of a depth-averaged model for turbulent flow in a compound channel." Proceedings of the Institution of Civil Engineers, Journal of Water, Maritime and Energy, Vol. 118, pp 151-159, September, 11017.

Knight, D.W. and Patel, H.S., (1985). "Boundary shear in smooth rectangular ducts." *Journal of Hydraulic Engineering*. ASCE, Vol. 111, No. 1, January, pp. 29-47.

Knight, D.W. and Shiono, K., (1996). "River channel and floodplain hydraulics." Chapter 5, Floodplain Processes, Editors Anderson, M.G., Walling, D.E. and Bates, P.D., John Wiley & Sons Ltd, Chichester.

Knight, D.W., (2001). "Flow and sediment transport in two-stage channels." Keynote Lecture, Proc. 2nd IAHR Symposium on River, Coastal and Estuarine Morphodynamics, September, Obihiro, Japan, 1-20.

Knight, D.W., (2006). "River flood hydraulics: theoretical issues and stage-discharge relationships." Chapter 17, River Basin Modelling for Flood Risk Mitigation, pp 301- 334, Editors DW Knight & A Y Shamseldin, Taylor & Francis.

Knight, D.W., and Demetriou, J. D. (1983). "Flood plain and main channel flow interaction." *J. Hydraul. Eng*., 10.1061/(ASCE)0733-9429(1983) 109:8(1073), 1073–1092.

Knight, D.W., Omran, M. and Tang, X., (2007). "Modelling depth-averaged velocity and boundary shear in trapezoidal channels with secondary flows." *Journal of Hydraulic Engineering*, ASCE, Vol. 133, No. 1, January, pp. 39-47.

Knight, D.W., Sellin, R.H.J. (1987). "The SERC flood channel facility." *J. Institution of Water and Env. Management* 1(2), 198–204.

Kolmogorov, A. N. (1942). "The equations of turbulent motion in an incompressible fluid." Izvestia Academy of Sciences, USSR; Physics 6, 56–58 (in Russian).

Kordi, H., Amini, R., Zahiri, A., & Kordi, E. (2015). "Improved Shiono and Knight Method for Overflow Modeling." *Journal of Hydrologic Engineering*, 20(12), 04015041.

Koussis, A. D. (1983) "Comparison of Muskingum method difference scheme." *Journal of Hydraulic Division*, ASCE, 106(5), 925–929.

Krishnappan, B. G., & Lau, Y. L. (1986). "Turbulence modeling of flood plain flows." *Journal of hydraulic engineering*, 112(4), 251-266.

Lambert, M. F., and Sellin, R. H. J. (1996). "Discharge prediction in straight compound channels using the mixing length concept." *J. Hydraul. Res.*, 34(3), 381–394.

Lambert, M.F. and Myers, W.R., (1998). "Estimating the discharge capacity in straight compound channels." Proceedings of the Institution of Civil Engineers, Journal of Water, Maritime and Energy, Vol. 130, pp 84-94, June, 11530.

Lambert, M.F., and Myers, W.R. (1998). "Estimating the discharge capacity in straight compound channels." Proceedings of the Institution of Civil Engineers, Journal of Water, Maritime and Energy, Vol. 130, pp 84-94, June, 11530,

Liu Z. and Todini E. (2002). "Towards a comprehensive physically based rainfall-runoff model." *Hydrol. Earth Syst. Sci.*, 6(5), 859–881.

Liu, C., Liu, X. N., & Yang, K. J. (2014). "Predictive model for stage-discharge curve in compound channels with vegetated floodplains." *Applied Mathematics and Mechanics*, 35(12), 1495-1508.

Liu, C., Luo, X., Liu, X., & Yang, K. (2013). "Modeling depth-averaged velocity and bed shear stress in compound channels with emergent and submerged vegetation." *Advances in Water Resources*, 60, 148-159.

Liu, Z. and Todini, E. (2004) "Assessing the TOPKAPI non-linear reservoir cascade approximation by means of a characteristic lines solution." *Hydrol. Processes*, 19(10), 1983–2006.

Lorena, M. (1992). "Meandering compound flow." Ph.D. thesis, Univ. of Glasgow, Glasgow, U.K.

Lotter, G.K. (1933). "Considerations on hydraulic design of channels with different roughness of walls." Translations of the All-Union Scientific Research Institute of Hydraulic Engineering, Leningrad, Vol. 9, pp 238-241.

Mays, L., Tung, Y. (2002). "Hydro-systems engineering and management." Highlands Ranch: Water Resources Publications, LLC.

McCarthy, G. T. (1940). "Flood Routing, Chap. V of 'Flood Control'." The Engineer School, Fort Belvoir, Virginia, pp. 127–177.

McCarthy, G.T., (1938). "The unit hydrograph and flood routing." In: Conf. North Atlantic Division, U.S. Army Corps of Engineers, New London, Conn.

McGahey, C. (2006). "A practical approach to estimating the flow capacity of rivers." PhD Thesis, Open University, Milton Keynes, UK.

McGahey, C., Samuels, P.G., Knight, D.W. (2006). "A practical approach to estimating the flow capacity of rivers: Application and analysis." RiverFlow 2006, Lisbon 1, 303– 312. Taylor & Francis, London, UK.

Merkel, W. (2002). "Muskingum-Cunge Flood Routing Procedure in NRCS Hydrologic Models." Proceedings of the second federal Interagency Hydrologic Modelling Conference, Chocorua.

Munson, B.R., Young, D.F. and Okiishi, T.H., (2002). "Fundamentals of fluid mechanics." *John Wiley & Sons*, 4th Edition.

Myers, W. R. C. (1978). "Momentum transfer in a compound channel." *J. Hydraul. Res.*, 16(2), 139–150.

Myers, W.R.C. & Elsawy, E.M., (1975). "Boundary shear in channel with flood plain." *Journal of the Hydraulics Division*, ASCE, Vol. 101, No. 7, pp 933-946.

Myers, W.R.C. and Brennan, E.K., (1990). "Flow resistance in compound channels." *Journal of Hydraulic Research*, IAHR, Vol. 28, No. 2, pp 141-155.

Myers, W.R.C., (1978). "Momentum transfer in a compound channel." *Journal of Hydraulic Research*, IAHR, Vol 16, No 2 p.139-150.

Nash, J. E. (1958). "The form of the instantaneous unit hydrograph." IUGG General Assembly of Toronto, Vol. III – IAHS Publ., 45, 114– 121.

Nezu, I and Nakagawa, H. (1993). "Turbulence in open-channel flows." In: IAHR Monograph Series. Rotterdam: Balkema.

Nezu, I. and Nakagawa, H., (1984). "Cellular secondary currents in straight conduit." *Journal of Hydraulic Engineering*, ASCE, Vo. 110, No. 2, February, pp. 173-193, Paper No. 18581.

Omran, M. (2008). "New developments in predicting stage–discharge curves, velocity and boundary shear stress distributions in open channel flow." *Water Environ. J.*, 22(2), 131– 136.

Omran, M., and Knight, D. W. (2010). "Modelling secondary cells and sediment transport in rectangular channels." *J. Hydraul. Res.*, 48(2), 205–212.

Parsaei, A., & Haghiabi, A. H. (2015). "Hydraulic analysis of compound open channel." *Journal of Applied Research in Water and Wastewater*, 2(1), 137-142.

Pasche, E.R.G., and Evers, P. (1985). "Flow in compound channels with extreme flood plain roughness." 21st IAHR Congress, Melbourne, Australia; 384–389.

Patankar, S. V. (1980). "Numerical Heat Transfer and Fluid Flow." Hemisphere Publishing Corporation, Taylor & Francis Group, New York.

Patel, V.C., (1965). "Calibration of the Preston tube and limitations on its use in pressure gradients." *Journal of Fluid Mechanics*. Cambridge University Press, Vol. 23, Part 1, pp 185-208.

Pavlovskii, N., (1931). "On a design for uniform movement in channels with nonhomogeneous walls." All-Union Scientific Research Institute of Hydraulic Engineering, Leningrad, Vol. 3, pp 157-164.

Perkins, H. J. (1970). "The formation of streamwise vorticity in turbulent flow." *J. Fluid Mech.*, 44(4), 721–740.

Perumal, M., & Price, R. K. (2013). "A fully mass conservative variable parameter McCarthy–Muskingum method: theory and verification." *Journal of Hydrology*, 502, 89-102.

Perumal, M., and Price, R.K. (2013). "A fully mass conservative variable parameter McCarthy–Muskingum method: theory and verification." *J Hydrol* 502:89–102. doi:10.1016/j.jhydrol.2013.08.023.

Perumal, M., Moramarco, T., Sahoo, B., and Barbetta, S. (2007). "A methodology for discharge estimation and rating curve development at ungauged river sites." *Water Resour Res* W02412 43(2):1–22. doi:10.1029/2005WR004609.

Perumal, M., Moramarco, T., Sahoo, B., and Barbetta, S. (2010). "On the practical applicability of the VPMS routing method for rating curve development at ungauged river sites." *Water Resour Res* 46(3):1–9. doi:10.1029/ 2009WR008103, W03522.

Perumal, M., O'Connell, P. E., and Ranga Raju, K. G. (2001). "Field Applications of a Variable-Parameter Muskingum Method." *J. Hydrol. Eng.*, ASCE, 6(3), 196–207.

Perumal, M., Sahoo, B., Moramarco, T., and Barbetta, S, (2009). "Multilinear Muskingum method for stage-hydrograph routing in compound channels." *J Hydrol Eng* ASCE 14(7):663–670. doi:10.1061/(ASCE)HE.1943-5584. 0000029.

Ponce, V. M. and Chaganti, P. V. (1994) "Variable-parameter Muskingum- Cunge revisited." *J. Hydrol.*, 162(3–4), 433–439.

Ponce, V. M. and Yevjevich, V. (1978). "Muskingum-Cunge method with variable parameters." *J. Hydraulic Division*, ASCE, 104(12), 1663–1667.

Ponce, V. M., & Changanti, P. V. (1994). "Variable-parameter Muskingum-Cunge method revisited." *Journal of Hydrology*, 162(3-4), 433-439.

Ponce, V. M., & Tsivoglou, A. J. (1981). "Modeling gradual dam breaches." *Journal of the Hydraulics Division*, 107(7), 829-838.

Ponce, V. M., and Theurer, F. D. (1982). "Accuracy criteria in diffusion routing." *J. Hydraul. Div*., ASCE., 108 (HY6): 747-757.

Ponce, V. M., and Yevjevich, V. (1978). "Muskingum-Cunge method with variable parameters." *J. Hydraul. Div*. ASCE, 104(HY12): 1663-1667.

Pope, S. B. (2000). "Turbulent flows." Cambridge University Press, Cambridge, United Kingdom. ISBN 0– 521–59886–9.

Prandtl, L., (1926). "Uber die ausgebildete turbulenz." Verh. 2nd Intl Kong. Fur Tech. Mech., Zurich [English translation, NACA Tech. Memo. 435].

Preston, J. H., (1954) "The Determination of Turbulent Skin Friction by means of Pitot Tubes." *Journal of Royal Aeronautical Society*, London, England, Vol. 58, 109–121.

Price, R. K. (2009). "Volume conservative non-linear flood routing." *J Hydraul Eng* ASCE 135(10):838–845

Proust, S., Fernandes, J. N., Peltier, Y., Leal, J. B., Riviere, N., & Cardoso, A. H. (2013). "Turbulent non-uniform flows in straight compound open-channels." *Journal of Hydraulic Research*, 51(6), 656-667.

Rajaratnam, N., Ahmadi, R., (1981). "Hydraulics of channel with flood-plains." *J. Hydraulic Res.* 19 (1), 43–60.

Rantz S.E. (1982). "Measurement and computation of streamflow." Volume 1 Measurement of Stage and Discharge U.S. Geological Survey Water Supply Paper 2175.

Reid, S. (2009). "Uncertainty and sensitivity analysis of the Muskingum-Cunge channel routing." Eisenhower Parkway: Pro Quest LLC.

Rhodes, D.G. and Knight, D.W., (1994). "Distribution of shear force on boundary of smooth rectangular duct." *Journal of Hydraulic Engineering*, ASCE, Vol. 120, No. 7, July, pp. 787-807, Paper No. 6195.

Richardson, L.F., (1922). "Weather prediction by numerical process." Cambridge University Press.

Rodi, W. (1980). "Turbulence models and their application in hydraulics: A state of the art review." IAHR Book Publications, Delft, Netherlands.

Rodi, W. (1993). "Turbulence models and their application in hydraulics." A. A. Balkema, Netherlands.

Rouse, H., (1965). "Critical analysis of open-channel resistance." *Journal of the Hydraulics Division*, ASCE, Vol. 91, No. 4387, HY4, pp 1-25.

Sahoo, B., Perumal, M., Moramarco, T., & Barbetta, S. (2014). "Rating curve development at ungauged river sites using variable parameter Muskingum discharge routing method." *Water resources management*, 28(11), 3783-3800.

Saint-Venant, B. D. (1871). "Theory of unsteady water flow, with application to river floods and to propagation of tides in river channels." French Academy of Science, 73(1871), 237-240.

Samuels, P.G., (1985). "Modelling of river and flood plain flow using the finite element method." PhD Thesis, University of Reading, November.

Sellin, R. H. J. (1964). "A laboratory investigation into the interaction between the flows in the channel of a river that is over its floodplain." La Houille Blanche, 7, 793–802.

Shiono, K. & Muto, Y., (1998). "Complex flow mechanisms in compound meandering channels with overbank flow." *Journal of Fluid Mechanics*, Cambridge University Press, Vol. 376: 221-261.

Shiono, K., and Knight, D. W. (1988). "Two-dimensional analytical solution for a compound channel." Proc., 3rd Int. Symp. Refined Flow Modelling and Turbulence Measurements, Y. Iwasa, N. Tamai, and A. Wada, eds., Universal Academy Press, Tokyo, 503–510.

Shiono, K., and Knight, D. W. (1991). "Turbulent open-channel flows with variable depth across the channel." *J. Fluid Mech.*, 222(1), 617–646.

Singh, V. (1996). "Kinematic wave modelling in water resources: surface-water hydrology." Hoboken: John Wiley & Sons.

Stelling, G. S and Verwey, A. (2005) "Numerical Flood Simulation, in Encyclopedia of Hydrological Sciences." *John Wiley & Sons Ltd*.

Stelling, G. S. and Duinmeijer, S. P. A. (2003). "A staggered conservative scheme for every Froude number in rapidly varied shallow water flows." *Int. J. Numer. Meth. Fluids*, 43, 1329–1354.

Sterling, M., Beaman, F., Morvan, H., and Wright, N. G. (2008). "Bed shear stress characteristics of a simple, prismatic, rectangular channel." *J. Eng. Mech.*, 134(12), 1085–1094.

Subramanya, K. (2009). "Flow In Open Channels", 3rd ed., New Delhi: Tata Mc Grow-Hill.

Tallaksen, L., Van Lanen, H. (2004). "Hydrological drought: processes and estimation methods for streamflow and Groundwater." Amesterdam: Elsevier.

Tang, X. and Knight, D.W, (2008). "A general model of lateral depth-averaged velocity distributions for open channel flows." Advances in Water Resources, Elsevier, Vol. 31, pp. 846-857.

Tang, X. and Samuels, P. G. (1999). "Variable Parameter Muskingum- Cunge Method for flood routing in a compound channel." *J. Hydraulic Res.*, 37, 591–614.

Tang, X., and Knight, D. W. (2008). "A general model of lateral depthaveraged velocity distributions for open channel flows." *Adv. Water Resour.*, 31(5), 846–857.

Tang, X., and Knight, D. W. (2009). "Analytical models for velocity distributions in open channel flows." *J. Hydraul.* Res., 47(4), 418–428.

Tang, X., Knight, D. W. and Samuels, P. G. (1999). "Volume conservation in Variable Parameter Muskingum-Cunge Method." *J. Hydraulic Eng.* (ASCE), 125(6), 610–620.

Te Chow, V. (1959). "Open channel hydraulics." McGraw-Hill, New York, 680.

Tewolde, M. (2005). "Flood Routing in Ungauged Catchments Using Muskingum Methods." Boca Raton: Dissertation.com.

Tewolde, M., Smithers, J., (2006)."Flood routing in ungauged catchments using Muskingum methods." Water SA [Online]. 32 (3). Available from: http://www.ajol.info/index.php/wsa/article/viewFile/5263/1371. [Accessed 1 October 2011].

Todini, E. (2009). "Predictive uncertainty assessment in real time flood forecasting." In Uncertainties in Environmental Modelling and Consequences for Policy Making (pp. 205-228). Springer Netherlands.

Todini, E., (2007). "A mass conservative and water storage consistent variable parameter Muskingum–Cunge approach." *Hydrol. Earth Syst. Sci*. 11, 1645– 1659.

Tominaga, A., and Nezu, I. (1991). "Turbulent structure in compound open channel flows." *J. Hydraul. Eng.*, 10.1061/(ASCE)0733-9429(1991) 117:1(21), 21–41.

Tominaga, A., Knight, D.W. (2004). "Numerical evaluation of secondary flow effects on lateral momentum transfer in overbank flows." RiverFlow 2004, 1, 353–361, M. Greco, A. Carravetta, R.D. De La Morte, eds. Balkema, Rotterdam, NL.

Tominaga, A., Nezu, I., Ezaki, K. and Nakagawa, H., (1989). "Three-dimensional turbulent structure in straight open channel flows." *Journal of Hydraulic Research*, IAHR, Vol. 27, No. 1, pp. 149-173.

Tominaga, Y. and Stathopoulos, T. (2007). "Turbulent Shmidt number for CFD analysis with various types of flowfield." *Atmospheric Environment* 41, 8091-8099.

U.S. Army Corps of Engineers (2005). "HEC-RAS User's Manual." http://www.hec.usace.army.mil/software/hec-ras/documents/ userman/index.html.

US Army Corps of Engineers (2008). "HEC-RAS, River Analysis System User's Manual, Version4, Davis: Institute for Water Resources Hydrologic Engineering Centre."

Vreugdenhil, C.B. and Wijbenga, J.H.A., (1982). "Computation of flow patterns in rivers." *Journal of the Hydraulic Division*, ASCE, Vol. 108, no. HY11, pp 1296- 1309.

Wark, J. B., Samuels, P.G., and Ervine, D.A., (1990). "A Practical method of estimating velocity and discharge in compound channels." Proceedings of the International Conference on River Flood Hydraulics, Wiley and Sons, UK, 163-172.

Wark, J.B., Slade, J.E. and Ramsbottom, D.M., (1991). "Flood discharge assessment by the lateral distribution method." *Hydraulics Research Limited*.

Wormleaton, P. R., and Merrett, D. J. (1990). "An improved method of the calculation for steady uniform flow in prismatic main channel/floodplain sections." *J. Hydraul. Res.*, 28(2), 157–174.

Wormleaton, P.R., (1988). "Determination of discharge in compound channels using the dynamic equation of lateral velocity distribution." Proceedings of the International Conference on Fluvial Hydraulics, IAHR, Budapest, Hungary.

Yang, K., Nie, R., Liu, X., & Cao, S. (2012). "Modeling depth-averaged velocity and boundary shear stress in rectangular compound channels with secondary flows." *Journal of Hydraulic Engineering*, 139(1), 76-83.

Yulistiyanto, B. (1997). "Flow around a cylinder installed in a fixed bed open channel." Ph.D. thesis, École Polytechnique Fédérale de Lausanne, Lausanne, Switzerland.

Zeng, Y. H., Guymer, I., Spence, K. J., & Huai, W. X. (2012). "Application of analytical solutions in trapezoidal compound channel flow." *River research and applications*, 28(1), 53-61.

Dissemination

International Journals

- P. Singh[1], K.K.Khatua[2]. "Prediction of velocity distribution, boundary shear stress and stage-discharge curves in compound channel" **Journal of Measurement Elsevier (Communicated).**

- P. Singh[1], S. Baneerjee[2], B. Naik [3], K.K.Khatua[4]. "Depth Average Velocity & Boundary Shear Stress in Gravel Bed", **ISH Journal of Hydraulic Engineering, Taylor & Francis Journals (Under Review)**

- S. Baneerjee [1], P. Singh [2], B. Naik [3], K.K.Khatua[4]. "Flow Resistance in Gravel Bed Open Channel Flows Case: Intense Transport Condition" , **ISH Journal of Hydraulic Engineering, Taylor & Francis Journals (Under Review)**

- B. Naik [1], K.K.Khatua[2],N.Knight[3], P.A. Sleigh[4], P.Singh[5]. "Numerical modelling of Converging Compound Channel Flow" , **ISH Journal of Hydraulic Engineering, Taylor & Francis Journals (Under Review)**

International Conference

- P. Singh[1], A. Kumar[2], K.K.Khatua[3]. " Concept of Turbulence Modelling and Its Application in Open Channel Flow" **Hydro-2016 International**, 21th Conference on Hydraulics, Water resources & Coastal Engineering. (Dec. 8-10th, 2016) Organized by CWPRS, Pune India.

- A. Kumar[1], P. Singh[2], K.K.Khatua[3]. "Comparison of 2D and 3D Modelling of Converging and Diverging Flood Plains" **Hydro-2016 International**, 21th Conference on Hydraulics, Water resources & Coastal Engineering. (Dec. 8-10th, 2016) Organized by CWPRS, Pune India.

National Conferences

- B.Naik[1], P. Singh[2], K.K.Khatua[3] . "Different techniques for boundary shear stress predictions for open channel flow", **National Conference on Water Resourses and Hydro Power**, June 17-18, 2016 , at Civil Engg. Dept. UPES, Dehradun.

Vitae

Prateek Kumar Singh

F-236 SD Hall of Residence

NATIONAL INSTITUTE OF TECHNOLOGY

ROURKELA

ODISHA, INDIA -769008

E mail: prateek.k.singh1992@gmail.com

Mobile – 9078068225

EDUCATIONAL QUQLIFICATION

- Maters' from Department of Civil Engineering with specialization water Resources Engineering in NIT Rourkela in the year 2017.
- Completed B.E in Mechanical Engineering from SRCOEM, Nagpur University in the year 2014.
- Completed +2 Science (Central Board for Secondary Education) securing 76% in the year 2010.
- Completed 10th standard (Central Board for Secondary Education) securing 84% in the year 2008.